SURE 静岡大学学術リポジトリ
Shizuoka University REpository

Study on Adsorption of Cesium Ions from Aqueous Solution by Using Plasma-induced Chitosan-grafted Nanomaterials

メタデータ	言語: en 出版者: Shizuoka University 公開日: 2015-12-17 キーワード (Ja): キーワード (En): 作成者: Yang, Shubin メールアドレス: 所属:
URL	https://doi.org/10.14945/00009274

THESIS

Study on Adsorption of Cesium Ions from Aqueous Solution by Using Plasma-induced Chitosan-grafted Nanomaterials

楊　樹斌

Department of Nanovision Technology
Graduate School of Science and Technology,
Educational Division, Shizuoka University

June 2015

静岡大学　博士論文

プラズマ誘起キトサン接合ベントナイトを用いた水溶液中セシウムイオン吸着に関する研究

楊樹斌

静岡大学
大学院自然科学系教育部
ナノビジョン工学専攻

2015 年 6 月

Acknowledgement

I would like to express my gratitude to everyone who helped me and made this thesis possible. In particular, I am deeply indebted to my supervior Prof. Massaki Nagatsu for his valuable guidance, advice, encouragement and support during my doctoral study in Shizuoka University. I also wish to thank him for gaving me the chance to study in Japan, and always supported me in my ideas.

Special appreciation is given to Prof. Wang Xiangke, my second supervisor, for his guidance for many helpful discussions that much stimulated my research. I also would thank to Dr. Changlun Chen for his valuable suggesting and comments for my research during my doctoral study.

Apart from above, I would like to thank Xiaoli, Peng Zhao, Mihai, Enbo, Anchu, Tomy, Naoyo Okada, Han Chou, et, al., everyone in Nagatus laboratory for the great help and support.

At last, I am deeply indebted to all my parents, my yonger sister and my youger brother for their love, selfless supporting and encouragement to finish my studies. Especial I would like to thank my husband, Dr. Yue Chen, who has always supported me so lot during the whole course.

I wish best of wish to all of you.

Thanks again.

Shubin Yang

Hamamatsu, 2015/04/16

Abstract

With the rapid increase industrialization in many countries, the pollution load on the environment is increasing. Radioactive cesium is of serious social and environment concern as it can be easily dissolved in water and has a high fission yield, long half-life ($T_{1/2}$ = 30.17 years). Although many research groups have made important contributions to search the high-efficiency sorbent for Cs^+ ions, and the mechanisms of Cs^+ adsorption are proposed, the detailed adsorption mechanisms still remain unclear. To search a high-efficiency adsorbent to remediate Cs^+ ions from contaminated water is an issue that needs to be addressed urgently. Therefore, an accurate and detail mechanism is required and calls for contribution to understand the adsorption process in order to facilitate the development of more efficient adsorbent. Among the traditional methods for the elimination of radioactive nuclides, such as precipitation, adsorption, ion exchange, and membrane filtration, adsorption has been suggested to be a promising technology for the treatment of wastewater with trace levels of radioactive nuclide ions for its simplicity, low cost and efficiency, although the success of the adsorption process is dependent on the choice of the appropriate material.

Plasma treatment is a useful means of surface modification, since it is solvent-free, time-efficient, versatile, and eco-friendly. The plasma-induced method can provide a wide range of different functional groups depending on the grafting material and the plasma discharge parameters, such as power, gas species, reaction time, and operating pressure. However, to the authors' knowledge, only a few studies regarding the modification of bentonite by plasma treatment have been reported. With these in mind, we herein designed a series of bentonite- and carbon nanotube-based materials by plasma modification to understand the detail of Cs^+ adsorption mechanisms.

In this thesis, **Chapter 1** presents the introduction of radioactive wastewater, including the fundamentals of radioactive wasterwater, the traditional treatments, an overview of the serious Fukushima Daiichi Nuclear Disaster and the fission and decay of radioactive cesium. The motivation and objectives of this thesis are also given in this chapter.

Chapter 2 introduces the principles of adsorption process, the application of adsorption in wastewater management and the influence factors for a successful adsorption separation process. The Langmuir isotherm and Freundlich isotherms, which are helpful to understand the adsorption mechanism, are also described in this chapter.

Chapter 3 describes the theory of plasma surface modification, and a briefly introduce about the plasma-induced grafting method. The plasma-induced method is considered to be a good way to enhance the chemical functionality of material. Several examples about the plasma science in space science and astrophysics are also listed in this chapter.

Chapter 4 provides the method to solve the question that "How important are the cation exchange and the hydroxyl exchange mechanisms to Cs^+ adsorption?" to study the detailed adsorption mechanisms of Cs^+. We have proved that the cation-exchange mechanism is much more effective than the hydroxyl group exchange. We cannot improve the Cs^+ adsorption capacity of material for Cs^+ only by increasing the amount of hydroxyl groups in any case.

Chapter 5 shows the study about designing a novel adsorbent with good magnetic properties, low turbidity, and high stability in aqueous solution as well as a significant adsorption capacity for Cs^+ ions. We found that the adsorption of Cs^+ by chitosan grafted magnetic bentonite was dependent on both pH and ionic strength. In the presence of Mg^{2+}, K^+, Li^+, and Na^+ ions, the Cs^+ exchange is constrained in the order of $Li^+ \approx Mg^{2+} < Na^+ < K^+$, primarily as a result of the hydrated radii and hydration energies of these cations in aqueous solution.

Finally **Chapter 6** is the summary and the conclusion of this work. The key points provided by this thesis are given in this chapter.

CONTENTS

CHAPTER 1 Radioactive Wastewater

This chapter deals with a little introduction about the problems of radioactive wastewater, the treatment methods, the main research conents, as well as the motivation of this work.

1.1 What is radioactive wastewater?

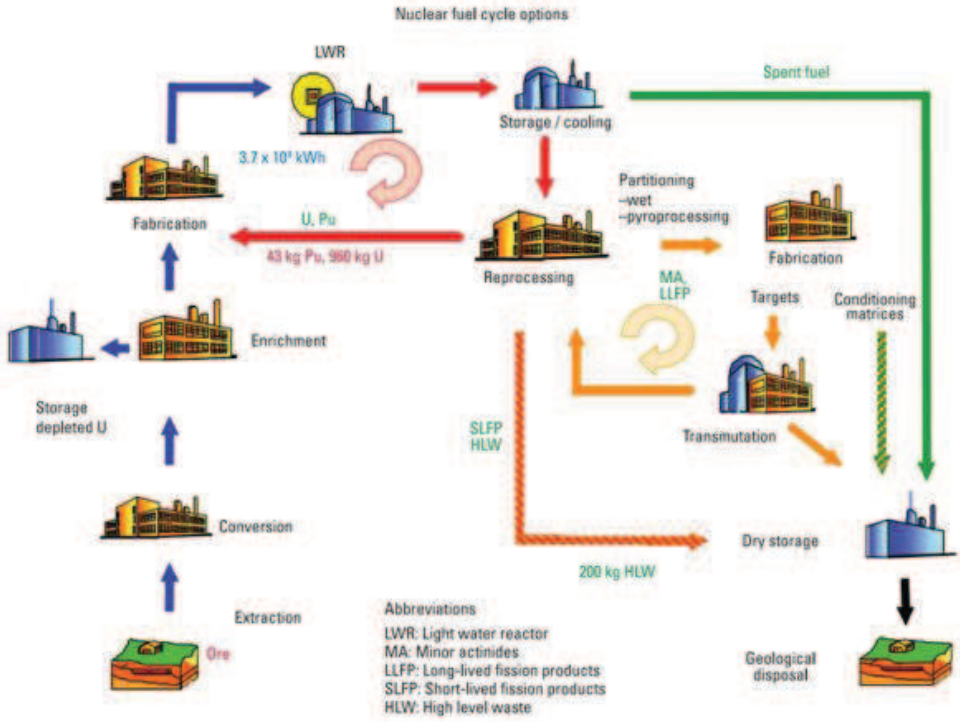

Fig.1.1 Diagram of the nuclear fuel cycle, showing the various options: once-through; conventional closed cycle; advanced closed cycle with partitioning and transmutation. Resultant high-level waste streams are also indicated.

Rapid increased in industrial development has led to the generation of large quantities of polluted industrial and municipal wastewaters. Wastewater, also written as waste water, is any water that has changed its natural characteristics and has been adversely affected in quality by anthropogenic influence.[1, 2] Wastewater can originate from a combination of domestic, industrial, commericial or agricultural activities, surface runoff or stormwater, and from sewer inflow or infiltration.[3, 4, 5] Nature water

is not normally reactive, but when adding some radioactive wastes such as ^{137}Cs, ^{235}U, etc., it produces highly reactive species, which cause nuclear radiation exposure. This kind of wastewater, which can affect human health and environment, also named radioactive wastewater.[2, 6]

Table 1.1 Socurces of radioactive wastewater.[8]

Source	Typical radioisotopes	Characteristics
Nuclear research centers	Might include relatively long lived, mixed with short lived	Generally uniform batches with nearly neutral pH from regeneration of ion exchange resins
Radioisotopes Lab. production	Wide variety depending upon production and purity of targets	Small volumes of high specific activity and high chemical concentrations
Radio-labeling and radiopharmaceuticals	^{14}C, ^{3}H, ^{32}P, ^{35}S, ^{125}I	Larger volume of low specific activity and small volume of predictable chemical composition
Medical diagnosis and treatment	^{99}Tcm, ^{131}I, ^{85}Sr	Large volumes of urine from patients and small volumes from preparation and treatment
Scientific research	Variable with short and long lived radioisotopes	Extremely variable
Industrial and pilot plants	Depends upon application	Volumes could be large and chemical composition underfined
Laundy and decontamination	Wide variety likely	Large volumes with low specific activity but containing complexing agents

Radioactive wastewater, which is generally believed to contain fission products, is any water systems that are either contaminated by radioactivity or radioactive itself, for which no further use.[9] Radioactive wastewater is usally generated during nuclear fuel cycle operation, production and other applications of nuclear fission or radioisotope, such as industry, agriculture, research and medicine, as well as a byproduct of natural resource exploitation, which includes mining and processing of ores, combustion of fossil fuels, or production of natural gas and oil.[8] Fig.1.1 shows

the diagram of the nuclear fuel cycle. The sources of radioactive wastewater are listed in Table 1.

1.2 Nuclear radiation and health effects

Radioactive wastewater is hazardous to most forms of life and the environment, and is regulated by government agencies in order to produce human health and the environment.[10, 11] The radioactive wastewater can be easily into the environment during the leaks of nuclear reactor, such as those that occurred at Chernobyl[12, 13, 14, 15] in 1986, at Three Mile Island[16, 17, 18] in Pennsylvania in 1979, and at Fukushima, Japan in 2011[19, 20, 21]. These serious accidents have been received the attention about fission products that could make their way into the food chain when present in the natural environment[22]. The diagram of the radioactive waste spread into the environment is illustrated in Fig. 1.2.

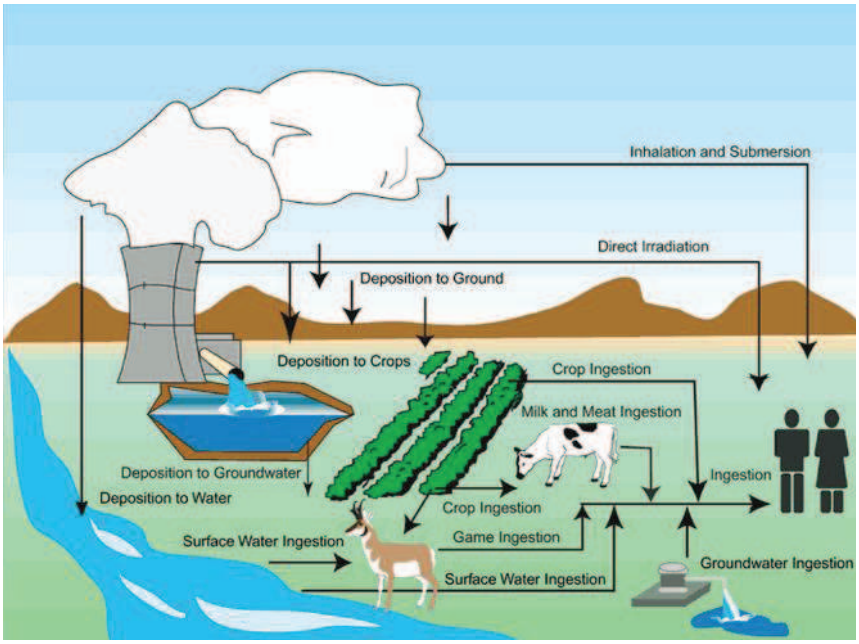

Fig.1.2 The diagram of the radioactive waste spread into the environment.

The radioactive wastewater could give rise to significant radiation exposure and do great harm to all the surrounding creatures and human beings. A chart released by the Japanese ministry of culture, sports, science and technology explaining the levels of

radiation that humans are explored to in daily life,[23, 24] see Fig. 1.3. Nuclear radiation arises from hundreds of different kinds of unstable atoms such as ^{131}I, ^{137}Cs, ^{90}Sr, ^{239}Pu, and ^{242}Am, which are mainly created in nuclear reactions.[25, 26] The radioactive nuclides could make their way to the food chain through the radioactive wastewater and consequently into human tissues. As these radioactive nuclides decays, or breaks down, ionizing radiation released into the environment can directly damage living tissues that is exposed to it. Expecially the nuclear radiation can cause mutations to DNA to become cancerous cells.[27] Prevously researches showed that lung, kidney and bones could receive the highest dose of radioactive uranium. Radiation poisoning or radiation sickness is a form of damage to organ tissue caused by excessive exposure to ionizing radiation.[28, 29]

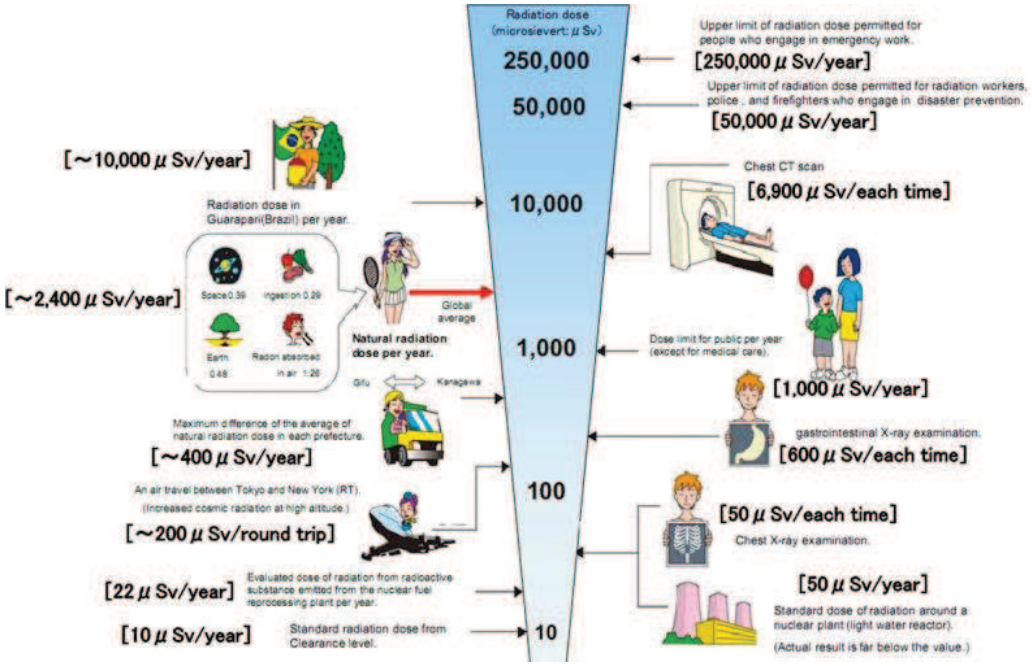

Fig.1.3 Radiation exposure in daily life.

1.3 High-level waste

In the nuclear power process, radioactive wastewater usually contains most of the radioactivity from the reprocessing of spent nuclear fuel, including liquid waster produced directly in reprocessing and any solid material derived from such liquid

waste that contains fission products in sufficient concentrations. This high level radioactive wastewater is defined as high-level liquid waste (HLW).[29, 30, 31] The chemical composites of typical high level liquid waste and its characteristics are list in Table 1.2. High-level waste is the type of nuclear waste with higest activity, which contains over 95% of the total fission products and transuranic elements generated in the reactor core.[32] Therefore, once accidentally nuclear leak occurred and released to the ground and sea, it must be a serious environmental crisis.

Table 1.2 Composites of typical high level liquid waste.

Composites		Concentration (mol/L)	Composites		Concentration (mol/L)
H^+		2.0	Corrosion products	Fe	0.054
NO_3^-		3.6		Cr	0.0096
Fission products	IA(Rb,Cs)	0.040		Ni	0.0034
	IIA(Sr,Ba)	0.040		Total	0.067
	III(Lanthanide)	0.148	PO_4^{3-}		0.042
	Zr	0.074	Actinides	U	0.053
	Mo	0.017		Np	0.003
	Tc	0.085		Pu	0.002
	VIIIA(Ru, Rh, Pd)	0.0078		Am	0.009
	others	0.0042		Cm	0.003
	total	0.416		Total	0.070

1.4 Wastewater management

To ensure the protection of human health and the environment from the hazard of these high level wastes, a planned integrated radioactive waste management practice should be applied. Therefore, their safe management has received considerable attention worldwide.

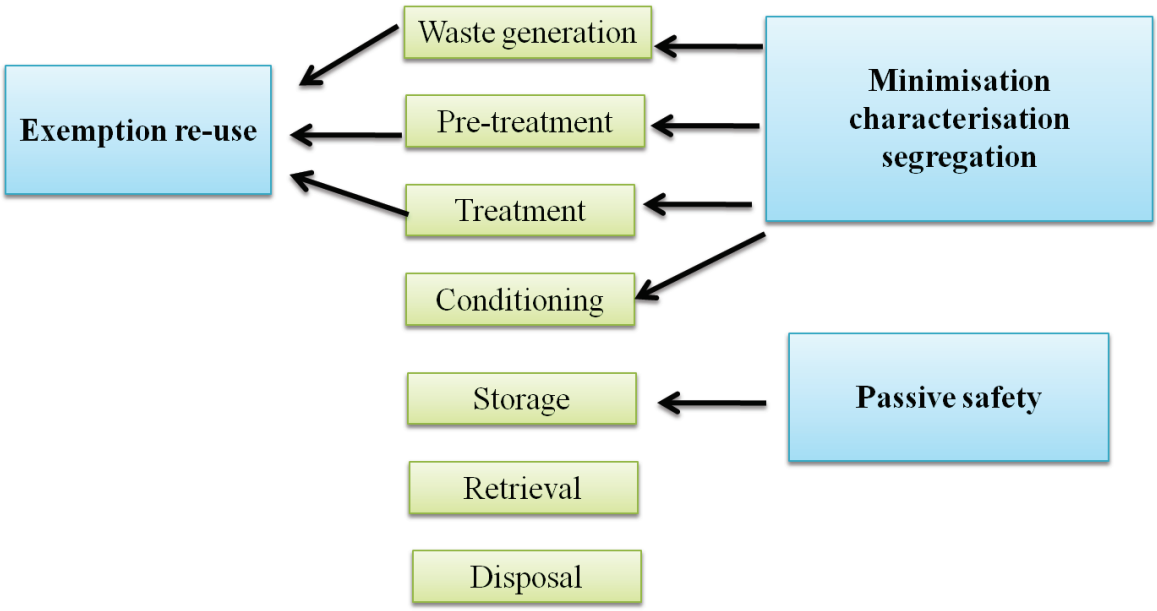

Fig.1.4 The basic steps of radioactive waste management.

Once accidentally nuclear leak occurred, radioactive waste will undergo some of the following stages depending on the type of waste and the strategy for its management.[26, 30, 33, 34, 35] The initial step is pretreatment, which involves collection, segregation, chemical adjustment and decontamination and may also include a period of interim storage, with the aim to segregate waste into stream to isolate non-radioactive wastes or those materials that can be recycled.[32] The second step is treatment. Typical treatment operations for the radioactive nuclides include sorption/ion exchange, chemical precipitation, evaporation, reverse osmosis, filtration and solvent extraction. The main features and limitation of these treatment processes are shown in Table 1.3. The third one is conditioning which involves transforming radioactive waste into a form that is suitable for handing, transportation, storage and disposal. This might also involve immobilization of radioactive waste, placing waste into containers or providing additional packaging. The following steps contain storage of radioactive waste to isolate it to help protect the environment, retrieval the waste package from storage, and disposal. These basic steps in radioactive waste management are shown in Fig. 1.4.

Table 1.3. Features and limitation of different aqueous liquid treatment optioins.[8]

Technology	Features	Limitations
Precipitation	Suitable for large volumes and high salt content waste Easy non-expensive operations	Low decontamination factor Efficiency depends on solid-liquid separation step
Sorption/ Ion-exchange	Good chemical, thermal and radiation stability Large choice of products ensuring high selectivity	Affected by high salt content Blockage problems Regeneration and recycling often difficult employed
Evaporation	High econtamination factor Well established technology High volume reduction factor Suitable for a variety of radionuclides	Process limitations (scaling, foaming, corrosion, volatility of certain radionuclides) High operation and capital costs
Reverse osmoses	Removes dissolved salts Economical Established for large scale operations	High preesure system Limited by osmotic pressure Non-back washable, subject to fouling
Ultrafiltration	Separation of dissolved salts from particulate and colloidal materials Good chemical and radiation stability for inorganic membranes	Fouling Organic membranes subject to radiation damage
Microfiltration	High recovery (99%) Low fouling when air backwash	Sensitive to impurities in waste stream
Solvant extraction	Selectivity enables removal, recovery or recycle of actinides	Generates aqueous and organic secondary waste

1.5 Fukushima nuclear accident

The huge Great East Japn Earthquake with a magnitude 9.0 on the Richter scale occurred on March 11, 2011 and induced a large tsunami that triggered the serious accident at the Fukushima Daiichi Nuclear Power Plant (FDNPP).[20, 36, 37, 38] The location of the FDNPP is shown in Fig.1.5. The FDNPP due to the catastrophic accident in particular lost reactor cooling systems, resulting in several explosions from four reactors, which involved the dispersion and spread of radioactive materials, and thus from both the political and economic perspectives.[9, 39] The first hydrogen explosion occurred at 15:36 Japan Standard Time (JST) on March 12 in unite 1, which the second one occurred at 11:01 on March 14 in unit 3. Worse still, two more explosions occurred in units 2 and 4 at approximately the same time around 06:00 on March 15.

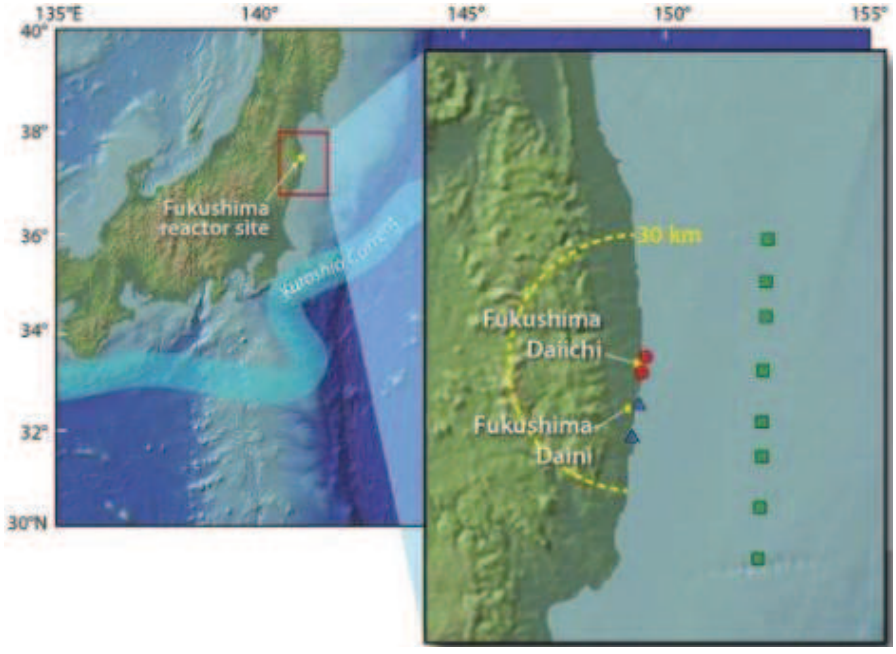

Fig.1.5 The location of the Fukushima Daiichi Nuclear Power Plant.

As a result of these explosions, huge amounts of radionuclides such as ^{131}I, ^{134}Cs, ^{137}Cs, ^{132}Te,^{140}Ba, ^{140}La and ^{90}Sr were emitted into the surrounding environment, and the eventual impact them will have on human health. The serious Fukushima nuclear

accidents had contaminated a vast area in Japan. The total amounts of ^{131}I and ^{137}Cs discharged into the atmosphere between 10:00 JST on March 12 and 00:00 JST on April 6 were estimated to be approximately $1.5 \times 10^{17}$and 1.3×10^{16}Bq, respectively.[20, 37, 39, 40] Therefore, the situation has become extremely severe for Japan since the countermeasures to deal with the nuclear accident had to be carried out along with dealing with the broader disaster. The serious accident became not only an issue for Japan itself but also an issue requiring internation crisis management, and it has raised concerns around the world about the safety of nuclear power generation.

1.6 Radioactive cesium

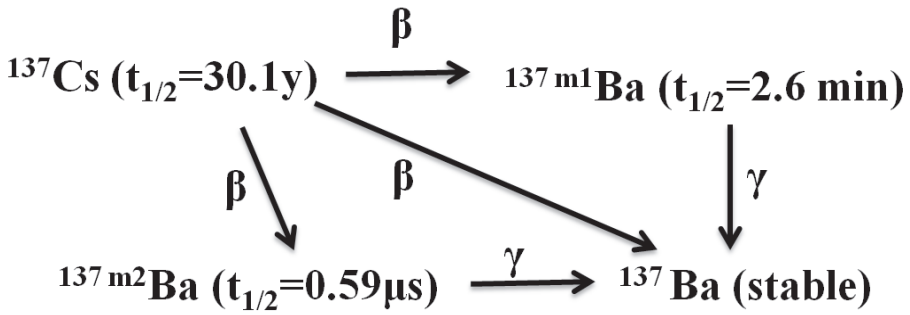

Fig.1.6 A brief description of the fission and decay pathway of ^{137}Cs to ^{137}Ba.

The radionuclides cesium (^{137}Cs and ^{134}Cs) are the products of uranium fission[41] and are biological hazard.[42, 43, 44, 45] Morisawa et al reported that the fallout of ^{137}Cs was higher than ^{90}Sr in Japan after Chernobyl. Radioactive cesium can stay in the environment for more than a century. The fission and decay pathway of ^{137}Cs to ^{137}Ba is discribed in Fig.6.

The serious Fukushima nuclear accident had releasted a significant amount of radioactive nuclides into the Pacific marine ecosystem.[19] Among the radionuclides emitted during the nuclear leak, ^{137}Cs with a long half-life of 30.1 yeas and ^{134}Cs with a long half-life of 2.1 yeas were of serious concern. There has been some reported evidence that radioactive cesium are being released into the environment from the malfunctioning nuclear reactions in Japan. The sorption and migration of radiocesium are important processes to evaluate its

physicochemical behavior in the natural environment.In addition, the radionuclide cesium could make its way into the food chain when present in the natural environment.[22] So the establishment of removal technology ofradio cesium from the nuclear waste before its discharge to the environment is very necessary.

1.7 Motivation and objectives of thesis

The Fukushima incident contaminated a vast area in eastern Japan [22] and, once the ^{137}Cs enters the food chain through uptake by plants, it can be readily ingested by both animals and human beings[46]. For these reasons, the capture of ^{137}Cs from wastewaters is currently an urgent priority. At present, the most commonly used methods for the separation and preconcentration of radionuclides include precipitation, solvent extraction, membrane dialysis, and adsorption [19, 47, 48, 49]. Among these methods, adsorption is both simple and economically feasible, although the success of the adsorption process is dependent on the choice of the appropriate material. Inorganic cation exchangers, such as crystalline silicotitanates, zeolites, clay minerals, and layered sulfide frameworks, have been studied for separation of Cs^+ ions, because of the ability of these adsorbents to withstand intense radiation, elevated temperatures, and high ion-exchange capacity.[19, 47, 48, 49, 50, 51, 52, 53] Although many research groups[19, 42, 54, 55] have made important contributions to search the high-efficiency sorbent for Cs^+ ions, and the mechanisms of Cs^+ sorption are proposed, the detailed adsorption mechanisms still remain unclear. Obviously, an accurate and detail mechanism is required and calls for contribution to understand the adsorption process in order to facilitate the development of more efficient adsorbent. This is very important for us to choose and design materials as a high-efficiency sorbent for Cs^+ ions.

Plasma treatment is a useful means of surface modification, since it is solvent-free, time-efficient, versatile, and eco-friendly[56, 57, 58]. It considered being a good way to enhance the chemical functionality of material. [57, 59, 60] The research on improving adsorption capacity of materials by plasma-induced grafting technique has profound significance in environmental pollution management.[61]

In the context of Cs^+ wastewaters, the informations of an accurate and detail mechanism for Cs^+ sorption as well as the designing non-toxic, low-cost, and high-efficiency adsorbent are important and useful for therapy of animals and humans affected by nuclear accident. Therefore, the motivation and objectives of this thesis are :

1) Use the Ar RF plasma-induced method to synthesize the CNTs- and bentonite-based composites as sorbents for Cs^+ ions in aqueous solutions
2) To understand "How important are the cation exchange and the hydroxyl exchange mechanisms to Cs^+ adsorption?"
3) Use the radio frequency Ar-plasma-induced method to prepare chitosan-grafted magnetic bentonite (CS-g-MB)
4) To design a better adsorbent by the plasma-induced graft method with good magnetic property, low turbidity, and a significant adsorption capacity for Cs^+ ions.
5) The stabilities of the new adsorbent in contaminated actual seawater and in simulated groundwater should be performed.
6) To give the future directions of new and selective adsorbents for the removal of Cs^+ ions in groundwater or wastewater.

Reference:

[1]. Crini, G.,Non-conventional low-cost adsorbents for dye removal: a review. *Bioresour. Technol.* **2006,** *97* (9), 1061-1085.

[2]. Awual, M. R.; Suzuki, S.; Taguchi, T.; Shiwaku, H.; Okamoto, Y.; Yaita, T.,Radioactive cesium removal from nuclear wastewater by novel inorganic and conjugate adsorbents. *Chem. Eng. J.* **2014,** *242* (0), 127-135.

[3]. Fu, W. G.; Li, P. P., Characteristics of Phosphorus Adsorption of Aerated Concrete in Wastewater Treatment. In *Environmental Biotechnology and Materials Engineering, Pts 1-3*, Shi, Y. G.; Zuo, J. L., Eds. 2011; Vol. 183-185, pp 466-470.

[4]. Gerente, C.; Lee, V. K. C.; Le Cloirec, P.; McKay, G.,Application of chitosan for the removal of metals from wastewaters by adsorption - Mechanisms and models review. *Crit. Rev. Environ. Sci. Technol.* **2007,** *37* (1), 41-127.

[5]. Levchuk, I.; Rueda-Márquez, J. J.; Suihkonen, S.; Manzano, M. A.; Sillanpää, M.,Application of UVA-LED based photocatalysis for plywood mill wastewater treatment. *Separation and Purification Technology* **2015,** *143*, 1-5.

[6]. Ren, X. M.; Chen, C. L.; Nagatsu, M.; Wang, X. K.,Carbon nanotubes as adsorbents in environmental pollution management: A review. *Chem. Eng. J.* **2011,** *170* (2-3), 395-410.
[7]. Dunicz, B. L.,Surface area of activated charcoal by Langmuir adsorption isotherm. *Journal of Chemical Education* **1961,** *38* (7), 357.
[8]. Rahman, R. O. A.; Ibrahium, H. A.; Hung, Y.-T.,Liquid Radioactive Wastes Treatment: A Review. *Water* **2011,** *3* (4), 551-565.
[9]. Tanaka, K.; Sakaguchi, A.; Kanai, Y.; Tsuruta, H.; Shinohara, A.; Takahashi, Y.,Heterogeneous distribution of radiocesium in aerosols, soil and particulate matters emitted by the Fukushima Daiichi Nuclear Power Plant accident: retention of micro-scale heterogeneity during the migration of radiocesium from the air into ground and river systems. *Journal of Radioanalytical and Nuclear Chemistry* **2013,** *295* (3), 1927-1937.
[10]. News Briefs : Radioactive waste disposal. *Environ Sci Technol* **2001,** *35* (15), 323A-323A.
[11]. Tavor, D.; Wolfson, A.; Shamaev, A.; Shvarzman, A.,Recycling of Industrial Wastewater by Its Immobilization in Geopolymer Cement. *Industrial & Engineering Chemistry Research* **2007,** *46* (21), 6801-6805.
[12]. Fessak, A.,Chernobyl, Ukraine: Not Chernobyl, Russia. *Journal of Chemical Education* **1990,** *67* (7), 630.
[13]. Danchenko, M.; Skultety, L.; Rashydov, N. M.; Berezhna, V. V.; Mátel, L. u.; Salaj, T.; Pret'ová, A.; Hajduch, M.,Proteomic Analysis of Mature Soybean Seeds from the Chernobyl Area Suggests Plant Adaptation to the Contaminated Environment. *Journal of Proteome Research* **2009,** *8* (6), 2915-2922.
[14]. Atwood, C. H.,Chernobyl-what happened? *Journal of Chemical Education* **1988,** *65* (12), 1037.
[15]. Flavin, C.,ES Views: Nuclear Safety After Chernobyl. *Environ Sci Technol* **1987,** *21* (7), 624-625.
[16]. Mammano, N. J.,A chemistry lesson at Three Mile Island. *Journal of Chemical Education* **1980,** *57* (4), 286.
[17]. Three Mile Island panel issues report. *Chemical & Engineering News Archive* **1979,** *57* (45), 7.
[18]. DOE will take Three Mile Island high-level waste. *Chemical & Engineering News Archive* **1981,** *59* (25), 23-24.
[19]. Yang, D.; Sarina, S.; Zhu, H.; Liu, H.; Zheng, Z.; Xie, M.; Smith, S. V.; Komarneni, S.,Capture of radioactive cesium and iodide ions from water by using titanate nanofibers and nanotubes. *Angew. Chem. Int. Ed.* **2011,** *50* (45), 10594-10598.
[20]. Merz, S.; Shozugawa, K.; Steinhauser, G.,Analysis of Japanese Radionuclide Monitoring Data of Food Before and After the Fukushima Nuclear Accident. *Environ Sci Technol* **2015,** *49* (5), 2875-2885.
[21]. Wang, Q.; Chen, X.,Nuclear Accident Like Fukushima Unlikely in the Rest of the World? *Environ Sci Technol* **2011,** *45* (23), 9831-9832.
[22]. Mizuno, T.; Kubo, H.,Overview of active cesium contamination of freshwater fish in fukushima and eastern Japan. *Sci. Rep.* **2013,** *3*, 1-4.

[23]. Kim, S.-H.; Kelly, P. B.; Clifford, A. J.,Calculating Radiation Exposures during Use of 14C-Labeled Nutrients, Food Components, and Biopharmaceuticals To Quantify Metabolic Behavior in Humans
Calculating Radiation Exposures during Use of 14C-Labeled Nutrien. *Journal of Agricultural and Food Chemistry* **2010**.
[24]. Bakshi, M. V.; Azimzadeh, O.; Barjaktarovic, Z.; Kempf, S. J.; Merl-Pham, J.; Hauck, S. M.; Buratovic, S.; Eriksson, P.; Atkinson, M. J.; Tapio, S.,Total Body Exposure to Low-Dose Ionizing Radiation Induces Long-Term Alterations to the Liver Proteome of Neonatally Exposed Mice. *Journal of Proteome Research* **2015,** *14* (1), 366-373.
[25]. Logan, S. R.,Instability of Large Nuclides with Respect to Decay by alpha-Particle Emission. *Journal of Chemical Education* **1994,** *71* (10), 888.
[26]. Lacy, W. J.; Laguna, W. d.,Decontaminating Radioactive Water. *Industrial & Engineering Chemistry* **1958,** *50* (8), 1193-1193.
[27]. Pearsall, S. G.; Wilshusen, W.,The disposal of chemical and radioactive waste - Part two. *Journal of Chemical Education* **1968,** *45* (9), A677.
[28]. Black, K. C. L.; Wang, Y.; Luehmann, H. P.; Cai, X.; Xing, W.; Pang, B.; Zhao, Y.; Cutler, C. S.; Wang, L. V.; Liu, Y.; Xia, Y.,Radioactive 198Au-Doped Nanostructures with Different Shapes for In Vivo Analyses of Their Biodistribution, Tumor Uptake, and Intratumoral Distribution. *ACS Nano* **2014,** *8* (5), 4385-4394.
[29]. Gruber, J.,High-level radioactive waste from fusion reactors. *Environ Sci Technol* **1983,** *17* (7), 425-431.
[30]. John E, M.; McELROY, J. L.; Allison M, P., High-Level Radioactive Waste Management Research and Development Program at Battelle Pacific. In *High-Level Radioactive Waste Management*, AMERICAN CHEMICAL SOCIETY: 1976; Vol. 153, pp 93-107.
[31]. James P, D., The High-Level Radioactive Waste Management Program at Nuclear Fuel Services. In *High-Level Radioactive Waste Management*, AMERICAN CHEMICAL SOCIETY: 1976; Vol. 153, pp 72-83.
[32]. Frank K, P., Management of Commercial High-Level Radioactive Waste. In *High-Level Radioactive Waste Management*, AMERICAN CHEMICAL SOCIETY: 1976; Vol. 153, pp 1-8.
[33]. Dantus, M. M.; High, K. A.,Economic Evaluation for the Retrofit of Chemical Processes through Waste Minimization and Process Integration. *Industrial & Engineering Chemistry Research* **1996,** *35* (12), 4566-4578.
[34]. High-level radioactive waste. *Environ Sci Technol* **1983,** *17* (9), 413A-414A.
[35]. Beal, J.; Weiss, R.; Densmore, D.; Adler, A.; Appleton, E.; Babb, J.; Bhatia, S.; Davidsohn, N.; Haddock, T.; Loyall, J.; Schantz, R.; Vasilev, V.; Yaman, F.,An End-to-End Workflow for Engineering of Biological Networks from High-Level Specifications. *ACS Synthetic Biology* **2012,** *1* (8), 317-331.
[36]. Buesseler, K.; Aoyama, M.; Fukasawa, M.,Impacts of the Fukushima Nuclear Power Plants on Marine Radioactivity. *Environ. Sci. Technol.* **2011,** *45* (23), 9931-9935.

[37]. Otosaka, S.; Nakanishi, T.; Suzuki, T.; Satoh, Y.; Narita, H.,Vertical and Lateral Transport of Particulate Radiocesium off Fukushima. *Environ. Sci. Technol.* **2014,** *48* (21), 12595-12602.

[38]. Mori, T.; Akamatsu, M.; Okamoto, K.; Sumita, M.; Tateyama, Y.; Sakai, H.; Hill, J. P.; Abe, M.; Ariga, K.,Micrometer-level naked-eye detection of caesium particulates in the solid state. *Sci. Technol. Adv. Mater.* **2013,** *14* (1).

[39]. Yamaguchi, S.; Kondo, K.; Kodera, S.,Fukushima Daiichi Nuclear Power Plant accident and its effect. *National Diet Library* **2011.6.23,** (Issue Brief 718).

[40]. Ishikawa, T.; Sorimachi, A.; Arae, H.; Sahoo, S. K.; Janik, M.; Hosoda, M.; Tokonami, S.,Simultaneous Sampling of Indoor and Outdoor Airborne Radioactivity after the Fukushima Daiichi Nuclear Power Plant Accident. *Environ Sci Technol* **2014,** *48* (4), 2430-2435.

[41]. Sheha, R. R.,Synthesis and characterization of magnetic hexacyanoferrate (II) polymeric nanocomposite for separation of cesium from radioactive waste solutions. *J. Colloid Interface Sci.* **2012,** *388*, 21-30.

[42]. Dwivedi, C.; Kumar, A.; Ajish, J. K.; Singh, K. K.; Kumar, M.; Wattal, P. K.; Bajaj, P. N.,Resorcinol-formaldehyde coated XAD resin beads for removal of cesium ions from radioactive waste: synthesis, sorption and kinetic studies. *RSC Adv.* **2012,** *2* (13), 5557-5564.

[43]. Hayes, R. L.; Butler, W. R.,Growth and decay of radionuclides: A demonstration. *Journal of Chemical Education* **1960,** *37* (11), 590.

[44]. Thomas, R. P. G., *Analytical Methods in Oceanography*. AMERICAN CHEMICAL SOCIETY: 1975; Vol. 147, p 252.

[45]. Ding, D.; Lei, Z.; Yang, Y.; Feng, C.; Zhang, Z.,Nickel Oxide Grafted Andic Soil for Efficient Cesium Removal from Aqueous Solution: Adsorption Behavior and Mechanisms. *ACS Appl Mater Interfaces* **2013,** *5* (20), 10151-10158.

[46]. Vipin, A. K.; Hu, B.; Fugetsu, B.,Prussian blue caged in alginate/calcium beads as adsorbents for removal of cesium ions from contaminated water. *J. Hazard. Mater.* **2013,** *258–259* (0), 93-101.

[47]. Ding, N.; Kanatzidis, M. G.,Selective incarceration of caesium ions by Venus flytrap action of a flexible framework sulfide. *Nat. Chem.* **2010,** *2* (3), 187-191.

[48]. Clearfield, A.,Ion-exchange materials seizing the caesium. *Nat. Chem.* **2010,** *2* (3), 161-162.

[49]. Celestian, A. J.; Kubicki, J. D.; Hanson, J.; Clearfield, A.; Parise, J. B.,The mechanism responsible for extraordinary Cs ion selectivity in crystalline silicotitanate. *J. Am. Chem. Soc.* **2008,** *130* (35), 11689-11694.

[50]. Celestian, A. J.; Parise, J. B.; Smith, R. I.; Toby, B. H.; Clearfield, A.,Role of the hydroxyl-water hydrogen-bond network in structural transitions and selectivity toward cesium in $Cs_{0.38}(D_{1.08}H_{0.54})SiTi_2O_7 \bullet (D_{0.86}H_{0.14})_2O$ crystalline silicotitanate. *Inorg. Chem.* **2007,** *46* (4), 1081-1089.

[51]. Chen, Q.; Du, G. H.; Zhang, S.; Peng, L. M.,The structure of trititanate nanotubes. *Acta Crystallogr., Sect. B: Struct. Sci.* **2002,** *58*, 587-593.

[52]. Dyer, A.; Pillinger, M.; Amin, S.,Ion exchange of caesium and strontium on a titanosilicate analogue of the mineral pharmacosiderite. *J. Mater. Chem.* **1999,** *9* (10), 2481-2487.

[53]. Kim, Y. I.; Salim, S.; Huq, M. J.; Mallouk, T. E.,Visible-light photolysis of hydrogen iodide using sensitized layered semiconductor particles. *J. Am. Chem. Soc.* **1991,** *113* (25), 9561-9563.

[54]. Delchet, C.; Tokarev, A.; Dumail, X.; Toquer, G.; Barre, Y.; Guari, Y.; Guerin, C.; Larionova, J.; Grandjean, A.,Extraction of radioactive cesium using innovative functionalized porous materials. *RSC Adv.* **2012,** *2* (13), 5707-5716.

[55]. Torad, N. L.; Hu, M.; Imura, M.; Naito, M.; Yamauchi, Y.,Large Cs adsorption capability of nanostructured Prussian Blue particles with high accessible surface areas. *J. Mater. Chem.* **2012,** *22* (35), 18261-18267.

[56]. Wei, Y.; Liu, Z. G.; Yu, X. Y.; Wang, L.; Liu, J. H.; Huang, X. J.,O_2-plasma oxidized multi-walled carbon nanotubes for Cd(II) and Pb(II) detection: Evidence of adsorption capacity for electrochemical sensing. *Electrochem. Commun.* **2011,** *13* (12), 1506-1509.

[57]. Chen, C. L.; Ogino, A.; Wang, X. K.; Nagatsu, M.,Plasma treatment of multiwall carbon nanotubes for dispersion improvement in water. *Appl. Phys. Lett.* **2010,** *96* (13), 131504-131503.

[58]. Shao, D. D.; Hu, J.; Wang, X. K.; Nagatsu, M.,Plasma induced grafting multiwall carbon nanotubes with chitosan for 4,4'-dichlorobiphenyl removal from aqueous solution. *Chem. Eng. J.* **2011,** *170* (2-3), 498-504.

[59]. Hu, J.; Shao, D. D.; Chen, C. L.; Sheng, G. D.; Li, J. X.; Wang, X. K.; Nagatsu, M.,Plasma-induced grafting of cyclodextrin onto multiwall carbon nanotube/iron oxides for adsorbent application. *J. Phys. Chem. B* **2010,** *114* (20), 6779-6785.

[60]. Chen, C. L.; Wang, X. K.; Nagatsu, M.,Europium adsorption on multiwall carbon nanotube/iron oxide magnetic composite in the presence of polyacrylic acid. *Environ. Sci. Technol.* **2009,** *43*, 2362-2367.

[61]. Yang, S. B.; Hu, J.; Chen, C. L.; Shao, D. D.; Wang, X. K.,Mutual effects of Pb(II) and humic acid adsorption on multiwalled carbon nanotubes/polyacrylamide composites from aqueous solutions. *Environ. Sci. Technol.* **2011,** *45* (8), 3621-3627.

CHAPTER 2 Liquid-Solid Adsorption

This chapter discussed briefy about the fundamental theory of adsorption, the application of adsoriton in wastewater management and the influence factors for a successful adsorption process. The difference of adsorption and absorption are discussed. The Langmuir isotherm and Freundlich isotherm, which are helpful to understand the adsorption mechanism, are also described.

2.1 Fundamental theory

Adsorption at liquid-solid interface is the process of transferring material from a fluid phase to a solid phase (e.g., the adsorption of an organic pollutant on activated carbon).[1, 2, 3, 4] In other words, adsorption is a separation process in which material or adsorbate is concentrated from a bulk vapor or liquid phase on to the surface of a porous solid.[5, 6, 7] In this system, the transferring material being adsorbed refers to adsorbate, while the solid material being used as the adsorbing phase is defined as adsorbent. A simple model of the liquid-solid adsoroption mechanism is described in Fig. 2.1.[8, 9, 10]

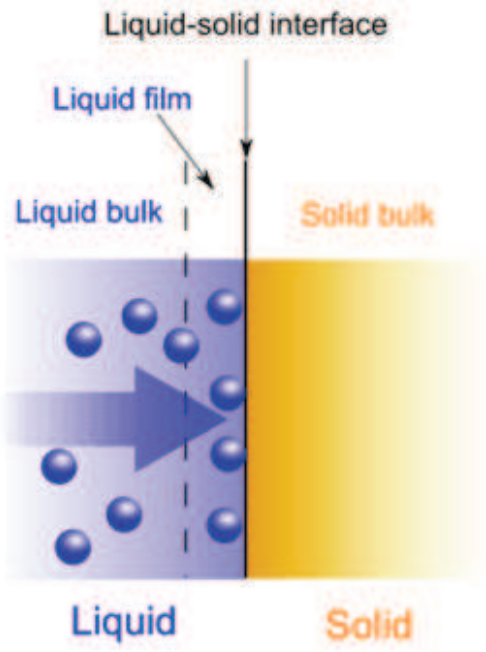

Fig. 2.1 Liquid-solid adsorption mechanism. Blue spheres are solute molecules.

Generally, the adsorption capacity (Q_e, mg/g) and removal efficiency ($E\%$) are calculated according to Eqs., (2-1) and (2-2) to evaluate the adsorption efficiency[11, 12, 13, 14, 15]:

$$Q_e = \frac{(C_o - C_t)V}{W} \tag{2-1}$$

$$E\% = \frac{(C_o - C_t)}{C_o} \times 100 \tag{2-2}$$

whereC_o is the initial concentration of adsorbate in solution (mg/L), C_t represents the concentration of adsorbate in supernatant at time t, W is the mass of adsorbent (g), V represents the total volume of the solution (L).

The driving force for adsorption is the reduction in interfacial tension between the fluid and the solid adsorbent as a result of the adsorption of the adsorbate on the surface of the solid. The surface or interfacial tension (σ) is the change in free energy (G) resulting when the area between two phases (A) is increased. The definition of interfacial tension (σ)[16] is:

$$\sigma = (\frac{\partial G}{\partial A})_{T,P,n_j} \tag{2-3}$$

The adsorption process is generally classified as physisorption (characteristic of weak van der Waals forces) and chemisorption (characteristic of covalent bonding) according to the forces involved in the binding at the surface. It may also occur due to electrostatic attration. Physical adsorption is the result of nonspecific, relatively weak van der Waals forces and adsorption energy usually not excessding 80 kJ/mol, with typical energies being considerably less.[17, 18] Physically adsorbed molecules may diffuse along the surface of the adsorbent and typically are not bound to a specific location on the surface.[19, 20, 21] Being only weakly bound, physical adsorption is easily reversed. On the other hand, chemisorption is much stronger than the physisorption with adsorption energy up to about 800 kJ/mol for chemical bonds. A chemical bond involves sharing of electrons between the adsorbate and the adsorbent and may be regarded as the formation of a surface compound. Due to the bond strength, chemical adsorption is difficult to reverse. In addition, physical adsoroption takes place on all surfaces provided that temperature and pressure conditions are favorable. Chemisorption, however, is

highly selective and occurs only between certain adsorptive and adsorbent species and only if the chemically active surface is cleaned of prvioulsy adsorbed molecules.

Sun et al. studied the adsorption processes of U(VI) ions on graphene and graphene oxides (GOs) by DFT calculation to understand the adsorption mechanisms.[22]They selected the –COOH, -COC and –OH functional groups as representative groups on GO, and employed the different GO models with uranyl ions to describe the adsorption of U(VI) ions on GOs with different oxygen-containing groups.(Fig. 2.2) According to the optimized structures and binding energies of uranyl ions on graphene and GOs, they fond the adsorption of U(VI) on graphene was physisorbed while the adsorption of U(VI) on GOs with COOH, OH or COO^- functional groups were chemisorption.

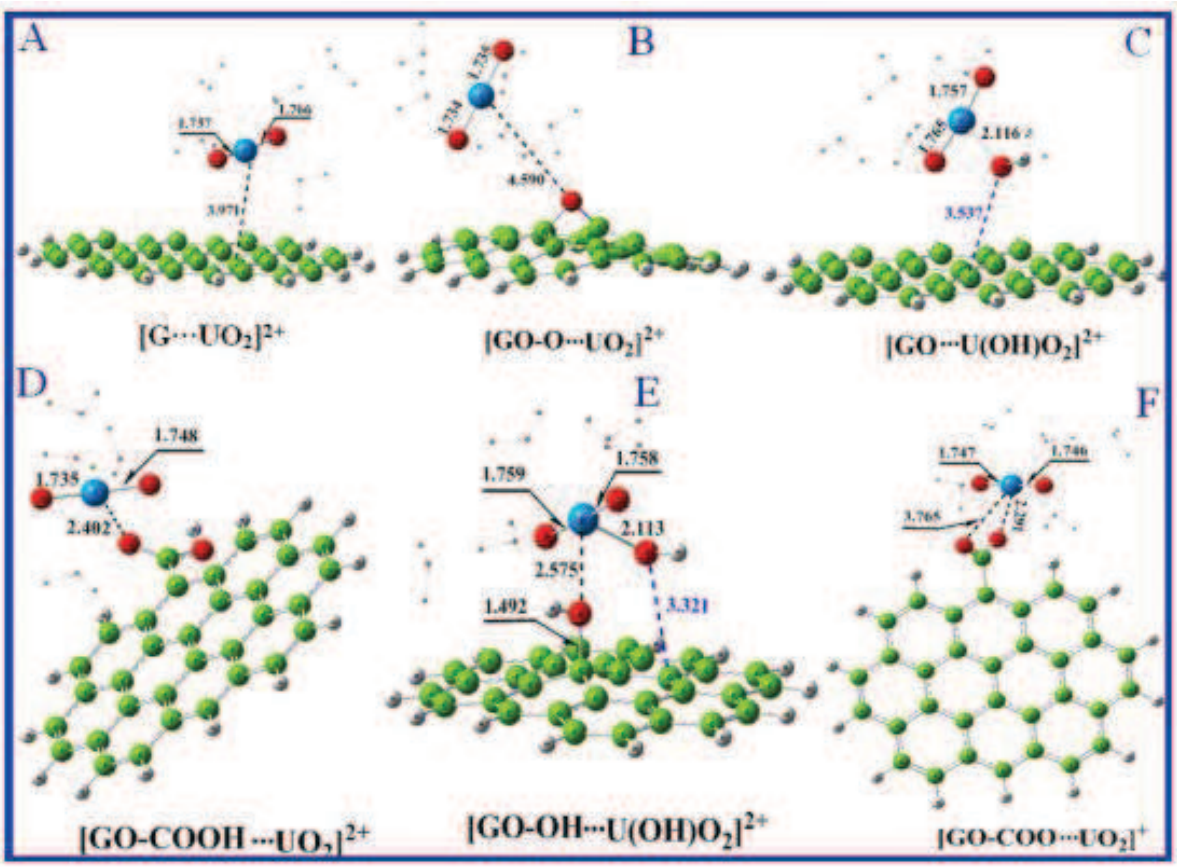

Fig. 2.2 The DFT optimized geometries of the graphene_uranyl complexes and GOs_uranyl complexes.

2.2 Absorption vs. Adsorption

Basically, "absorption"[23, 24] and "adsorption"[5, 25, 26] are both sorption process but different phenomena. The term sorption encompasses both processes, while desorption is the reverse of it. Absorption is the process in which a fluid is dissolved by a liquid or a solid (absorbent).[27, 28, 29, 30] Adsorption is the process in which atoms, ions or molecules from a substance (it could be gas, liquid or dissolved solid) adhere to a surface of the adsorbent. Adsorption is a surface-based process where a film of adsorbate is created on the surface while absorption involves the entire volume of the absorbing substance. More differences of the two processes are listed in Table 2.1.

Table 2.1 Comparion chart of the adsoroption and absorption processes.

	Adsorption	Absorption
Definition	Accumulation of the molecular species at the surface rather than in the bulk of the solid or liquid	Assimilation of molecular species throughout the bulk of the solid or liquid
Phenomenon	A surface phenomenon	A bulk phenomenon
Heat exchange	Exothermic process	Endothermic process
Temperature	Favoured by low temperature	No effect
Rate of reaction	It steadily increases and reach to equilibrium	A uniform rate
Concentration	Concentration on the surface of adsorbent is different from that in the bulk	It is same throughout the material

2.3 Adsorption in wasterwater treatment

Water pollution caused by heavy metal ions and radioactive nuclides is a crucial worldwide environmental problem with significant effect on human health and environment.[31, 32] A

number of conventional methods for the wasterwater treatment have been reported such as ion exchange, electrochemical reduction reverse osmosis, chemical precipitation, and membrane filtration.[33, 34, 35, 36] However, since some of them have a few problems such as their operational demerits, high cost and time-consuming. As an economically feasible, simple and efficient method, adsorption technique has been widely applied in wasterwater management. The detailed motications for the use of adsorption processes in wasterwater treatment are summarized as following:

1) The pollutants in the wastewater are toxic or hazardous
2) The pollutants are difficult to remove via the conventionally secondary treatment
3) Some of the pollutants are volatile and cannot be transferred to the atmosphere
4) The pollutants have the potential for creating noxious vapors or odors, or for impacting color to the wastewater
5) There have many drawbacks for the conventional methods
6) The concentration of pollutants is so low that it is difficult to remove them via other methods

2.4 Influence Factor for Adsorption

The success of the adsorption process is dependent on the choice of the appropriate material and the environmental conditions such as pH, ionic strength, and other parameters. The appropriate material with good chemical stability, large specific surface area, hollow, layered nanosized structures, no color and low turbidity has been proved to be good candidates as adsorbent.[32, 37]

2.4.1 Specific surface area

The monolayer of chemisorptions capacity is strongly corresponds relate to the quantity of number of accessible active sites of adsorbent. The efficient utilization of the adsorption sites correspond to the specific surface area of adsorbent.[38, 39, 40, 41, 42] Specific surface area is a property of solids which is the total surface area of a material per unite of mass, solid or bulk volume, or cross-sectional area. Generally, the amount adsorbed is only a fraction of a

monolayer. Therefore, to adsorb a substantial amount of material, the adsorbent must have a large specific surface area. The specific surface area of typical adsorbents ranges from 0.1 to 1.0 km^2/kg, i.e. the area of a football field in a kg of adsorbent. Some common examples of adsorption are the carbon canister to adsorb gasoline vapor in automobile fuel tanks, silica gel packets to adsorb moisture from packaged electronic or optical equipment, and carbon "filter" to deodorize drinking water. [42, 43] The specific surface area can be measured by N_2 adsorption using the BET isotherm. This has the advantage of measuring the surface of fine structures and deep texture on the particles. However, the results can differ markedly depending on the substance adsorbed.

2.4.2 Dispersion vs. Solubilization

Basically, "dispersion" and "solubilization" are different phenomena.[44, 45, 46, 47, 48] In statistics, dispersion denotes how stretched or squeezed a distribution is. In dispersion, it is possible to identify interfaces among components of different chemical nature or composition, as in the case of phase equilibra, whereas in solution the components are mixed at the molecular scale. Thus, the interface or better interphase plays a dominant role in the liquid-solid adsorption. The adsorbent with good dispersion could avoid agglomerating and bundling[44, 49, 50, 51], resulting in extending of the active surface for adsorption,[52, 53] therefore, more efficient utilization of the respective adsorption sites could be achieved in the sorbent.

Solubilization is a short form micellar solubilization, a term used in colloidal and surface chemistry. It is the process of incorporating the solubilizate into or onto the micelles. Materials with poor solubilization will always exist in the form of agglomerates, and this agglomeration can assist in avoiding significant increases in the turbidity of untreated water as well as in the separation of the material from the solution.[54, 55, 56, 57] In addition, color and turbidity are very important factors with regard to drinking water, and therefore the removal of turbidity from untreated water

is an important factor in water management. So an appropriate adsorbent in water management should also exhibits low solubilization and no color.

2.4.3 pH value

The initial solution pH is an important parameter in adsorption process, which affects the protonation or deprotonation of functional groups from the adsorbent surface and the distribution of adsorbate in aqueous solutions.[58, 59, 60, 61, 62] The pH-dependence of many heavy metal ions and radioactive nuclides adsorption had been studied extensively.[63, 64, 65, 66, 67]

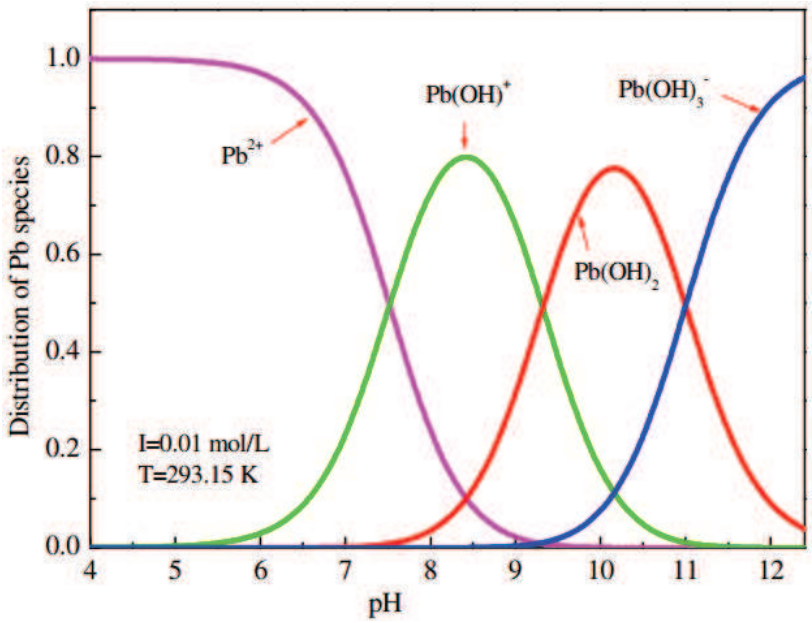

Fig. 2.3 Distribution of Pb(II) species as a function of pH based on the equilibrium constants.

As the change of solution pH, many acid or basic functional groups such as –OH, -COOH and -NH_2 will have proton transfer reaction in aqueous solution, resulting in the point of zero charge (pzc) of material.[68, 69, 70] The point of zero charge describes the condition when the electrical charge density on a surface is zero. Therefore, when the pH is equal to the pH_{pzc}value, the electrode potential of material is zero.[69] When the pH is lower than the pH_{pzc}value, the surface of material is positively charged,

which is not good for the adsorption of positively metal ions. However, when the pH >pH_{pzc}, the surface of material is negaticely charged, which benefits to absorb the positive metial ions.[32]

Changes in the solution pH can also affect the distribution of adsorbate species in solution. For example, the different hydrolysis constants ($logk_1$=6.48, $logk_2$=11.16, and $logk_3$=14.16) suggest that the Pb(II) species are present as Pb^{2+}, $Pb(OH)^{+}$, $Pb(OH)_2^0$, and $Pb(OH)^{3-}$ at different pH values, see Fig. 2.3.[32, 71] At pH < 7, the main species is Pb^{2+}, while the main species present in the pH range 7-10 are $Pb(OH)^{+}$ and $Pb(OH)_2^0$. From the precipitation constant of $Pb(OH)_2$(s) (1.2×10^{-15}), at a Pb(II) initioal concentration of 120 mg/L, Pb(II) ions begin to form a precipitation at pH ~8.1.[71, 72] Therefore, in the suspension of the mixture solution at pH>8.1, it is difficult to avoid the precipitation of $Pb(OH)_2$. In addition, according to the solubility equilibrium equations:

$$Pb(OH)_2 \rightleftharpoons Pb(OH)^{+} + OH^{-} \quad (2\text{-}4)$$

$$Pb(OH)^{+} \rightleftharpoons Pb^{2+} + OH^{-} \quad (2\text{-}5)$$

The equilibrium of the reactions will be shifted with the adsorption reaction and the pH value. So the change of pH value plays an important part in the adsoriton process.

2.4.4 Ionic strength

The ionic strength of a solution is a measure of the concentration of ions in that solution. Ionic compounds, when dissolved in water, dissociate into ions.[73, 74] The total electrolyte concentration in solution will affect important properties such as the dissociation or the solubility of different salts. One of the main characteristics of a solution with dissolved ions is the ionic strength. The ionic strength can influence the double electrode layer thickness and interface potential of solid particles, thereby can affect the binding of the adsorbed species. Special, outer-sphere surface coordination is more impressionable to ionic strength variations than inner-sphere surface

coordination as the background electrolyte ions are placed in the same plan for our-sphere surface complexes.[37, 73]

The ionic strength (*I*) of the solution was calculatedby the following equation [75]:

$$I = \frac{1}{2}\sum_{i=1}^{n} c_i z_i^2 \tag{2-6}$$

where ci is the ionic concentration (M, mol/L), zi is the charge of the ion and the summation is used to account for all ions in the solution.

2.4.5 Other factors

Except the influence factors mented above, other factors such as temperature, pore size, foreign ions, and color of the adsorbent' solution are all relate to the success of the adsorption process.

2.5 Adsorption isotherms

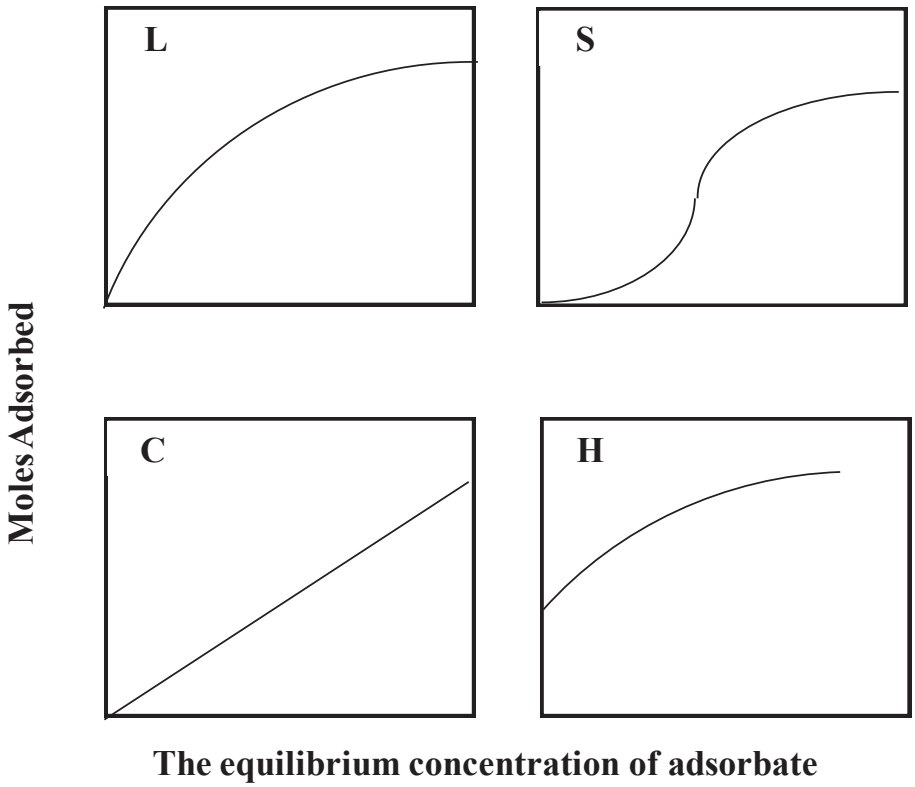

Fig. 2.4 Forms of experimental adsorption isotherms.

Adsorption is usually described through isotherms, that is, the amount of adsorbate on the adsorbent as a function of its pressure or concentration at constant temperature. The quantity adsorbed is nearly always normalized by the mass of the adsorbent to allow comparison of different materials. To date, 15 different isotherm models were developed. The classification of experimental adsorption isotherms are shown in Fig.2.4. Langmuir and Freundlich isotherm models are the most widely used ones among the abundant isotherm models, to fit the experimental data to understand the adsorption mechanism.[20, 32, 37]

2.5.1 Freundlich adsorption isotherm

The so-called Freundlich empirical equation was firstly proposed by van Bemmelen in 1888.[76, 77] The first mathematical fit to an isotherm was published by Freundlich and Küster (1894) and is a purely empirical formula for gaseous adsorbates.[78, 79, 80] It is known in literature as Freundlich equation, because Freundlich assigned great importance to it and popularized its use. The Freundlich equation is:

$$\frac{x}{m} = kC^{\frac{1}{n}} \qquad (2\text{-}7)$$

whereχ is the quantity of adsorbate adsorbed in moles, m is the mass of the adsorbent, C is the concentration of adsorbate. k and n are empirical constants for each adsorbent-adsorbate pair at a given temperature. As the temperature increases, the constants k and n change to reflect the empirical observation that the quantity adsorbed rises more slowly and higher concentration are required to saturate the surface.

2.5.2 Langmuir adsorption isotherm

In 1916, Irving Langmuir hypothesized that a given surface has a certain number of equivalent sites that a species can “stick”, eigher by physisorption or chemisorptions.[81] Based on the theory, he derived Langmuir equation and presented his model for the adsorption of species onto simple surfaces. Langmuir, for the first time, introduced a clear concept of the monomolecular adsorption on energetically homogeneous surface. The statement proposed by

Langmuir was applied to chemisorptions and with some restrictions to physical adsorption.[82] In 1932, Langmuir was awarded the Nobel Prize in chemistry for his discoveries and researches in the realm of surface chemistry. Inherent within this model, the following basic assumptions of Langmuir adsorption isotherm are valid specifically for the simplest case[83]:

1) The surface of the adsorbant is in contact with a solution containing an adsorbate which is strongly attracted to the surface.

2) The surface has a specific number of sites where the solution molecules can be adsorbed.

3) The adsorption involves the attachment of only one layer of molecules to the surface, i. e. monolayer adsorption.

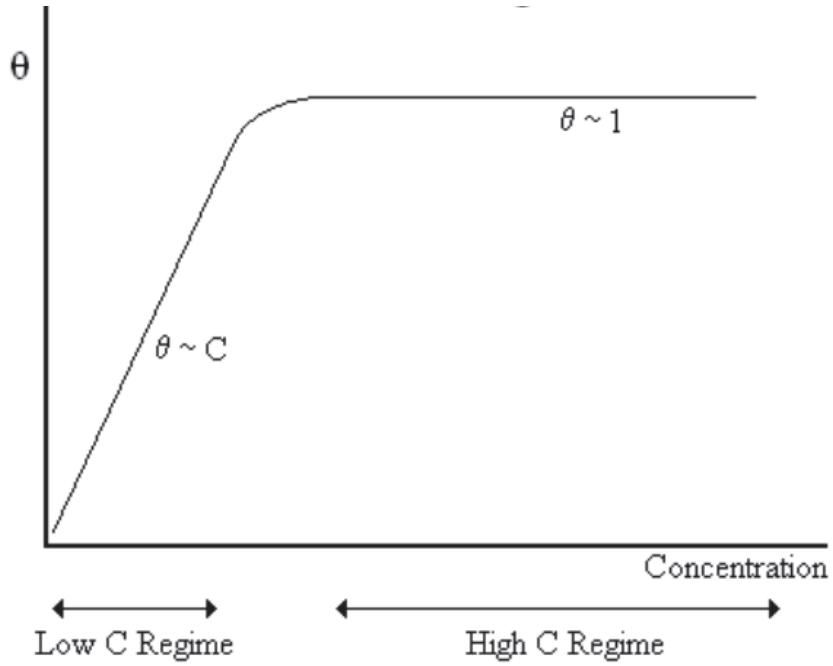

Fig. 2.5 The general form of the Langmuir isotherm.

The chemical reaction for monolayer adsorption can be represented as follows:

$$A(g) + B(s) \underset{desorption}{\overset{adsorpton}{\rightleftharpoons}} AB \qquad (2\text{-}8)$$

where A (g) is the adsorbate, B(s) is adsorbant and AB represents a solute molecule bound to a surface site on B. The equilibrium constant $K_{ads}$for this reacton is given by:

$$K_{ads} = \frac{[AB]}{[A][B]} \tag{2-9}$$

where [A] denotes the concentration of A, while the other two terms [B] and [AB] are two-dimensional analogs of concentration and are expressed in unites such as mol/cm^2. The complete form of the Langmuir isotherm considers in terms of surface converage θ, which is defined as the fraction of the adsorption sites occupied. Given these definitions, we can rewrite the term $\frac{[AB]}{[B]}$ as

$$\frac{[AB]}{[B]} = \frac{\theta}{1-\theta} \tag{2-10}$$

Therefore, the equilibrium constant K_{ads} can be rewritedas :

$$K_{ads} = \frac{\theta}{[A](1-\theta)} \tag{2-8}$$

Rearranging, we obtain the final form of the Langmuir adsorption isotherm (Fig.2.5):

$$\theta = \frac{K_{ads}[A]}{1+K_{ads}[A]} \tag{2-9}$$

Reference:

[1]. Chang, C. H.; Franses, E. I.,adsorption dynamics of surfactants at the air/water interface-A critical review of mathematical models, data, and mechanisms. *Colloid Surf. A-Physicochem. Eng. Asp.* **1995,** *100*, 1-45.

[2]. Volkov, A. G., Liquid-Liquid Interfaces. In *Theory and Methods*, Deamer, D. W., Ed. CRC Press: Boca Raton, New York, 1996.

[3]. Volkov, A. G., Liquid-liquid interfaces : theory and methods. Deamer, D. W., Ed. CRC Press: Boca Raton, New York :, 1996.

[4]. Crawford, S.; Lim, S. K.; Gradečak, S.,Fundamental Insights into Nanowire Diameter Modulation and the Liquid/Solid Interface. *Nano Letters* **2013,** *13* (1), 226-232.

[5]. Harris, B. L.,Adsorption. *Industrial & Engineering Chemistry* **1952,** *44* (1), 30-38.

[6]. Renneckar, S.; Zhou, Y.,Nanoscale Coatings on Wood: Polyelectrolyte Adsorption and Layer-by-Layer Assembled Film Formation. *ACS Appl Mater Interfaces* **2009,** *1* (3), 559-566.

[7]. Dabrowski, A.,Adsorption from theory to practice. *Adv. Colloid Interface Sci.* **2001,** *93* (1-3), 135-224.

[8]. Kudish, A. T.; Eirich, F. R., Adsorption of Gelatin at Solid-Liquid Interfaces. In *Proteins at Interfaces*, American Chemical Society: 1987; Vol. 343, pp 261-277.

[9]. King, C. V.,Reaction Rates at Solid—Liquid Interfaces. *Journal of the American Chemical Society* **1935,** *57* (5), 828-831.

[10]. Jordens, S.; Riley, E. E.; Usov, I.; Isa, L.; Olmsted, P. D.; Mezzenga, R.,Adsorption at Liquid Interfaces Induces Amyloid Fibril Bending and Ring Formation. *ACS Nano* **2014,** *8* (11), 11071-11079.

[11]. Hu, J.; Shao, D. D.; Chen, C. L.; Sheng, G. D.; Li, J. X.; Wang, X. K.; Nagatsu, M.,Plasma-induced grafting of cyclodextrin onto multiwall carbon nanotube/iron oxides for adsorbent application. *J. Phys. Chem. B* **2010,** *114* (20), 6779-6785.

[12]. Hu, J.; Zhang, C. X.; Cong, J.; Toyoda, H.; Nagatsu, M.; Meng, Y. D.,Plasma-grafted alkaline anion-exchange membranes based on polyvinyl chloride for potential application in direct alcohol fuel cell. *Journal of Power Sources* **2011,** *196* (10), 4483-4490.

[13]. Hu, R.; Shao, D.; Wang, X., Graphene oxide/polypyrrole composites for highly selective enrichment of U(vi) from aqueous solutions. In *Polymer Chemistry*, The Royal Society of Chemistry: 2014; Vol. 5, pp 6207-6215.

[14]. Shao, D.; Hou, G.; Li, J.; Wen, T.; Ren, X.; Wang, X.,PANI/GO as a super adsorbent for the selective adsorption of uranium(VI). *Chemical Engineering Journal* **2014,** *255* (0), 604-612.

[15]. Shao, D. D.; Ren, X. M.; Hu, J.; Chen, Y. X.; Wang, X. K.,Preconcentration of Pb^{2+} from aqueous solution using poly(acrylamide) and poly(N,N-dimethylacrylamide) grafted multiwalled carbon nanotubes. *Colloids Surf., A* **2010,** *360* (1-3), 74-84.

[16]. Anastasiadis, S. H.; Gancarz, I.; Koberstein, J. T.,Interfacial tension of immiscible polymer blends: temperature and molecular weight dependence. *Macromolecules* **1988,** *21* (10), 2980-2987.

[17]. Glezakou, V. A.; deJong, W. A.,Cluster-models for uranyl(VI) adsorption on alpha-alumina. *The journal of physical chemistry. A* **2011,** *115* (7), 1257-1263.

[18]. Lan, J. H. C., D. P.; Wang, W. C.; Smit, B. ,Doping of alkali, alkaline-earth, and transition metals in covalent-organic frameworks for enhancing CO_2 capture by first-principles calculations and molecular simulations. *ACS Nano* **2010,** *4* (7), 4225-4237.

[19]. Sun, Y.; Chen, C.; Shao, D.; Li, J.; Tan, X.; Zhao, G.; Yang, S.; Wang, X.,Enhanced adsorption of ionizable aromatic compounds on humic acid-coated carbonaceous adsorbents. *RSC Adv.* **2012,** *2* (27), 10359-10364.

[20]. Yang, S.; Chen, C.; Chen, Y.; Li, J.; Wang, D.; Wang, X.; Hu, W.,Competitive Adsorption of Pb^{II}, Ni^{II}, and Sr^{II} Ions on Graphene Oxides: A Combined Experimental and Theoretical Study. *ChemPlusChem* **2014,** *80* (3), 480-484.

[21]. Yang, S.; Ding, C.; Cheng, W.; Jin, Z.; Sun, Y.,Effect of microbes on Ni(II) diffusion onto sepiolite. *J. Mol. Liq.* **2015,** *204*, 170-175.

[22]. Sun, Y.; Yang, S.; Chen, Y.; Ding, C.; Cheng, W.; Wang, X.,Adsorption and Desorption of U(VI) on Functionalized Graphene Oxides: A Combined Experimental and Theoretical Study. *Environ. Sci. Technol.* **2015,** *49* (7), 4255-4262.

[23]. Acik, M.; Lee, G.; Mattevi, C.; Chhowalla, M.; Cho, K.; Chabal, Y. J.,Unusual infrared-absorption mechanism in thermally reduced graphene oxide. *Nat Mater* **2010,** *9* (10), 840-845.

[24]. Shaviv, E.; Schubert, O.; Alves-Santos, M.; Goldoni, G.; Di Felice, R.; Vallée, F.; Del Fatti, N.; Banin, U.; Sönnichsen, C.,Absorption Properties of Metal–Semiconductor Hybrid Nanoparticles. *ACS Nano* **2011,** *5* (6), 4712-4719.

[25]. Xu, N.; Braida, W.; Christodoulatos, C.; Chen, J. P.,A Review of Molybdenum Adsorption in Soils/Bed Sediments: Speciation, Mechanism, and Model Applications. *Soil. Sediment. Contam.* **2013,** *22* (8), 912-929.

[26]. Paria, S.; Khilar, K. C.,A review on experimental studies of surfactant adsorption at the hydrophilic solid-water interface. *Adv. Colloid Interface Sci.* **2004,** *110* (3), 75-95.

[27]. Cuomo, J.; Appendino, G.; Dern, A. S.; Schneider, E.; McKinnon, T. P.; Brown, M. J.; Togni, S.; Dixon, B. M.,Comparative Absorption of a Standardized Curcuminoid Mixture and Its Lecithin Formulation. *Journal of Natural Products* **2011,** *74* (4), 664-669.

[28]. Giblin, J.; Kuno, M.,Nanostructure Absorption: A Comparative Study of Nanowire and Colloidal Quantum Dot Absorption Cross Sections. *The Journal of Physical Chemistry Letters* **2010,** *1* (23), 3340-3348.

[29]. Hargis, L. G.; Howell, J. A.; Sutton, R. E.,Ultraviolet and Light Absorption Spectrometry. *Analytical Chemistry* **1996,** *68* (12), 169-184.

[30]. Howell, J. A.; Sutton, R. E.,Ultraviolet and Absorption Light Spectrometry. *Analytical Chemistry* **1998,** *70* (12), 107-118.

[31]. Yang, S. B.; Wu, X. L.; Chen, C. L.; Dong, H. L.; Hu, W. P.; Wang, X. K.,Spherical α-$Ni(OH)_2$ nanoarchitecture grown on graphene as advanced electrochemical pseudocapacitor materials. *Chem. Commun.* **2012,** *48* (22), 2773-2775.

[32]. Yang, S. B.; Hu, J.; Chen, C. L.; Shao, D. D.; Wang, X. K.,Mutual effects of Pb(II) and humic acid adsorption on multiwalled carbon nanotubes/polyacrylamide composites from aqueous solutions. *Environ. Sci. Technol.* **2011,** *45* (8), 3621-3627.

[33]. Yang, D.; Sarina, S.; Zhu, H.; Liu, H.; Zheng, Z.; Xie, M.; Smith, S. V.; Komarneni, S.,Capture of radioactive cesium and iodide ions from water by using titanate nanofibers and nanotubes. *Angew. Chem. Int. Ed.* **2011,** *50* (45), 10594-10598.

[34]. Ding, N.; Kanatzidis, M. G.,Selective incarceration of caesium ions by Venus flytrap action of a flexible framework sulfide. *Nat. Chem.* **2010,** *2* (3), 187-191.

[35]. Clearfield, A.,Ion-exchange materials seizing the caesium. *Nat. Chem.* **2010,** *2* (3), 161-162.

[36]. Celestian, A. J.; Kubicki, J. D.; Hanson, J.; Clearfield, A.; Parise, J. B.,The mechanism responsible for extraordinary Cs ion selectivity in crystalline silicotitanate. *J. Am. Chem. Soc.* **2008,** *130* (35), 11689-11694.

[37]. Yang, S. B.; Shao, D. D.; Wang, X. K.; Nagatsu, M.,Localized in situ polymerization on carbon nanotube surfaces for stabilized carbon nanotube dispersions and application for cobalt(II) removal. *RSC Adv.* **2014,** *4* (10), 4856-4863.

[38]. Tiwari, D.; Lalhmunsiama; Choi, S. I.; Lee, S. M.,Activated Sericite: An Efficient and Effective Natural Clay Material for Attenuation of Cesium from Aquatic Environment. *Pedosphere* **2014,** *24* (6), 731-742.

[39]. Karimi, L.; Salem, A.,Analysis of bentonite specific surface area by kinetic model during activation process in presence of sodium carbonate. *Microporous and Mesoporous Materials* **2011,** *141* (1–3), 81-87.

[40]. Wei, Z.; Kowalska, E.; Ohtani, B.,Influence of post-treatment operations on structural properties and photocatalytic activity of octahedral anatase titania particles prepared by an ultrasonication-hydrothermal reaction. *Molecules* **2014,** *19* (12), 19573-19587.

[41]. Kaufhold, S.; Dohrmann, R.; Klinkenberg, M.; Siegesmund, S.; Ufer, K.,N_2-BET specific surface area of bentonites. *J. Colloid Interface Sci.* **2010,** *349* (1), 275-282.

[42]. Jandak, J.,Values of specific surface area in agricultural soils in the region of southwestern Moravia. *Rostl. Vyroba* **1996,** *42* (1), 23-28.

[43]. Volynskii, A. L.; Grokhovskaya, T. E.; Kulebyakina, A. I.; Bakeev, N. F.,Specifics of change in the surface area of amorphous poly(vinyl chloride) during its inelastic deformation. *Polym. Sci. Ser. A* **2007,** *49* (1), 35-41.

[44]. Premkumar, T.; Mezzenga, R.; Geckeler, K. E.,Carbon nanotubes in the liquid phase: addressing the issue of dispersion. *Small* **2012,** *8* (9), 1299-1313.

[45]. Paredes, J. I.; Villar-Rodil, S.; Martínez-Alonso, A.; Tascón, J. M. D.,Graphene Oxide Dispersions in Organic Solvents. *Langmuir* **2008,** *24* (19), 10560-10564.

[46]. McBride, M. B.,A critique of diffuse double layer models applied to colloid and surface chemistry. *Clay Clay Min.* **1997,** *45* (4), 598-608.

[47]. Uddin, A. J.; Watanabe, A.; Gotoh, Y.; Saito, T.; Yumura, M.,Green tea-aided dispersion of single-walled carbon nanotubes in non-water media: Application for extraordinary reinforcement of nanocomposite fibers. *Text. Res. J.* **2012,** *82* (9), 911-919.

[48]. Locke, D.; Koreen, I. V.; Harris, A. L.,Isoelectric points and post-translational modifications of connexin26 and connexin32. *Faseb J.* **2006,** *20* (8), 1221-+.

[49]. Lou, X.; Detrembleur, C.; Pagnoulle, C.; Jérôme, R.; Bocharova, V.; Kiriy, A.; Stamm, M.,Surface Modification of Multiwalled Carbon Nanotubes by Poly(2-vinylpyridine):

Dispersion, Selective Deposition, and Decoration of the Nanotubes. *Adv. Mater.* **2004,** *16* (23-24), 2123-2127.

[50]. Chen, C. L.; Ogino, A.; Wang, X. K.; Nagatsu, M.,Plasma treatment of multiwall carbon nanotubes for dispersion improvement in water. *Appl. Phys. Lett.* **2010,** *96* (13), 131504-131503.

[51]. Das, S.; Wajid, A. S.; Shelburne, J. L.; Liao, Y. C.; Green, M. J.,Localized in situ polymerization on graphene surfaces for stabilized graphene dispersions. *ACS Appl. Mater. Interfaces* **2011,** *3* (6), 1844-1851.

[52]. Rao, G. P.; Lu, C.; Su, F.,Sorption of divalent metal ions from aqueous solution by carbon nanotubes: A review. *Sep. Purif Technol.* **2007,** *58* (1), 224-231.

[53]. Ren, X. M.; Chen, C. L.; Nagatsu, M.; Wang, X. K.,Carbon nanotubes as adsorbents in environmental pollution management: A review. *Chem. Eng. J.* **2011,** *170* (2-3), 395-410.

[54]. Klevens, H. B.,Solubilization. *Chemical Reviews* **1950,** *47* (1), 1-74.

[55]. Merrill, R. C.; McBain, J. W.,Studies on Solubilization. *The Journal of Physical Chemistry* **1942,** *46* (1), 10-19.

[56]. Osipow, L.,Solubilization and related phenomena. *Journal of Chemical Education* **1956,** *33* (4), 190.

[57]. Prajapati, R. N.; Tekade, R. K.; Gupta, U.; Gajbhiye, V.; Jain, N. K.,Dendimer-Mediated Solubilization, Formulation Development and in Vitro−in Vivo Assessment of Piroxicam. *Molecular Pharmaceutics* **2009,** *6* (3), 940-950.

[58]. Wang, Q.; Chen, L.; Sun, Y. B.,Removal of radiocobalt from aqueous solution by oxidized MWCNT. *J. Radioanal. Nucl. Chem.* **2012,** *291* (3), 787-795.

[59]. Liu, M. C.; Chen, C. L.; Hu, J.; Wu, X. L.; Wang, X. K.,Synthesis of magnetite/graphene oxide composite and application for cobalt(II) removal. *J. Phys. Chem. C* **2011,** *115* (51), 25234-25240.

[60]. Zhang, S. W.; Niu, H. H.; Guo, Z. Q.; Chen, Z. S.; Wang, H. P.; Xu, J. Z.,Impact of environmental conditions on the sorption behavior of radiocobalt in TiO_2/eggshell suspensions. *J. Radioanal. Nucl. Chem.* **2011,** *289* (2), 479-487.

[61]. Guo, Z. Q.; Xu, D. P.; Zhao, D. L.; Zhang, S. W.; Xu, J. Z.,Influence of pH, ionic strength, foreign ions and FA on adsorption of radiocobalt on goethite. *J. Radioanal. Nucl. Chem.* **2011,** *287* (2), 505-512.

[62]. Dong, W. M.; Wang, X. K.; Shen, Y.; Zhao, X. D.; Tao, Z. Y.,Sorption of radiocobalt on bentonite and kaolinite. *J. Radioanal. Nucl. Chem.* **2000,** *245* (2), 431-434.

[63]. Mesquita, M. E.; Silva, J.,Preliminary study of pH effect in the application of Langmuir and Freundlich isotherms to Cu-Zn competitive adsorption. *Geoderma* **2002,** *106* (3-4), 219-234.

[64]. Yu, X. Y.; Luo, T.; Zhang, Y. X.; Jia, Y.; Zhu, B. J.; Fu, X. C.; Liu, J. H.; Huang, X. J.,Adsorption of lead(II) on O_2-plasma-oxidized multiwalled carbon nanotubes: thermodynamics, kinetics, and desorption. *ACS Appl. Mater. Interfaces* **2011,** *3* (7), 2585-2593.

[65]. Dastgheib, S. A.; Rockstraw, D. A.,A model for the adsorption of single metal ion solutes in aqueous solution onto activated carbon produced from pecan shells. *Carbon* **2002,** *40* (11), 1843-1851.

[66]. Ferro-García, M. A.; Rivera-Utrilla, J.; Rodríguez-Gordillo, J.; Bautista-Toledo, I.,Adsorption of zinc, cadmium, and copper on activated carbons obtained from agricultural by-products. *Carbon* **1988,** *26* (3), 363-373.

[67]. Boddu, V. M.; Abburi, K.; Talbott, J. L.; Smith, E. D.; Haasch, R.,Removal of arsenic(III) and arsenic(V) from aqueous medium using chitosan-coated biosorbent. *Water Res.* **2008,** *42* (3), 633-642.

[68]. Preocanin, T.; Kallay, N.,Point of zero charge and surface charge density of TiO2 in aqueous electrolyte solution as obtained by potentiometric mass titration. *Croat. Chem. Acta* **2006,** *79* (1), 95-106.

[69]. Appel, C.; Ma, L. Q.; Rhue, R. D.; Kennelley, E.,Point of zero charge determination in soils and minerals via traditional methods and detection of electroacoustic mobility. *Geoderma* **2003,** *113* (1-2), 77-93.

[70]. Zuyi, T.; Taiwei, C.,Points of zero charge and potentiometric titrations. *Adsorpt. Sci. Technol.* **2003,** *21* (6), 607-616.

[71]. Zhao, G. X.; Ren, X. M.; Gao, X.; Tan, X. L.; Li, J. X.; Chen, C. L.; Huang, Y. Y.; Wang, X. K.,Removal of Pb(II) ions from aqueous solutions on few-layered graphene oxide nanosheets. *Dalton Trans.* **2011,** *40* (41), 10945-10952.

[72]. Xu, D.; Tan, X.; Chen, C.; Wang, X.,Removal of Pb(II) from aqueous solution by oxidized multiwalled carbon nanotubes. *J. Hazard. Mater.* **2008,** *154* (1-3), 407-416.

[73]. Zhao, D.; Yang, S.; Chen, S.; Guo, Z.; Yang, X.,Effect of pH, ionic strength and humic substances on the adsorption of Uranium (VI) onto Na-rectorite. *Journal of Radioanalytical and Nuclear Chemistry* **2011,** *287* (2), 557-565.

[74]. Liu, C. X.; Zachara, J. M.; Smith, S. C.,A cation exchange model to describe Cs^+ sorption at high ionic strength in subsurface sediments at Hanford site, USA. *J. Contam. Hydrol.* **2004,** *68* (3-4), 217-238.

[75]. Solomon, T.,The Definition and Unit of Ionic Strength. *J. Chem. Educ.* **2001,** *78* (12), 1691.

[76]. Freundlich, H.,Adsorptionstechnik. By Franz Krzil. *The Journal of Physical Chemistry* **1935,** *40* (6), 857-858.

[77]. Professor Herbert Freundlich, 1880. *Journal of Chemical Education* **1934,** *11* (5), 257.

[78]. Midgley, T.,The Chemistry of Rubber (Freundlich, H.). *Journal of Chemical Education* **1938,** *15* (2), 99.

[79]. Rogers, W.; Sclar, M.,A Modification of the Freundlich Adsorption Isotherm. *The Journal of Physical Chemistry* **1931,** *36* (8), 2284-2291.

[80]. Haring, M. M.,Colloid and Capillary Chemistry (Freundlich, Herbert). *Journal of Chemical Education* **1926,** *3* (12), 1454.

[81]. Dunicz, B. L.,Surface area of activated charcoal by Langmuir adsorption isotherm. *Journal of Chemical Education* **1961,** *38* (7), 357.

[82]. Langmuir, I.,Surface Chemistry. *Chemical Reviews* **1933,** *13* (2), 147-191.

[83]. Bird, P. G.,A derivation of Langmuir's adsorption isotherm. *Journal of Chemical Education* **1933,** *10* (4), 237.

CHAPTER 3 Plasma Surface Modifications

In this chapter, the plasma physics and radio frequency charge are introduced briefly. Several examples about the plasma science in space science and astrophysics are listed. This chapter is mainly related to the theory of plasma modification in nanomaterial. But, as always, the idears and concepts developed in the field proved to be of a wide and interest for the theory. In this thesis too, we only deal with the plasma-induced process, one of the methods about the plasma surface modification.

3.1 What is plasma?

Plasma is matter heated beyond its gaseous state, heated to a temperature so high that atoms are stripped of at least one electron in their ourter shells, so that what remains are positive ions in a sea of free electrons.[1, 2] These components have many of the properties of a normal gas.[3] For example they can be describled by their particle density and temperature. However, a plasma has two characteristic properties. Firstly, the electric charge density of the two species is so large that any substantial separation would lead to a very restoring force, and as a consequence that ion and electron charge densities in a plasm are almost equal. The second property is the ability to carry a current as result of a relative drift between the ions and electrons.

In the ionization process, not all the atoms have to be ionized: the cooler plasmas used in plasma processing are only 1-10% ionized, with the rest of the gas remaining as neutral atoms or molecules. The extent of ionization depends on the power source and determines the temperature of the plasma.[4]

Outside the earth in the ionosphere or outer space, almost everything is in the plasma state. In fact, what we see in the sky is visible only because plasmas emit light. Thus, the most obvious application of plasma science[5] is in space science and astrophysics.[5, 6, 7, 8] Here are some examples (Fig. 3.1):

1) Aurora borealis
2) Solar wind
3) Magnetospheres of earth and Jupiter

4) Solar corona and sunspots
5) Comet tails
6) Gaseous nebulae
7) Stellar interiors and atmospheres
8) Galactic arms
9) Quasars, pulsars, novas, and black holes

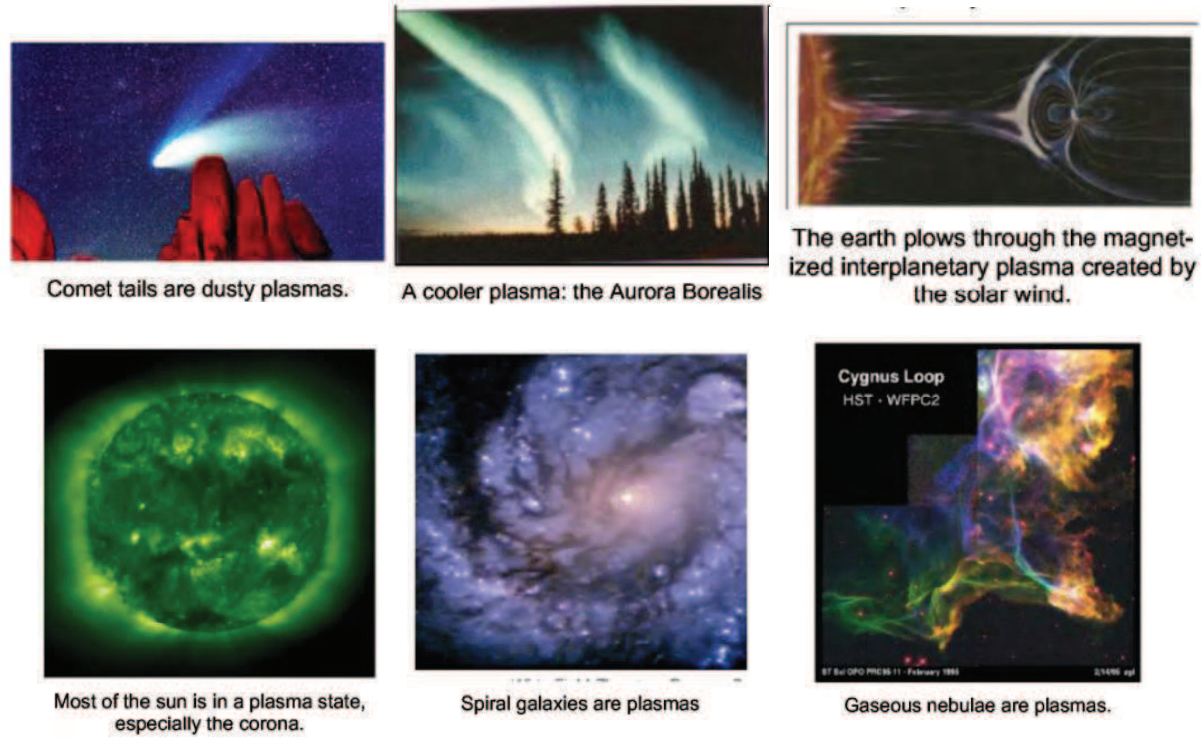

Fig. 3.1 The plasma in space sicence and astrophysics.

3.2 Radio frequency discharge

To ionize and heat a plasma, electrical power is applied either at radio frequency (RF) or at a microwace frequency.[9, 10] The vast majority of sources use the industrially assigned frequency is 13.56 MHz. Some work at a harmonic or subharmonic of this, and some experimental sources run at frequencies higher or lower than this range. RF source are usually driven by a solid-state power amplifier with a buit-in oscillator to generate the signal.[9, 10]

Regarding their structure, the radio frequency sources can work with a high or low power supply. It influences the properties of the plasma and thus its potensial applications. The impedance matching can be eigher inductive (high powered discharges) or capacitive. The RF discharge device used in this work is shown in Fig. 3.2. More details about the experimental device and conditions are described in the following chapters.[11]

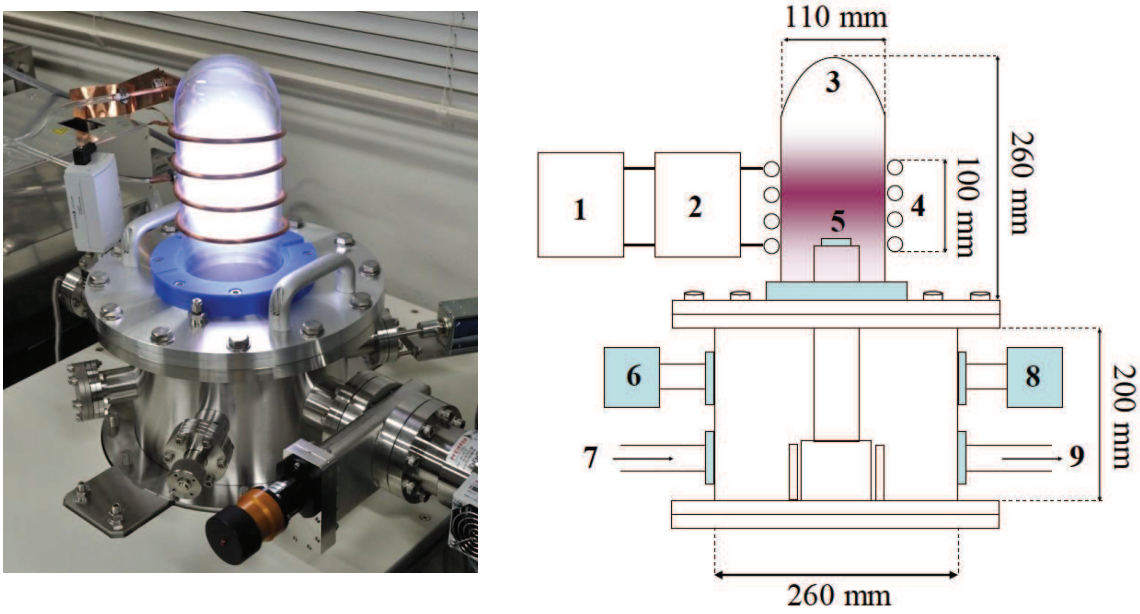

Fig.3.2 Schematic view of experimental setup of inductively coupled RF plasma. (1) RF powers supply, (2) Matching Box, (3) Glass jar, (4) Cupper coil connected to the water cooling system, (5) Sample place, (6) Pressure gauge, (7) Gas inlet, (8) Leaking valve, (9) Gas outlet connected to the turbo and rotary pump.

3.3 Plasma surface modification

Plasma treatment is a useful means of surface modification, since it is solvent-free, time-efficient, versatile, and eco-friendly[12, 13, 14]. Plasma treatment utilizes gases such as Ar, O_2, N_2, NH_3, CF_4, and H_2O to insert or substitute functional groups onto the substrate or to creat radicals, electrons, ions, and VUV/UV light to strongly interact with the surfaces of materials and create active sites for the binding of functional groups.[10, 15, 16, 17, 18, 19] A reasonable set of steps for plasma surface interaction is as follows (Fig.3.3).

Surface modification processes of low temperature plasma were first developed in the 1960s.[20, 21, 22] They have been widely recognized and several successful applications have emerged in the last 20 years. For surface modification application, low temperature plasma has many particulary appreciated advantages for instance, free radicals, charged particles, especially, energetic electrons. Researches have been extended to include the surface modification of carbon nanotubes (CNTs) by plasma treatment to improve its physical and chemical properties.[13, 15, 23, 24, 25] The CNTscan be activated easily in plasma treatment process[25]and without altering the material bulk properties.[25, 26, 27, 28] In our earlier work, we confirmed that a radio frequency Ar plasma is able to split C-C bonds to increase the reactivity of the surfaces of CNTs as the result of Ar ion bombardment [23, 24, 26, 29].

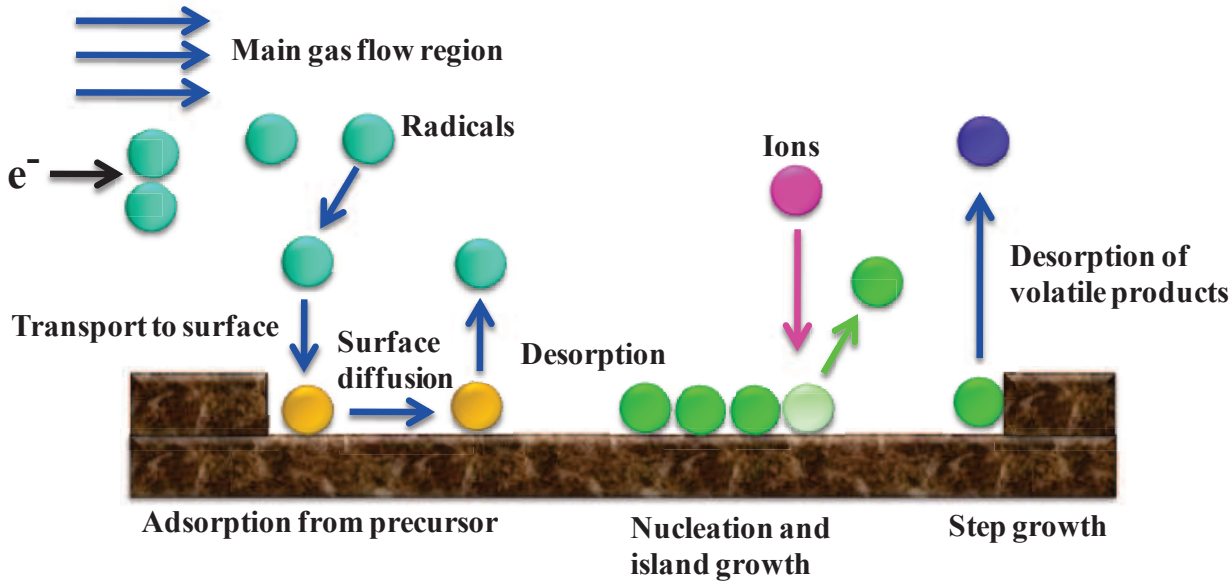

Fig.3.3 Schematic diagram of plasma surface interaction.

3.4 Plasma-induced grafting method

Plasma treatment is an effective tool for the surface modification with amine, carboxy, hydroxyl, and aldehyde groups, because of its compatibility with well-established chemical reactions for grafting of organic materials such as chitosan, carboxymethyl cellulose, cysteine, and acrylamide.[8, 30] This process through plasma treatment to graft the organic material on the substrate called plasma-induced method. Plasma-induced grafting technique is an efficient

method in the field of surface modifications.[12, 13, 14] It considered being a good way to enhance the chemical functionality of material. This technique always consistes of two-step successive processes: surface activation of substrate and organic material grafting process. This plasma-induced method can provide a wide range of different functional groups depending on the grafting material and the plasma discharge parameters, such as power, gas species, reaction time, and operating pressure.The research on improving adsorption capacity of materials by plasma-induced grafting technique has profound significance in environmental pollution management.[13, 23, 31]

We have used the plasma-induced method to decorate poly (N,N-dimethylacrylamide) (PNDA) on the surface of CNTs to synthesize the MWCNT/PNDA composites. The composite shows excellent dispersion property and high-efficient properties in the preconcentration and separation of Co(II) ions from aqueous solutions.[29] The proposed mechanisms of N_2 plasma induced grafting PNDA on MWCNTs are shown in Fig. 3.4.

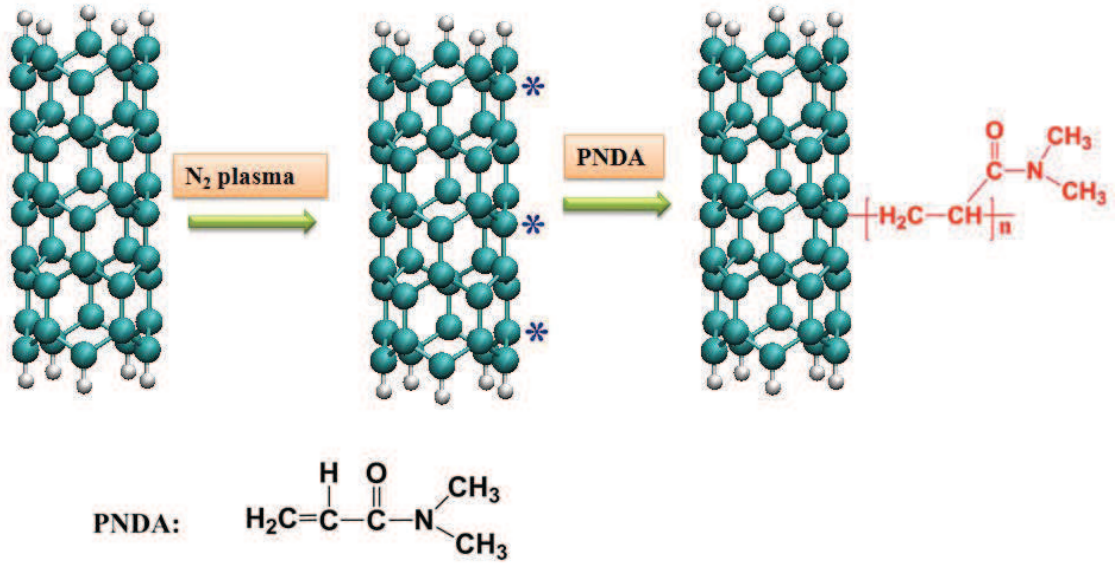

Fig.3.4 The synthesis route of MWCNT/PNDA composites by plasma-induced grafting route method.

Reference:

[1]. Tendero, C.; Tixier, C.; Tristant, P.; Desmaison, J.; Leprince, P.,Atmospheric pressure plasmas: A review. *Spectrochimica Acta Part B: Atomic Spectroscopy* **2006,** *61* (1), 2-30.

[2]. Schutze, A.; Jeong, J. Y.; Babayan, S. E.; Park, J.; Selwyn, G. S.; Hicks, R. F.,The atmospheric-pressure plasma jet: A review and comparison to other plasma sources. *IEEE Trans. Plasma Sci.* **1998,** *26* (6), 1685-1694.

[3]. Hume, D. N.,Techniques and Applications of Plasma Chemistry (Hollahan, John R.; Bell, Alexis T., eds.). *Journal of Chemical Education* **1975,** *52* (12), A564.

[4]. J. A, M.; D. W, H., Plasma Etching. In *Introduction to Microlithography*, AMERICAN CHEMICAL SOCIETY: 1983; Vol. 219, pp 215-285.

[5]. Wilson, E.,ASTROPHYSICS Spacecraft detects waves that could heat sun's corona, accelerate solar wind. *Chemical & Engineering News Archive* **2007,** *85* (50), 9.

[6]. Night Light, Errant Spoons. *Chemical & Engineering News Archive* **2013,** *91* (7), 72.

[7]. Katzenstein, W.; Apt, J.,Air Emissions Due To Wind And Solar Power. *Environ Sci Technol* **2009,** *43* (2), 253-258.

[8]. Wu, S.; Liu, X.; Yeung, A.; Yeung, K. W. K.; Kao, R. Y. T.; Wu, G.; Hu, T.; Xu, Z.; Chu, P. K.,Plasma-Modified Biomaterials for Self-Antimicrobial Applications. *ACS Appl Mater Interfaces* **2011,** *3* (8), 2851-2860.

[9]. Zhao, P.; Zheng, W.; Meng, Y. D.; Nagatsu, M.,Low Temperature Deposition of Cu Thin Film on Polyimide Using RF-driven Atmospheric Pressure Plasma Jet in Nitrogen Atmosphere. *J. Photopolym Sci. Technol.* **2013,** *26* (4), 549-554.

[10]. Saraswati, T. E.; Ogino, A.; Nagatsu, M.,Plasma-activated immobilization of biomolecules onto graphite-encapsulated magnetic nanoparticles. *Carbon* **2012,** *50* (3), 1253-1261.

[11]. Saraswati, T. E.; Matsuda, T.; Ogino, A.; Nagatsu, M.,Surface modification of graphite encapsulated iron nanoparticles by plasma processing. *Diamond Relat. Mater.* **2011,** *20* (3), 359-363.

[12]. Wei, Y.; Liu, Z. G.; Yu, X. Y.; Wang, L.; Liu, J. H.; Huang, X. J.,O_2-plasma oxidized multi-walled carbon nanotubes for Cd(II) and Pb(II) detection: Evidence of adsorption capacity for electrochemical sensing. *Electrochem. Commun.* **2011,** *13* (12), 1506-1509.

[13]. Chen, C. L.; Ogino, A.; Wang, X. K.; Nagatsu, M.,Plasma treatment of multiwall carbon nanotubes for dispersion improvement in water. *Appl. Phys. Lett.* **2010,** *96* (13), 131504-131503.

[14]. Shao, D. D.; Hu, J.; Wang, X. K.; Nagatsu, M.,Plasma induced grafting multiwall carbon nanotubes with chitosan for 4,4'-dichlorobiphenyl removal from aqueous solution. *Chem. Eng. J.* **2011,** *170* (2-3), 498-504.

[15]. Chen, C. L.; Ogino, A.; Wang, X. K.; Nagatsu, M.,Oxygen functionalization of multiwall carbon nanotubes by Ar/H_2O plasma treatment. *Diamond Relat. Mater.* **2011,** *20* (2), 153-156.

[16]. Ogino, A.; Noguchi, S.; Nagatsu, M., Low Temperature Plasma Treatment for Immobilization of Biomaterials on Polymer Surface. In *Inter Academia 2010: Global Research and Education*, Medvids, A., Ed. 2011; Vol. 222, pp 297-300.

[17]. Ogino, A.; Noguchi, S.; Nagatsu, M.,Effect of Plasma Pretreatment on Heparin Immobilization on Polymer Sheet. *J. Photopolym Sci. Technol.* **2009,** *22* (4), 461-466.

[18]. Nagatsu, M.; Saraswati, T. E.; Ogino, A., Surface Functionalization of Graphene Layer-Encapsulated Magnetic Nanoparticles by Inductively Coupled Plasma. In *Inter Academia 2010: Global Research and Education*, Medvids, A., Ed. 2011; Vol. 222, pp 134-137.

[19]. Ma, Q. A.; Saraswati, T. E.; Ogino, A.; Nagatsu, M.,Improvement of UV emission from highly crystalline ZnO nanoparticles by pulsed laser ablation under O-2/He glow discharge. *Appl. Phys. Lett.* **2011,** *98* (5).

[20]. Jiang, B.; Zheng, J.; Qiu, S.; Wu, M.; Zhang, Q.; Yan, Z.; Xue, Q.,Review on electrical discharge plasma technology for wastewater remediation. *Chemical Engineering Journal* **2014,** *236* (0), 348-368.

[21]. Zhong;, S.; Meng;, Y.; Ou, Q.,Plasma induced grafting of PMMA onto titanium dioxide powder. *Plasma Sci. Technol.* **2005,** *7* (4), 2955-2958.

[22]. McTaggart, F. K.,Plasma chemistry in electrical discharges. *Amsterdam: Elsevier* **1970**.

[23]. Chen, C. L.; Wang, X. K.; Nagatsu, M.,Europium adsorption on multiwall carbon nanotube/iron oxide magnetic composite in the presence of polyacrylic acid. *Environ. Sci. Technol.* **2009,** *43*, 2362-2367.

[24]. Chen, C. L.; Liang, B.; Lu, D.; Ogino, A.; Wang, X. K.; Nagatsu, M.,Amino group introduction onto multiwall carbon nanotubes by NH3/Ar plasma treatment. *Carbon* **2010,** *48* (4), 939-948.

[25]. Shao, D. D.; Jiang, Z. Q.; Wang, X. K.; Li, J. X.; Meng, Y. D.,Plasma induced grafting carboxymethyl cellulose on multiwalled carbon nanotubes for the removal of UO_2^{2+} from aqueous solution. *J. Phys. Chem. B* **2009,** *113* (4), 860-864.

[26]. Yang, S. B.; Hu, J.; Chen, C. L.; Shao, D. D.; Wang, X. K.,Mutual effects of Pb(II) and humic acid adsorption on multiwalled carbon nanotubes/polyacrylamide composites from aqueous solutions. *Environ. Sci. Technol.* **2011,** *45* (8), 3621-3627.

[27]. Shao, D. D.; Hu, J.; Wang, X. K.,Plasma induced grafting multiwalled carbon nanotube with chitosan and its application for removal of UO_2^{2+}, Cu^{2+}, and Pb^{2+} from aqueous solutions. *Plasma Process. Polym.* **2010,** *7* (12), 977-985.

[28]. Naseh, M. V.; Khodadadi, A. A.; Mortazavi, Y.; Pourfayaz, F.; Alizadeh, O.; Maghrebi, M.,Fast and clean functionalization of carbon nanotubes by dielectric barrier discharge plasma in air compared to acid treatment. *Carbon* **2010,** *48* (5), 1369-1379.

[29]. Yang, S. B.; Shao, D. D.; Wang, X. K.; Nagatsu, M.,Localized in situ polymerization on carbon nanotube surfaces for stabilized carbon nanotube dispersions and application for cobalt(II) removal. *RSC Adv.* **2014,** *4* (10), 4856-4863.

[30]. Mitchel, S.; Alexis T, B., A Review of Recent Advances in Plasma Polymerization. In *Plasma Polymerization*, AMERICAN CHEMICAL SOCIETY: 1979; Vol. 108, pp 1-33.

[31]. Hu, J.; Shao, D. D.; Chen, C. L.; Sheng, G. D.; Li, J. X.; Wang, X. K.; Nagatsu, M.,Plasma-induced grafting of cyclodextrin onto multiwall carbon nanotube/iron oxides for adsorbent application. *J. Phys. Chem. B* **2010,** *114* (20), 6779-6785.

CHAPTER 4 Study on the Adsorption Mechanism of Cesium ion

4.1The importance of cation exchange and the hydroxyl exchange in Cs^+ sorption

Radioactive cesium contamination of water is of serious social and environment concern as it is the product of uranium fission[1]. These fission products can be easily dissolved in water during the leaks of nuclear reactor, such as those that occurred at Chernobyl in 1986, at Three Mile Island in Pennsylvania in 1979, and at Fukushima, Japan in 2011[2]. The serious Fukushima nuclear accidents had contaminated a vast area in Japan. These serious accidents have been received the attention about fission products that could make their way into the food chain when present in the natural environment[3]. The radionuclide cesium-137 (^{137}Cs) has a long half-life of 30.1 y and is biological hazard.[4] The sorption and migration of radiocesium are important processes to evaluate the physicochemical behavior of radiocesium in the natural environment. So the establishment of removal technology ofradio cesium from the nuclear waste before its discharge to the environment is very necessary. Ding et al.[5] synthesized a framework sulfide as Cs sorbent, and proposed that the ion-exchange was the main mechanism for Cs removal. Yang et al.[2] demonstrated a method to capture^{137}Cs from contaminated water by using titanate nanotubes and nanofibers. Lin et al.[6, 7] synthesized copper ferrocyanide immobilized within a mesoporous silica matrix as a novel Cs sorbent. Although many research groups[2, 4, 8, 9] have made important contributions to search the high-efficiency sorbent for Cs^+ ions, and the mechanisms of Cs^+ sorption are proposed, the detailed adsorption mechanisms still remain unclear. Obviously, an accurate and detail mechanism is required and calls for contribution to understand the adsorption process in order to facilitate the development of more efficient adsorbent.

Previous researches show that the ion exchange mechanism is the very important part for Cs^+ sorption.[5, 7, 10, 11] In addition, the ion exchange process contains exchange with cation and with some functional groups (such as hydroxyl groups and carboxyl groups). The monovalent

cesium ions can be competed for reactive sites by monovalent Group I and divalent Group II cations. Recently, Dwivedi et al.[4] showed that the resorcinol-formaldhyde resin had an exceptionally high affinity for Cs^+ ions which was attributed to the presence of the –OH group. Functional groups on the substance surface affect the chemical functionality. In addition, the ionization of hydroxyl groups can affect the pH of the solution and the surface charge of the material. Yang et al.[2] demonstrated that the competitive effect of highly concentrated hydronium ions can decrease the adsorption capacity of the adsorbents at low pH. Therefore, how important are the cation exchange and the hydroxyl exchange mechanisms to Cs^+ sorption? And whether can we improve the sorption capacity of the material by increasing the amount of hydroxyl groups? This is very important for us to choose and design materials as a high-efficiency sorbent for Cs^+ ions.

Carbon nanotubes (CNTs)[12, 13] and bentonite[14, 15] have been proved to be good candidates as adsorbents owing to their good chemical stability and relatively large specific area. Bentonite is a 2:1 type aluminosilicate with high cation-exchange capacity (CEC)[14, 16, 17], the unit layer which consists of one Al^{3+} octahedral sheet between two Si^{4+} sheets.[18, 19] It is a good candidate as buffer material for disposingthe high-level radioactive waste. To modify bentonite by intercalation or sorption has been reported by many researchers[16, 20, 21, 22, 23, 24]. Chitosan (CS) is a nontoxic, hydrophilic, and biocompatible compound having a large number of hydroxyl groups with high activity as adsorption sites[25, 26]. Various techniques have been reported to graft CS on different materials to modify hydroxyl groups and to improve the dispersion property and the adsorption capacity for metal ions.[25, 27, 28] Plasma-induced grafting techniqueis an efficient method in the field of surface modifications.[27, 29, 30] It considered tobe a good way to enhance the chemical functionality of material. The research on improving adsorption capacity of materials by plasma-induced grafting technique has profound significance in environmental pollution management.[30, 31, 32]

In order to understand the effect of hydroxyl groups on Cs^+ adsorption process, herein we synthesized the CS-g-CNTs and CS-g-bentonite composites by the plasma-induced

grafting method[13] and compared their adsorption capacities with the pristine CNTs and bentonite for Cs^+ ions. In this work, CNTs and bentonite were used as low[33, 34] and high[14, 16, 17] CEC materials, respectively. The interactions of Cs^+ ion with the CS-g-CNTs and CS-g-bentonite composites were researched by cesium adsorption experiment. Based on the excellent CEC of bentonite, we also compared the bentonite-based material with the CNTs-based materials to evaluate the effect of cation-exchange on Cs^+ adsorption process. Our approach is depicted in Fig. 4.1. The effects of pH, ionic strength and contact time on Cs sorption process were also investigated to understand the mechanism of Cs^+ adsorption reactions.

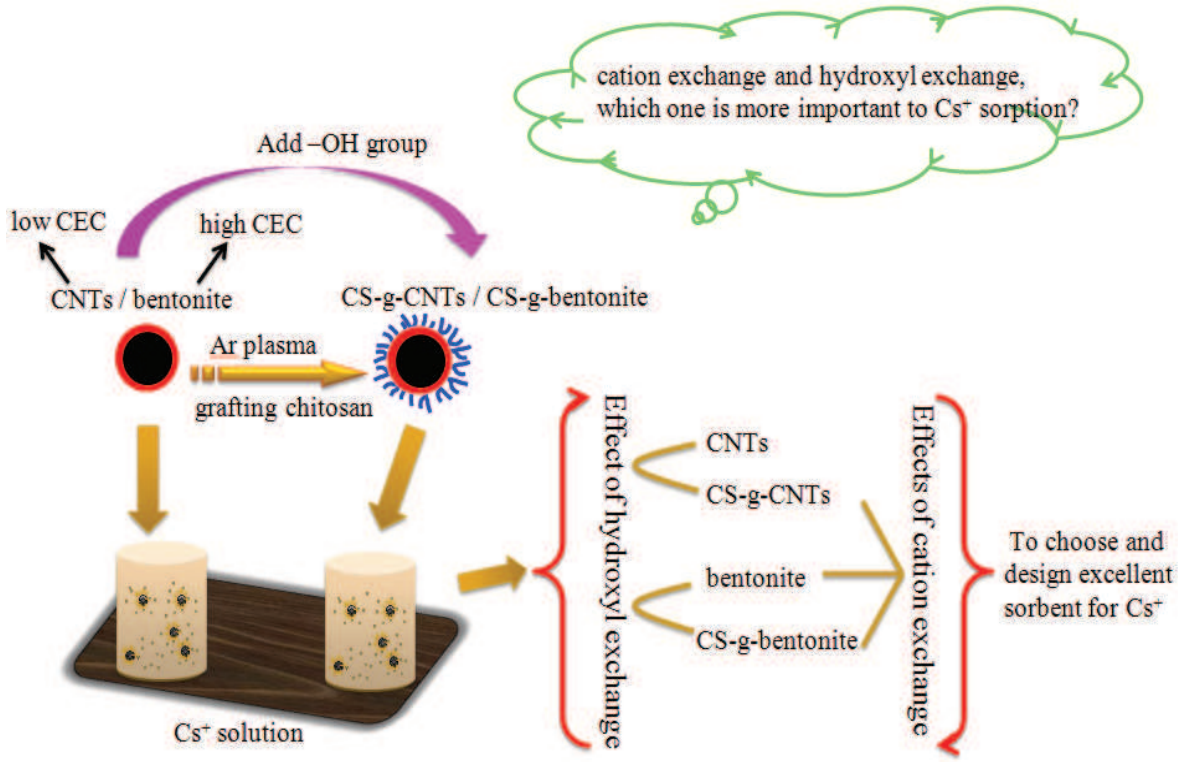

Fig. 4.1. Schematic illustration of the research approach.

4.2 Experimental details

4.2.1 Instruments and reagents

The pristine CNTs were synthesized by chemical vapor deposition using Ni-Fe nanoparticles as catalysts as previously reported[13, 32]. Bentonite was obtained from

Gaomiaozicounty (Inner Mongolia, China). Chitosan 100, phosphoric acid, cesium chloride, sodium hydroxide, magnesium chloride, sodium acetate, and potassium chloride were available from Wako Pure Chemical Industries, Ltd. All chemicals used were of analytical grade and used without further purification. Milli-Q water was used to prepare all the solutions in the experiments.

Table 4.1 Summary table of reagents used in this study.

Reagents	**degree**	**Compony**
CNTs	>97%	Shenzhen Nanotech Port Co., Ltd
Bentonite	Gaomiaozi county	Inner Mongolia, China
Chitosan	100%	Wako Pure Chemical Industries, Ltd.
H_3PO_4	Analytical grade	Wako Pure Chemical Industries, Ltd.
CsCl	Analytical grade	Wako Pure Chemical Industries, Ltd.
NaOH	Analytical grade	Wako Pure Chemical Industries, Ltd.
$MgCl_2$	Analytical grade	Wako Pure Chemical Industries, Ltd.
CH_3COOH	Analytical grade	Wako Pure Chemical Industries, Ltd.
KCl	Analytical grade	Wako Pure Chemical Industries, Ltd.
NaCl	Analytical grade	Wako Pure Chemical Industries, Ltd.
HCl	37%	Wako Pure Chemical Industries, Ltd.
CsCl standard solution	1001 mg/L	Wako Pure Chemical Industries, Ltd.
LiCl	Analytical grade	Wako Pure Chemical Industries, Ltd.

Table 4.2 Summary table of instruments used in this study.

Instruments	Model	Compony
Pipet	200µl, 1000µl	Wako Pure Chemical Industries, Ltd.
FE-SEM	JSM-7001F	JEOL
XRD (Cu Kα radiation)	RINT-Ultima	Rogaku
XPS (Mg Kα X-ray source)	ESCA-3400	Shimadzu
TGA	DTG-60A	Shimadzu
BET	BELSORP MINI II	BELSORP
pH meter	pH 15-7Mo	LABINDIA
Atomic absorption spectroscopy	Solar S4-AA	THERMO ELECTRON

4.2.2 Synthesis of CS-g-CNTs and CS-g-bentonite composites by plasma induced grafting procedure

In this study, we employed an inductivelycoupled radio frequency plasma device, described in our previous papers.[35, 36] A schematic diagram of the compact experimental setup is shown in Fig. 4.2. The plasma-induced grafting chitosan on CNTs and bentonite consisted of two successive processes: surface activation and chitosan grafting. For instance, 0.1 g pristine CNTs were treated using Ar plasma for 10 min at a pressure of 50Pa with an RF power of 80W. Ar plasma treatment is expected to activate the surfaces by bond breaking due to Ar-ion bombardment and to increase the reactivity of CNTs surface.[37] Then 150 mL 1.5g/L CS solution was immediately injected into the plasma treated CNTs to anchor CS at 80ºC. After stirring vigorously for 24 hours, the CS-g-CNTs composites were collected by centrifuging, washed several times with 0.01 mol/L H_3PO_4 solution and distilled water, and finally dried in a vacuum oven at room temperature.

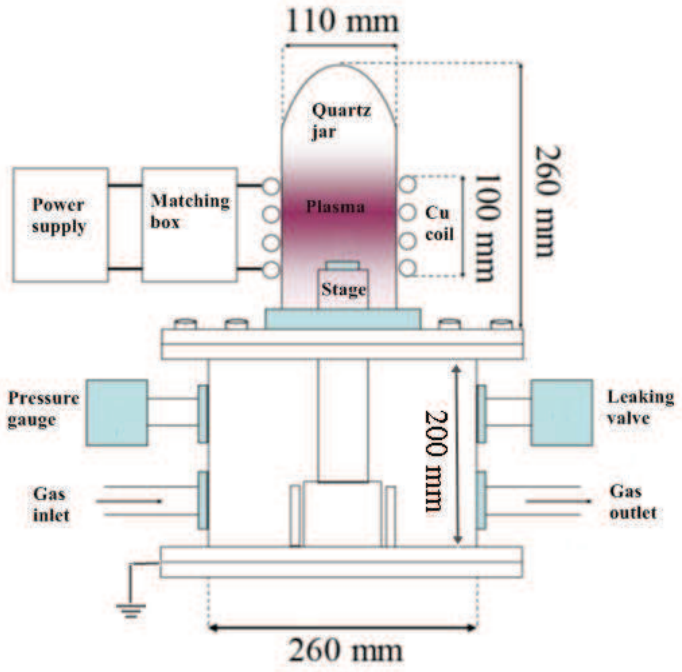

Fig. 4.2. Schematic view of experimental setup for inductively coupled RF plasma.

4.2.3 Sample characterization

After the plasma induced grafting procedure, the samples were characterized by using field emission scanning electron microscopy (FE-SEM), X-ray diffraction (XRD), X-ray photoelectron spectroscopy (XPS), Thermo-gravimetric analysis (TGA) and Brunauer-Emmett-Teller (BET). The surface morphology was obtained by FE-SEM performed on a JEOL JSM-7001F electron microscope. The crystal structures were analyzed by XRD (ROGAKU, RINT-Ultima). The XPS measurements were performed by Shimadzu ESCA-3400 equipped with an Mg Kα X-ray source. The crystal structures were analyzed by XRD equipped with Cu Kα (λ=0.15418nm) radiation. TGA was performed using a Shimadzu DTG-60A analyzer under 25%/Ar/75% air atmosphere, and the samples were hearted at a rate of 10ºC/min from 35 ºC to 800 ºC. The BET equation was obtained with a BELSORP MINI II. The pH of suspensions was measured using LABINDIA pH meter. Elemental chemical analyses for sodium solution were analysis by atomic absorption spectroscopy (THERMO ELECTRON, Solar S4-AA).

4.2.4 Cesium adsorption experiment

3.6 mg adsorbent was added to 6 mL aqueous solution of CsCl at concentrations ranging from 1.0 ppm to 42.0 ppm. The system was adjusted to the desired pH by adding small volumes of 0.01 or 0.1 mol/L $HClO_4$ or NaOH. The suspension was then shaken at ambient temperature for the required contact time. After appropriate time intervals, the adsorbent was separated from the solution by centrifuging at 14000 rpm for 30 min, and then the supernatant was filtered through a 0.45 μm membrane filter. Aliquots of supernatants were sampled to determine the concentration of Cs^+ ions in solution by atomic absorption spectroscopy.

The adsorption capacity (Q_e, mg/g) and removal efficiency ($E\%$) are calculated according to Eqs., (4-1) and (4-2):

$$Q_e = \frac{(C_o - C_t)V}{W} \tag{4-1}$$

$$E\% = \frac{(C_o - C_t)}{C_o} \times 100 \tag{4-2}$$

Where C_o is the initial concentration of Cs^+ in solution (mg/L), C_t represents the concentration of Cs^+ in supernatant at time t, W is the mass of adsorbent (g), V represents the total volume of the solution (L).

4.3 Results and discussion

4.3.1 Material characterization

The CS-g-CNTs and CS-g-bentonite composites were synthesized via a two-step method by low-temperature plasma-induced grafting procedure in Ar atmosphere; see Fig. 4.2. According to N_2-BET measurements, the surface area for CNTs, CS-g-CNTs, bentonite and CS-g-bentonite composites are 71.29 m^2/g, 78.82 m^2/g, 18.52 m^2/g and 27.92 m^2/g, respectively. The morphology and microstructures of the samples were characterized by SEM. The CNTs (Fig. 4.3a) have very smooth surfaces and the nanotubes are highly bundled with

about 10~30 nm in diameter. Afterloaded CS,many nanoplate-like CS nanostructures with a fairly uniform size of about 0.88 μm in diameter coated on the surface can be seen (Fig.4.3b). The SEM images show distinctly that the nanoplate structures are randomly decorated on the surface of CNTs, indicating that CS-g-CNTscomposites are synthesized successfully. The stacking morphology of CS-g-CNTs is due to the strong interaction between CNTs and the hydroxyl group of CS.[26] Fig.4.3c reveals that the bentonite has a rough surface with same crumples and a three-dimensional network structure.

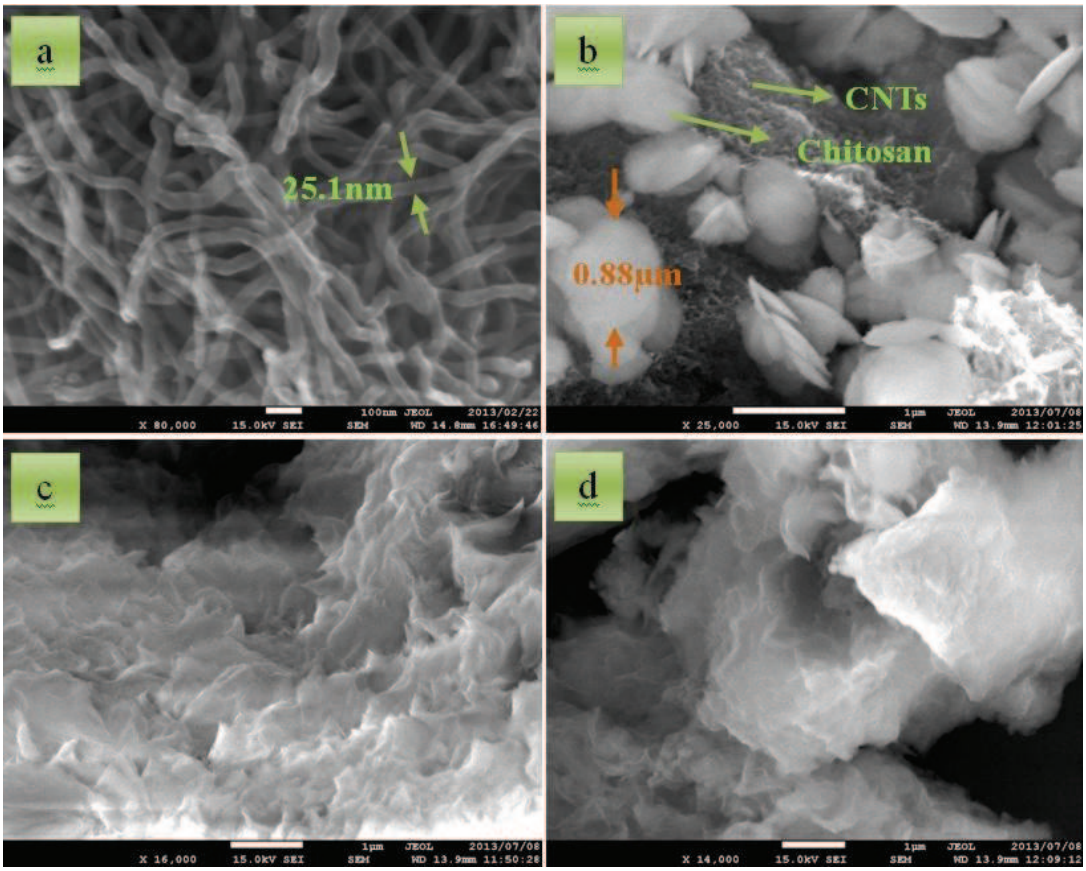

Fig.4.3 SEM images of pristine CNTs (a), CS-g-CNTs (b), pristine bentonite (c) and CS-g-bentonite (d)

A comparison is also made between pristine bentonite and CS-g-bentonite composite. The SEM image of CS-g-bentonite (Fig. 4.3d) shows agglomerated structure with a surface abundant in folds. And the crumpled structures are apparently much more transparent than that of bentonite, which can be attributed to the rearrangement of bentonite layers, suggesting

the existence of partial exfoliation of the bentonite layer.[23, 38] Therefore, due to the introduced CS, the bentonite layer has partially opened.[39]The results suggest the formation of CS-g-bentonite structures exist some degree of intercalated and exfoliated structures. In other words, the CS was intercalated into the bentonite interlayer as many previously reported[19, 40] rather than immobilized on the surface of bentonite.

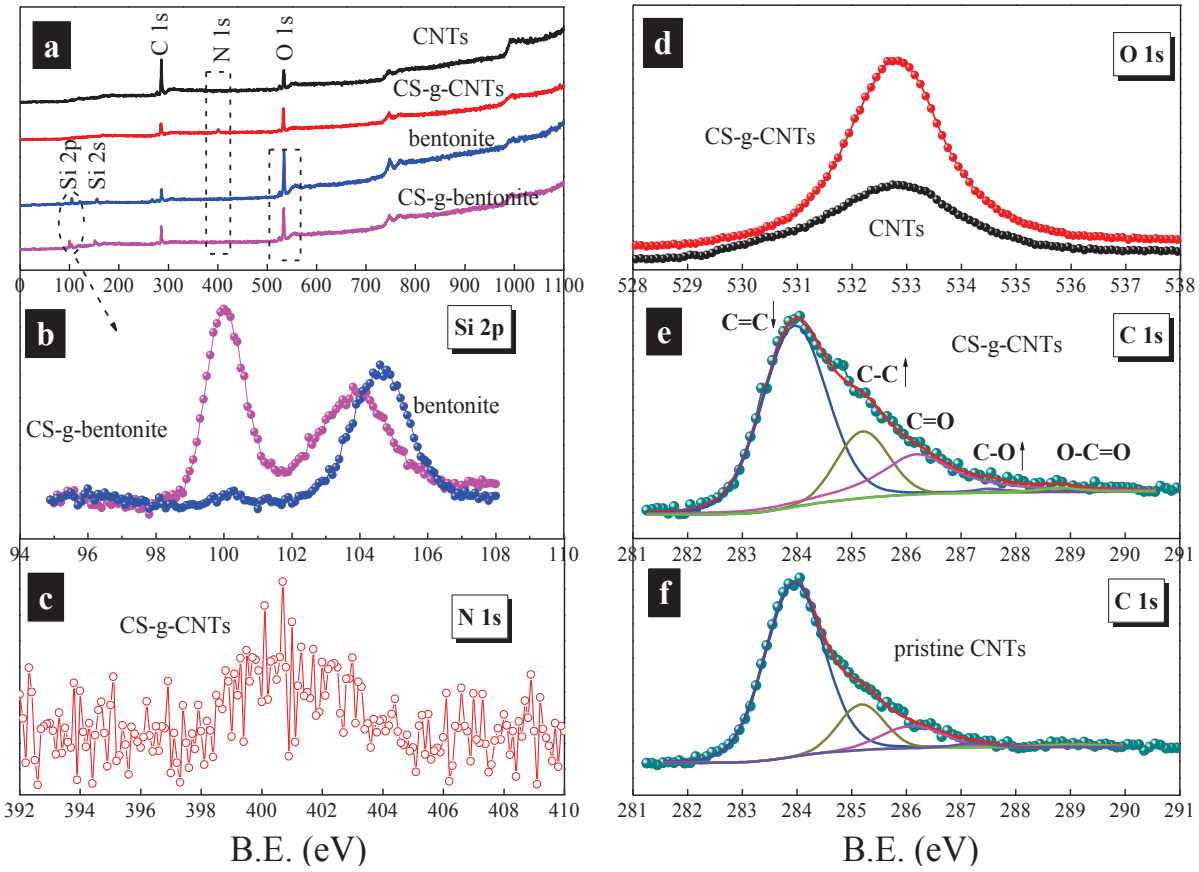

Fig. 4.4 XPS spectra of survey scan (a), Si 2p spectrum (b), N 1s spectrum (c), O 1s spectrum (d), C 1s spectrum of CS-g-CNTs (e), and C 1s spectrum of pristine CNTs (f).

In order to verify the above viewpoint, the element characterizations of the obtained samples were analyzed by XPS. Fig. 4.4a shows the presence of Si, C, N and O in the surface of samples. For all the samples, the survey spectra show mainly carbon (C 1s) and oxygen (O 1s) species (Fig. 4.4a). The spectra of XPS for CS-g-bentonite and bentonite exist the characteristic peaks of Si 2s and Si 2p, which attribute to the tetrahedral silica sheets of bentonite.[19, 38] From Fig. 4.4b, we can also find that the Si 2p spectrum of CS-g-bentonite shows double strong peaks. This is due to the new bond formation of silica with CS, which

can cause deformation of the silica tetrahedral sheets. And the further proof was offered from the decreased O 1s peak intensity in CS-g-bentonite (Fig. 4.4a). These results confirmed the effective connection of CS onto bentonite.

Table 4.1. Curve fitting results of XPS C1s spectra of CNTs and CS-g-CNTs

peak (%) / Content	C=C	C-C	C-O	C=O	O-C=O
B.E. (eV)	284.4	285.4	286.2	287.6	288.9
CNTs	74.2	14.2	9.33	1.00	1.25
CNTs-g-CS	60.0	16.7	21.2	1.02	1.16

Since nitrogen only exists in chitosan[41] not in CNTs and bentonite, the atomic concentration of N can be an indication of the extent of surface coverage by CS. However, no peak belongs to nitrogen that can be observed in CS-g-bentonite composites as previously reported[19, 22]. This is due to the XPS analysis is only used to ensure the elemental composition at the surface. Therefore, the CS is intercalated into the bentonite interlayer structure instead of on the surface. The result is consistent with the SEM results.

The N 1s peak (400.5 eV) of CS-g-CNTs composites was found in Fig. 4.4a and 4.4c, which was attributed to the amino groups in chitosan. This indicates CS has been grafted on the surface of CNTs, and therefore the CS-g-bentonite composites are successfully synthesized. Besides, after plasma and CS grafting treatment, the O 1s (533 eV) peak intensity increased (Fig. 4.4a and d), which was assigned to the hydroxyl groups of CS. On the other hand, the C 1s peak intensity decreased after the plasma induced grafting procedure, because during the pre-treatment, Ar plasma broke carbon double bonds in the graphene structure as previously reported[32, 35]. The comparison of C 1s region of CNTs and CS-g-CNTs are shown in Fig. 4.4e and 4.4f.And more detailed analysis is shown in Table 4.1. The C1s spectra can be deconvoluted into five Gaussian peaks[32]: (1) the C=C peak (284.4 eV); (2) the

carbon in C-C peak (285.4 eV); (3) the C-O peak (286.2 eV), (4) the carbonyl carbon (C=O, 287.6 eV); and (5) the carboxylate carbon peak (O-C=O, 288.9 eV). As can be seen from the quantitative analysis (Table 4.1)of C 1s spectra of CNTs and CS-g-CNTs, the peak fractions of C=C and O-C=O decrease, whereas the C-C and C-O fractions increase after grafting CS. It is reasonable because: a) the C=C bonds were partly broke during the plasma treatment; b) CS is a polysaccharide, which contains large amount of C-C, C-OH, and C-O-C groups.[42, 43] The XPS analysis presents a confirmation of the success of the CS immobilized on CNTs and bentonite structures. It was concluded that CS was grafted on the surface of CNTs, while the CS are intercalated into the bentonite interlayer in CS-g-bentonite composites.

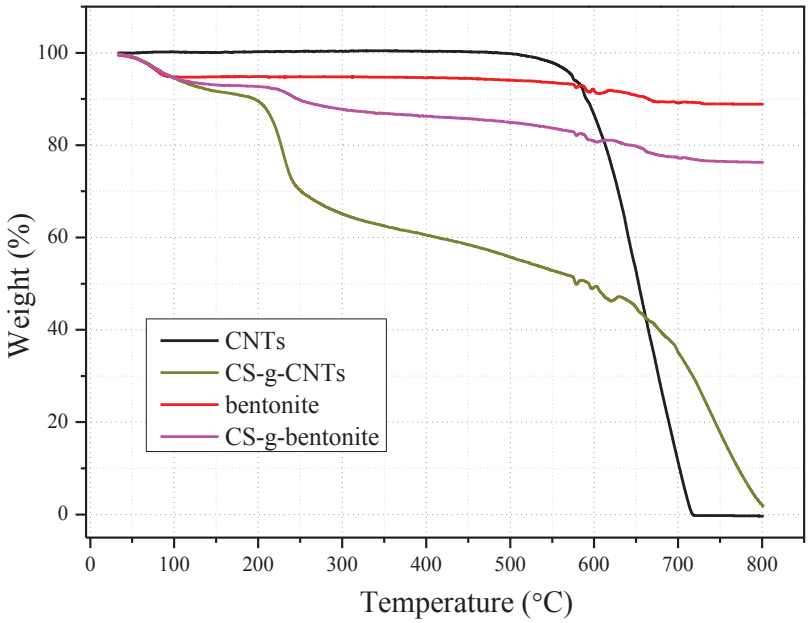

Fig. 4.5 TGA curves of CNTs, CS-g-CNTs, bentonite, and CS-g-bentonite.

The chitosan content in CS-g-CNTs and CS-g-bentonite composites can be determined by thermogravimetric analysis (TGA) to be about 36.7 wt% and 8.7 wt%, respectively. (see Fig. 4.5). The TGA curve of CS-g-CNTs showed three steps of weight loss. About 7.2% of weight loss occurred from room temperature to around 130 ºC, which was attributed to the elimination of absorbed water. As shown in Fig.4.5, the weight loss of CNTs is negligible before 500 ºC. Therefore, the second weight loss about 36.7% from 150 ºC to 500 ºC corresponding to the content of chitosan in the hybrid material. Up to 800 ºC, the weight loss

is mostly attributed to the combustion of CNTs. For CS-g-bentonite, the same trend of degradation was also observed. As mentioned above, the weight loss of 6.3% before 130 ºC is attributed to the loss of moisture. The weight loss of bentonite is negligible from 150 to 500 ºC. Therefore, the second weight loss about 8.4% was caused by decomposition of chitosan in the CS-g-bentonite composites.

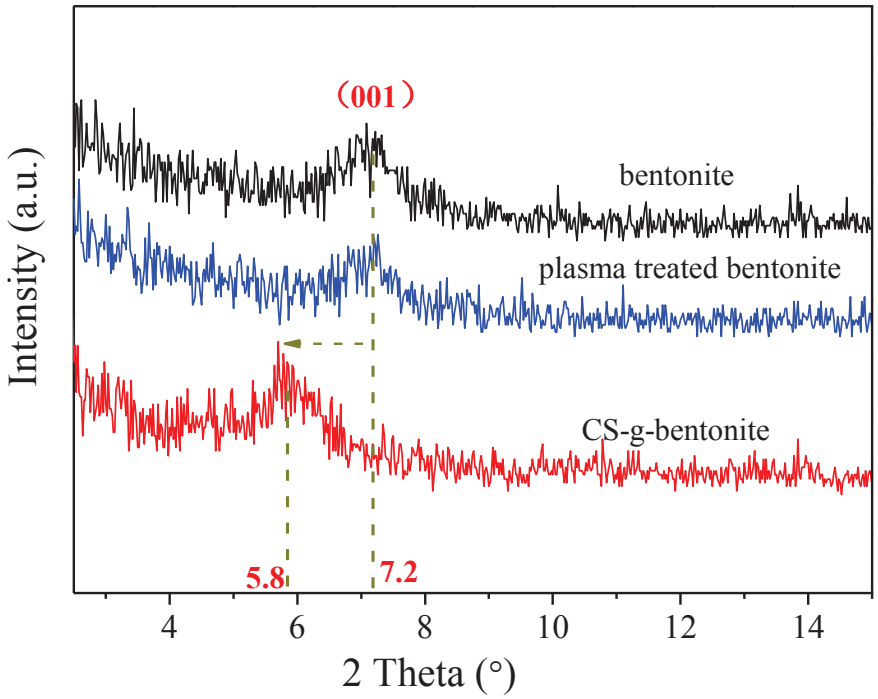

Fig. 4.6 XRD patterns of pristine bentonite, plasma treated bentonite, and CS-g-bentonite.

In addition, the XRD patterns of the obtained samples were characterized, which is a powerful technique to help to clarify the microscopic status of the intercalated molecule in the bentonite structure.The XRD patterns of pristine bentonite and plasma treated bentonite exhibit the (001) diffraction peak at 2θ = 7.2°, corresponding to the typical reflections of montmorillonite (see Fig. 4.6).[44] However a negative shift in the position of the d_{001} peak from 12.2Å to 15.2Å, showing an expansion of the basal interplanar distance, indicating the intercalation of the CS molecule in the bentonite structure.[19, 45]

4.3.2 Kinetics of Cs^+ adsorption

Fig. 4.7a shows the removal of Cs^+ from aqueous solution by bentonite at pH 7.0 as a function of contact time. It is noted that the adsorption of Cs^+ ions increases quickly with increasing contact time and a saturation value of 89% is reached at 7h. After contact time about 10 h, the adsorption of Cs^+ on bentonite maintains level with increasing contact time. The same trends of the contact time effect for Cs^+ onto the other sorbents were also observed; see Fig. 4.8. In the following experiments, the contact time for all the Cs^+ sorption measurements was kept 24h.

4.3.3 pH effect and adsorption isotherms.

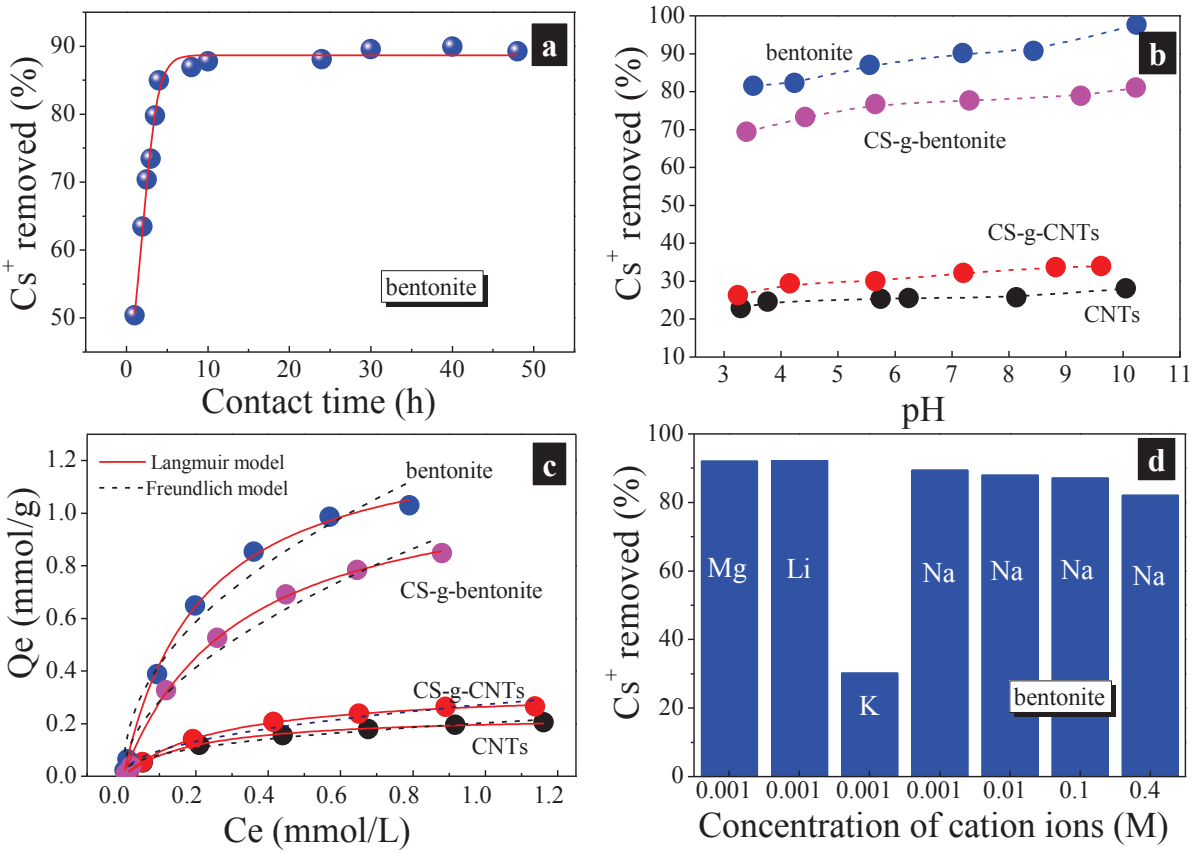

Fig. 4.7 (a) Kinetic curve of Cs^+ adsorption by bentonite, (b) Effects of initial pH and sorbent forCs^+ adsorption,(c) Adsorption isotherms forCs^+ uptake by the sorbents, and (d) Effect of ionic strength forCs^+ adsorption on bentonite, with T=20 ± 1 ºC, $m_{sorbent}/V_{solvent}$=0.6g/L, $[Cs^+]_{initial}$=10.0 mg/L.

An additional important characteristic of Cs^+ sorption is pH-dependence. The pH effect of Cs^+ sorption has been studied by many researchers[2, 46, 47], and the results indicated that pH of solution exerts a modest effect on the uptake of Cs^+ ions. It is noted that the adsorption of Cs^+ ions increases gradually with increasing pH (Fig.4.7b), because the highly concentrated hydronium ions are able to compete with Cs^+ ions to uptake onto the sorbents at low pH. In order to investigate the effects of cation exchange and hydroxyl exchange on Cs^+ sorption process, the comparisons of these sorbents for Cs adsorption capacity are made (Fig.4.7b). The removal of Cs^+ ions decreased in the order of bentonite > CS-g-bentonite > CS-g-CNTs > CNTs. And a further proof was offered by the adsorption isotherms, as shown in Fig.4.7c. The Langmuir[13] and Freundlich[13]isotherm models, both of which are the most widely used among the abundant isotherm models, were applied to fit the experimental data to understand the adsorption mechanism. The Langmuir (Eq. 4-3) and Freundlich (Eq. 4-4) models are expressed as follow:

$$Q_e = \frac{Q_m K_L C_e}{1 + K_L C_e} \qquad (4\text{-}3)$$

$$Q_e = K_F C_e^{1/n} \qquad (4\text{-}4)$$

Where Q_e is the equilibrated cesium ion concentration,Q_m (mg/g) is the maximum sorption capacity,K_L (L/mg) is the Langmuir adsorption constant and and$1/n$is the Freundlich adsorption constant.

The parameters calculated from Langmuir and Freundlich isotherms are listed in Table 4.2. One can see that the Langmuir model fits the experimental data better than the Freundlich one. It can be calculated that the sorption capacity Q_m of Cs^+ on CS-g-CNTs is 0.333mmol/g, which is about 1.4 times higher than that ofCs^+ on CNTs (0.235mmol/g). Based on low CEC[33, 34], CNTs-based materials capture the Cs^+ ions mainly by the width of tubes and the functional groups on the surface. The enhanced sorption of Cs^+ on CS-g-CNTs is due to the modified hydroxyl groups which are derived from the grafted CS. Therefore, the effect of hydroxyl

groups to the Cs^+ adsorption process onto the CNTs-based materials is positive. Compared to the CS-g-CNTs, the sorption capacity of Cs^+isabout 3 times higher than that of Cs^+ onCS-g-bentonite (1.164 mmol/g) and 4 times higher than that of Cs^+ onbentonite (1.334 mmol/g). Due to the excellent CEC of bentonite, we can see that the cation-exchange mechanism is much more effective than that of hydroxyl exchange in Cs^+ adsorption process.

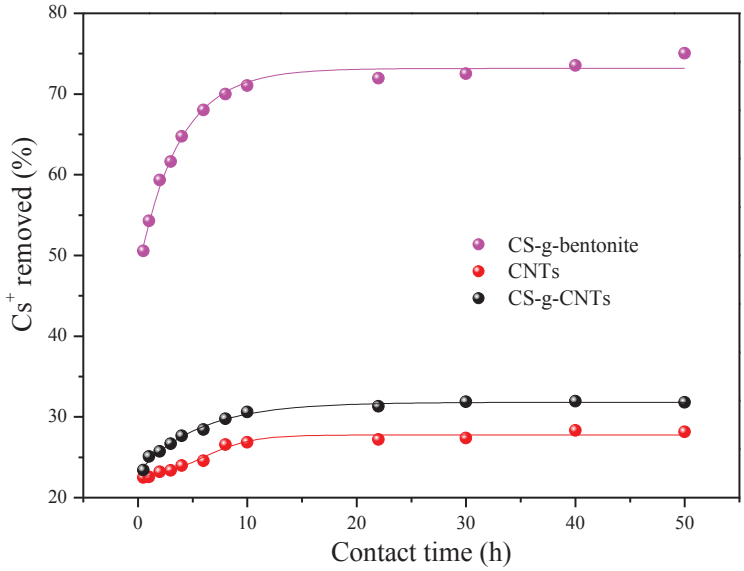

Fig. 4.8 The effects of contact time for Cs^+ adsorption onto CNTs, CS-g-CNTs, and CS-g-bentonite. T=20 ± 1 ºC,$m_{sorbent}/V_{solvent}$=0.6g/L, $[Cs^+]_{initial}$=10.0 mg/L.

Table 4.2 Sorption constants for Langmuir and Freundlich isotherm models.

Sorbent	Langmuir			Freundlich		
	Q_m (mmol/g)	K_L (L/mmol)	R^2	n	K_F (mmol/g)	R^2
bentonite	1.334	4.69	0.999	2.13	1.248	0.963
CS-g-bentonite	1.164	3.16	0.997	1.88	0.974	0.963
CS-g-CNTs	0.333	3.82	0.998	2.22	0.273	0.955
CNTs	0.235	4.99	0.991	2.52	0.203	0.978

Compared to the bentonite, one can see that the sorption capacity of Cs^+ on CS-g-bentonite is clearly lower by 13%, which may be due to the grafted CS. We considered that there are two main reasons for the decreased adsorption capacity of Cs^+ on bentonite after modified with hydroxyl groups: 1) the first is the partial exfoliation of the bentonite layer resulted from the intercalated CS; and 2) the second one is the lower ion-exchange properties of hydroxyl groups than the bentonite layer structures.[16, 48]

4.3.4 Effect of ionic strength.

The effect of the background electrolyte concentrations on Cs^+ adsorption to bentonite at pH 7 is shown in Fig. 4.7d. Due to the isomorphous substitution within the bentonite layers (e.g. Al^{3+} replaced by Mg^{2+} or Fe^{2+}), the clay layer is negatively charged, which is counter-balanced by cations (e.g., Na^+, Ca^{2+}) in the galleries between layers.[18, 49] In the four different Na^+ solution concentrations, the adsorption capacity increases with the decreasing ionic strength, because a large fraction of the cation ions at the interlayer are exchanged with Na^+ions and thus the uptake of Cs^+ ions is decreased. The main mechanism of Cs^+ adsorption on bentonite is cation-exchange. The effect of other cations is also shown in Fig. 4.7d. One can see that the sorption of Cs^+ on bentonite is strongly dependent on the background cations. The sorption of Cs^+ is mainly dominated by strong cation exchange with cation (i.e., alkali metal and alkaline earth metal ions) such as Mg^{2+}, Na^+, and K^+ ions. This is due to the Cs^+ ions leak chemical unique characteristic and can be competed for reactive sites by monovalent Group I and divalent Group II cations. And the adsorption capacity decreased in the following sequence: $Mg^{2+} \approx Li^+ > Na^+ > K^+$. The ionic radius and the configuration of the hydrated metal ions in aqueous solution are listed in Table 4.3. It is noted that the ionic radius increased in the reverse order of $Mg^{2+} \approx Li^+ < Na^+ < K^+ < Cs^+$. The alkali metal ions are highly hydrated. The smaller the size of the ion, the greater is the degree of hydration. Thus, the effective size of the hydrated Li^+ ions is much bigger than that of hydrated Cs^+ ions. Therefore, it is more difficult for $Li(H_2O)_6^+$ to compete the adsorption sites of the sorbent than $Cs(H_2O)_{12}^+$. For Mg^{2+} and Li^+ ions, they have the same configuration and ionic radius, resulting in the same

hydrated radius. Among these cations, the presence of K^+ strongly constraints the Cs^+ adsorption, because with similar radius and hydration energy[46], K^+ can compete more effectively against Cs^+ ions on the sorbent surface.[50] Therefore, the adsorption capacity and the hydrated radiuses of the cations are in the same sequence: $Mg^{2+} \approx Li^+ > Na^+ > K^+$. With increasing the hydrated radius of the cations in solution, the Cs adsorption capacity constraint decreases.

Table 4.3 The M-O bond distance, ionic radius and configuration of hydrated metal ions in aqueous solution.

Aqua complex	M-O distance /Å	M^{n+}'s ion radius/Å	Configuration	References
$Li(H_2O)_6^+$	2.10	0.76	Octahedron	51, 52, 53, 54
$Na(H_2O)_6^+$	2.43	1.09	Octahedron	53, 55
$K(H_2O)_8^+$	2.84	1.50	Square antiprism	53, 55
$Cs(H_2O)_{12}^+$	3.25	1.91	12-coordination	53, 54, 55
$Mg(H_2O)_6^{2+}$	2.10	0.76	Octahedron	53, 54

Finally, the results indicate that based on the high CEC, bentonite-based composite can be considered as promising material for the cesium contamination management. And the effect of hydroxyl groups to Cs^+ adsorption process is dependent on the property of the matrix. For the material based on low CEC such as CNTs, the effect of hydroxyl groups is positive. For the material based on excellent CEC such as bentonite, the effect of hydroxyl groups is weak or negative. One can draw a conclusion that

we cannot improve the Cs^+ adsorption capacity of material only by increasing the amount of hydroxyl groups in any case. Therefore, the spatial structure and CEC of the material are very important factors for choosing the sorbent for Cs^+ removal from radioactive waste water.

4.4 Conclusions

In summary, we have successful synthesized the CS-g-CNTs and CS-g-bentonite composites by the plasma-induced grafting method. This study demonstrates that cation-exchange mechanism is much more effective than the hydroxyl group to Cs^+ adsorption process. And the effect of hydroxyl groups to Cs^+ adsorption is dependent on the property of the matrix. We cannot improve the Cs^+ adsorption capacity of material only by increasing the amount of hydroxyl groups in any case. The sorption of Cs^+ ions was strongly dependent on pH andbackground cations. And it was mainly dominated by strong cation exchange with alkali and alkaline-earth cations. The spatial structure and CEC of the material are very important factors for high-efficiency sorbent for Cs^+ ions. Our findings are important for estimating and optimizing the sorbent for Cs^+ ions and give the future directions of new and selective adsorbents for the removal of Cs^+ ions in groundwater or wastewater.

Reference:

[1]. Sheha, R. R.,Synthesis and characterization of magnetic hexacyanoferrate (II) polymeric nanocomposite for separation of cesium from radioactive waste solutions. *J. Colloid Interface Sci.* **2012,** *388*, 21-30.
[2]. Yang, D.; Sarina, S.; Zhu, H.; Liu, H.; Zheng, Z.; Xie, M.; Smith, S. V.; Komarneni, S.,Capture of radioactive cesium and iodide ions from water by using titanate nanofibers and nanotubes. *Angew. Chem. Int. Ed.* **2011,** *50* (45), 10594-10598.
[3]. Mizuno, T.; Kubo, H.,Overview of active cesium contamination of freshwater fish in fukushima and eastern Japan. *Sci. Rep.* **2013,** *3*, 1-4.
[4]. Dwivedi, C.; Kumar, A.; Ajish, J. K.; Singh, K. K.; Kumar, M.; Wattal, P. K.; Bajaj, P. N.,Resorcinol-formaldehyde coated XAD resin beads for removal of cesium ions from radioactive waste: synthesis, sorption and kinetic studies. *RSC Adv.* **2012,** *2* (13), 5557-5564.
[5]. Ding, N.; Kanatzidis, M. G.,Selective incarceration of caesium ions by Venus flytrap action of a flexible framework sulfide. *Nat. Chem.* **2010,** *2* (3), 187-191.
[6]. Lin, Y.; Fryxell, G. E.; Wu, H.; Engelhard, M.,Selective sorption of cesium using self-assembled monolayers on mesoporous supports. *Environ. Sci. Technol.* **2001,** *35* (19), 3962-3966.
[7]. Clearfield, A.,Ion-exchange materials seizing the caesium. *Nat. Chem.* **2010,** *2* (3), 161-162.
[8]. Delchet, C.; Tokarev, A.; Dumail, X.; Toquer, G.; Barre, Y.; Guari, Y.; Guerin, C.; Larionova, J.; Grandjean, A.,Extraction of radioactive cesium using innovative functionalized porous materials. *RSC Adv.* **2012,** *2* (13), 5707-5716.

[9]. Torad, N. L.; Hu, M.; Imura, M.; Naito, M.; Yamauchi, Y.,Large Cs adsorption capability of nanostructured Prussian Blue particles with high accessible surface areas. *J. Mater. Chem.* **2012,** *22* (35), 18261-18267.

[10]. Dyer, A.; Pillinger, M.; Amin, S.,Ion exchange of caesium and strontium on a titanosilicate analogue of the mineral pharmacosiderite. *J. Mater. Chem.* **1999,** *9* (10), 2481-2487.

[11]. Kozaki, T.; Sato, H.; Sato, S.; Ohashi, H.,Diffusion mechanism of cesium ions in compacted montmorillonite. *Eng. Geol.* **1999,** *54* (1-2), 223-230.

[12]. Long, R. Q.; Yang, R. T.,Carbon nanotubes as superior sorbent for dioxin removal. *J. Am. Chem. Soc.* **2001,** *123* (9), 2058-2059.

[13]. Yang, S. B.; Hu, J.; Chen, C. L.; Shao, D. D.; Wang, X. K.,Mutual effects of Pb(II) and humic acid adsorption on multiwalled carbon nanotubes/polyacrylamide composites from aqueous solutions. *Environ. Sci. Technol.* **2011,** *45* (8), 3621-3627.

[14]. Zhao, D.; Chen, S.; Yang, S.; Yang, X.; Yang, S.,Investigation of the sorption behavior of Cd(II) on GMZ bentonite as affected by solution chemistry. *Chem. Eng. J.* **2011,** *166* (3), 1010-1016.

[15]. Wang, X. K.,Diffusion of Cs-137 in compacted bentonite: effect of pH and concentration. *J. Radioanal. Nucl. Chem.* **2003,** *258* (2), 315-319.

[16]. Seckin, T.; Gultek, A.; Onal, Y.; Yakinci, M. E.; Aksoy, I.,Synthesis, characterization and thermal properties of bentonite-polyacrylate sol-gel materials. *J. Mater. Chem.* **1997,** *7* (2), 265-269.

[17]. Kahr, G.; Madsen, F. T.,Determination of the cation exchange capacity and the surface area of bentonite, illite and kaolinite by methylene blue adsorption. *Appl. Clay Sci.* **1995,** *9* (5), 327-336.

[18]. Wei, J. M.; Zhu, R. L.; Zhu, J. X.; Ge, F.; Yuan, P.; He, H. P.; Ming, C.,Simultaneous sorption of crystal violet and 2-naphthol to bentonite with different CECs. *J. Hazard. Mater.* **2009,** *166* (1), 195-199.

[19]. Wan Ngah, W. S.; Teong, L. C.; Hanafiah, M. A. K. M.,Adsorption of dyes and heavy metal ions by chitosan composites: A review. *Carbohydr. Polym.* **2011,** *83* (4), 1446-1456.

[20]. Jiang, D. L.; Weng, Y. L.; Tong, R. T.,Preparation and characteristics of polyaniline/bentonite layered nanocomposites. *Acta Phys.-Chim. Sin.* **1999,** *15* (1), 69-72.

[21]. Lee, D. C.; Jang, L. W.,Characterization of epoxy-clay hybrid composite prepared by emulsion polymerization. *J. Appl. Polym. Sci.* **1998,** *68* (12), 1997-2005.

[22]. Anirudhan, T. S.; Rijith, S.,Synthesis and characterization of carboxyl terminated poly(methacrylic acid) grafted chitosan/bentonite composite and its application for the recovery of uranium(VI) from aqueous media. *Journal of environmental radioactivity* **2012,** *106*, 8-19.

[23]. Anirudhan, T. S.; Rijith, S.; Tharun, A. R.,Adsorptive removal of thorium(IV) from aqueous solutions using poly(methacrylic acid)-grafted chitosan/bentonite composite matrix: process design and equilibrium studies. *Colloids Surf., A* **2010,** *368* (1-3), 13-22.

[24]. Guo, Z. Q.; Li, Y.; Zhang, S. W.; Niu, H. H.; Chen, Z. S.; Xu, J. Z.,Enhanced sorption of radiocobalt from water by Bi(III) modified montmorillonite: a novel adsorbent. *J. Hazard. Mater.* **2011,** *192* (1), 168-175.

[25]. Tang, X. H.; Zhang, X. M.; Guo, C. C.; Zhou, A. L.,Adsorption of Pb^{2+} on chitosan cross-Linked with triethylene-tetramine. *Chem. Eng. Technol.* **2007,** *30* (7), 955-961.

[26]. Shao, D. D.; Hu, J.; Wang, X. K.,Plasma induced grafting multiwalled carbon nanotube with chitosan and its application for removal of UO_2^{2+}, Cu^{2+}, and Pb^{2+} from aqueous solutions. *Plasma Process. Polym.* **2010,** *7* (12), 977-985.

[27]. Shao, D. D.; Hu, J.; Wang, X. K.; Nagatsu, M.,Plasma induced grafting multiwall carbon nanotubes with chitosan for 4,4'-dichlorobiphenyl removal from aqueous solution. *Chem. Eng. J.* **2011,** *170* (2-3), 498-504.

[28]. Boddu, V. M.; Abburi, K.; Talbott, J. L.; Smith, E. D.; Haasch, R.,Removal of arsenic(III) and arsenic(V) from aqueous medium using chitosan-coated biosorbent. *Water Res.* **2008,** *42* (3), 633-642.

[29]. Wei, Y.; Liu, Z. G.; Yu, X. Y.; Wang, L.; Liu, J. H.; Huang, X. J.,O_2-plasma oxidized multi-walled carbon nanotubes for Cd(II) and Pb(II) detection: Evidence of adsorption capacity for electrochemical sensing. *Electrochem. Commun.* **2011,** *13* (12), 1506-1509.

[30]. Chen, C. L.; Ogino, A.; Wang, X. K.; Nagatsu, M.,Plasma treatment of multiwall carbon nanotubes for dispersion improvement in water. *Appl. Phys. Lett.* **2010,** *96* (13), 131504-131503.

[31]. Hu, J.; Shao, D. D.; Chen, C. L.; Sheng, G. D.; Li, J. X.; Wang, X. K.; Nagatsu, M.,Plasma-induced grafting of cyclodextrin onto multiwall carbon nanotube/iron oxides for adsorbent application. *J. Phys. Chem. B* **2010,** *114* (20), 6779-6785.

[32]. Chen, C. L.; Wang, X. K.; Nagatsu, M.,Europium adsorption on multiwall carbon nanotube/iron oxide magnetic composite in the presence of polyacrylic acid. *Environ. Sci. Technol.* **2009,** *43*, 2362-2367.

[33]. Rao, G. P.; Lu, C.; Su, F.,Sorption of divalent metal ions from aqueous solution by carbon nanotubes: A review. *Sep. Purif Technol.* **2007,** *58* (1), 224-231.

[34]. Li, Y. H.; Ding, J.; Luan, Z.; Di, Z.; Zhu, Y.; Xu, C.; Wu, D.; Wei, B.,Competitive adsorption of Pb^{2+}, Cu^{2+} and Cd^{2+} ions from aqueous solutions by multiwalled carbon nanotubes. *Carbon* **2003,** *41* (14), 2787-2792.

[35]. Saraswati, T. E.; Ogino, A.; Nagatsu, M.,Plasma-activated immobilization of biomolecules onto graphite-encapsulated magnetic nanoparticles. *Carbon* **2012,** *50* (3), 1253-1261.

[36]. Saraswati, T. E.; Matsuda, T.; Ogino, A.; Nagatsu, M.,Surface modification of graphite encapsulated iron nanoparticles by plasma processing. *Diamond Relat. Mater.* **2011,** *20* (3), 359-363.

[37]. Chen, C. L.; Ogino, A.; Wang, X. K.; Nagatsu, M.,Oxygen functionalization of multiwall carbon nanotubes by Ar/H_2O plasma treatment. *Diamond Relat. Mater.* **2011,** *20* (2), 153-156.

[38]. Dietsche, F.; Thomann, Y.; Thomann, R.; Mülhaupt, R.,Translucent acrylic nanocomposites containing anisotropic laminated nanoparticles derived from intercalated layered silicates. *J. Appl. Polym. Sci.* **2000,** *75* (3), 396-405.

[39]. Paiva, L. B.; Morales, A. R.,Organophilic bentonites based on argentinean and brazilian bentonites. Part 2: potential evaluation to obtain nanocomposites. *Braz. J. Chem. Eng.* **2012,** *29* (3), 525-536.

[40]. Guo, J.; Chen, S.; Liu, L.; Li, B.; Yang, P.; Zhang, L.; Feng, Y.,Adsorption of dye from wastewater using chitosan-CTAB modified bentonites. *J. Colloid Interface Sci.* **2012,** *382* (1), 61-66.

[41]. Yang, M. H.; Jong, S. B.; Lu, C. Y.; Lin, Y. F.; Chiang, P. W.; Tyan, Y. C.; Chung, T. W.,Assessing the responses of cellular proteins induced by hyaluronic acid-modified surfaces utilizing a mass spectrometry-based profiling system: over-expression of CD36, CD44, CDK9, and PP2A. *Analyst* **2012,** *137* (21), 4921-4933.

[42]. Kyzas, G. Z.; Deliyanni, E. A.,Mercury(II) removal with modified magnetic chitosan adsorbents. *Molecules* **2013,** *18* (6), 6193-6214.

[43]. Crini, G.,Non-conventional low-cost adsorbents for dye removal: a review. *Bioresour. Technol.* **2006,** *97* (9), 1061-1085.

[44]. Ma, J.; Zou, J.; Li, L.; Yao, C.; Zhang, T.; Li, D.,Synthesis and characterization of Ag_3PO_4 immobilized in bentonite for the sunlight-driven degradation of orange II. *Appl. Catal. B* **2013,** *134–135* (0), 1-6.

[45]. Darder, M.; Ruiz Hitzky, E.,Caramel–clay nanocomposites. *J. Mater. Chem.* **2005,** *15* (35-36), 3913.

[46]. Bouzidi, A.; Souahi, F.; Hanini, S.,Sorption behavior of cesium on ain oussera soil under different physicochemical conditions. *J. Hazard. Mater.* **2010,** *184* (1-3), 640-646.

[47]. Celestian, A. J.; Kubicki, J. D.; Hanson, J.; Clearfield, A.; Parise, J. B.,The mechanism responsible for extraordinary Cs ion selectivity in crystalline silicotitanate. *J. Am. Chem. Soc.* **2008,** *130* (35), 11689-11694.

[48]. Wang, X. K.; Tan, X. L.; Chen, C. L.; Chen, L.,The concentration and pH dependent diffusion Of Cs-137 in compacted bentonite by using capillary method. *J. Nucl. Mater.* **2005,** *345* (2-3), 184-191.

[49]. Eloussaief, M.; Benzina, M.,Efficiency of natural and acid-activated clays in the removal of Pb(II) from aqueous solutions. *J. Hazard. Mater.* **2010,** *178* (1-3), 753-757.

[50]. Liu, C. X.; Zachara, J. M.; Smith, S. C.; McKinley, J. P.; Ainsworth, C. C.,Desorption kinetics of radiocesium from subsurface sediments at Hanford Site, USA. *Geochim. Cosmochim. Acta* **2003,** *67* (16), 2893-2912.

[51]. Inorganic Crystal Structure Database 1.4.6. *Release 2009-1* **2009,** *FIZ Karlsruhe* (FIZ Karlsruhe).

[52]. Cambridge Structure Database. *Release* **2008**.

[53]. Ohtaki, H.; Radnai, T.,Structure and dynamics of hydrated ions. *Chem. Rev.* **1993,** *93* (3), 1157-1204.

[54]. Johansson, G., Structures of complexes in solution derived from X-Ray diffraction measurements. In *Adv. Inorg. Chem.*, Sykes, A. G., Ed. Academic Press: 1992; Vol. Volume 39, pp 159-232.
[55]. Persson, I.,Hydrated metal ions in aqueous solution: How regular are their structures? *Pure Appl. Chem.* **2010,** *82* (10), 1901-1917.

CHAPTER 5 Highly Effective Removal of Cs^+ by Low Turbidity Chitosan-Grafted Magnetic Bentonite

5.1 Introduction

The hazards of radioactive cesium contamination have attracted significant attention following the crisis at the Fukushima Daiichi Nuclear Power Plant in Japan in 2011[1]. Although three years have passed, concerns regarding radioactive ^{137}Cs have come to the forefront as the most significant concern because of the harmful health effects of this isotope and its potential to persist for decades [2]. The Fukushima incident contaminated a vast area in eastern Japan [3] and, once the ^{137}Cs enters the food chain through uptake by plants, it can be readily ingested by both animals and human beings [4]. For these reasons, the capture of ^{137}Cs from wastewaters is currently an urgent priority.

At present, the most commonly used methods for the separation and preconcentration of radionuclides include precipitation, solvent extraction, membrane dialysis, and adsorption [5, 6, 7, 8]. Among these methods, adsorption is both simple and economically feasible, although the success of the adsorption process is dependent on the choice of the appropriate material. Bentonite has traditionally been employed as an inorganic cation exchanger and, in addition to being stable under conditions of intense radiation and elevated temperatures, exhibits high cation exchange capacity [9, 10, 11]. Bentonite is a geological term for soil materials with high contents of a swelling clay mineral, typically montmorillonite[12]. The layered structure of bentonite consists of two silica tetrahedral sheets fused to one alumina octahedral sheet, and the main chemical composition of bentonite can be summarized as $E_x(H_2O)_4\{(Al_{2-x},Mg_x)_2[(Si,Al)_4O_{10}](OH)_2\}$, where E indicates exchangeable cations between the layers, including Na^+, Ca^{2+}, K^+, and others (Fig. 5.1a). Bentonite is capable of capturing Cs^+ ions through these exchangeable cations[12, 13, 14]. It is also known that solutions of bentonite will typically have a net negative charge due to the isomorphic substitutions of of Si^{4+} for Al^{3+} and Al^{3+} for Mg^{2+}. [15]

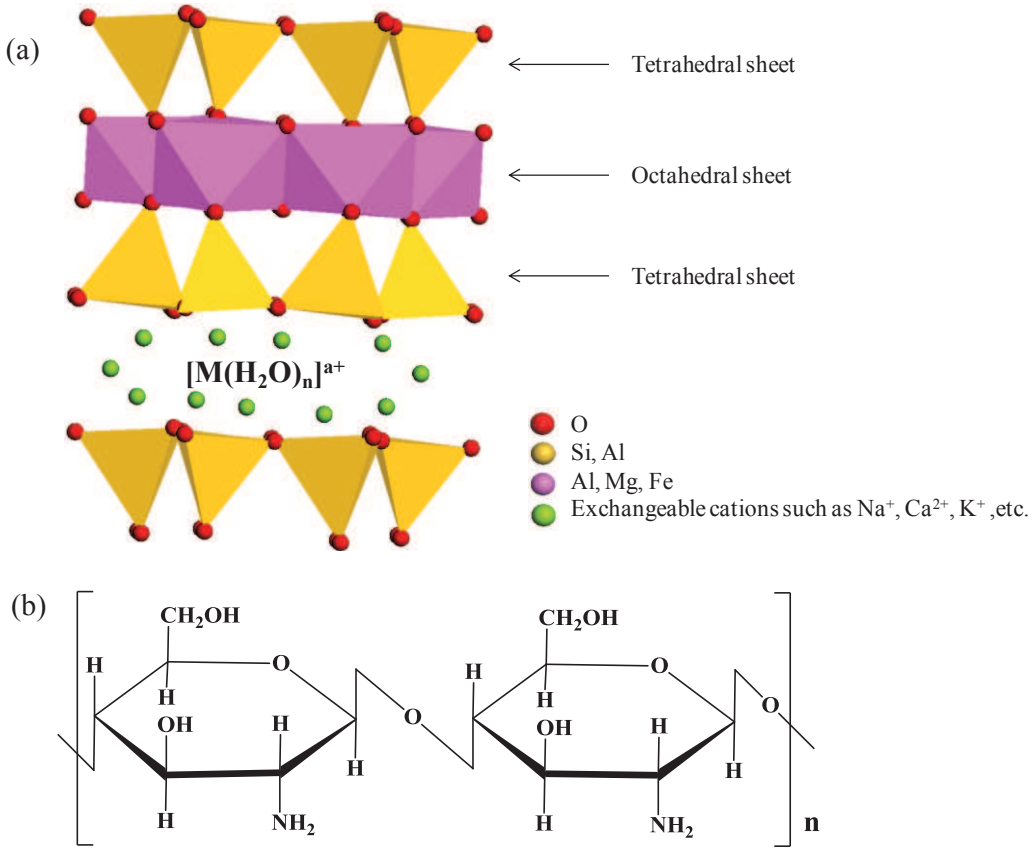

Fig.5.1. Schematic structures of bentonite (a) and (b) chitosan.

Color and turbidity are very important factors with regard to drinking water, and therefore the removal of turbidity from untreated water is an important factor in water management. The most common technique for the removal of turbidity uses both alum and polyaluminum chloride as coagulants. However, extensive alum intake has been associated with Alzheimer's disease [16, 17] and therefore novel materials with good adsorption properties and poor dispersion that do not increase the turbidity of water during the remediation process are required. Previous studies have identified chitosan as an eco-friendly coagulant and flocculant [18]. Previous studies have identified chitosan as an eco-friendly coagulant and flocculant due to its high cationic charge density, long polymer chains, bridging of aggregates, precipitation in neutral or alkaline pH conditions as well as its non-toxic and non-corrosive properties [18, 19]. Ahmad et al had successfully harvested of microalgae cells by coagulation using chitosan [20]. Chitosan (CS, Fig.5.1b) is a hydrophilic, nontoxic copolymer with abundant amino and hydroxyl groups that allow it to exhibit significant adsorption capacity for dyes and metal ions

[21, 22, 23]. As such, the enhancement of the coagulation abilities of kaolinite and bentonite suspensions by the addition of modified chitosan has been studied [24, 25, 26]. Diverse methods have also been applied to synthesize chitosan-modified bentonite and the bentonite/chitosan composite matrix has been widely used to adsorb heavy metal ions [24, 25], organic pollutants [10], dyes [25, 27], and other environmental contaminants [28].

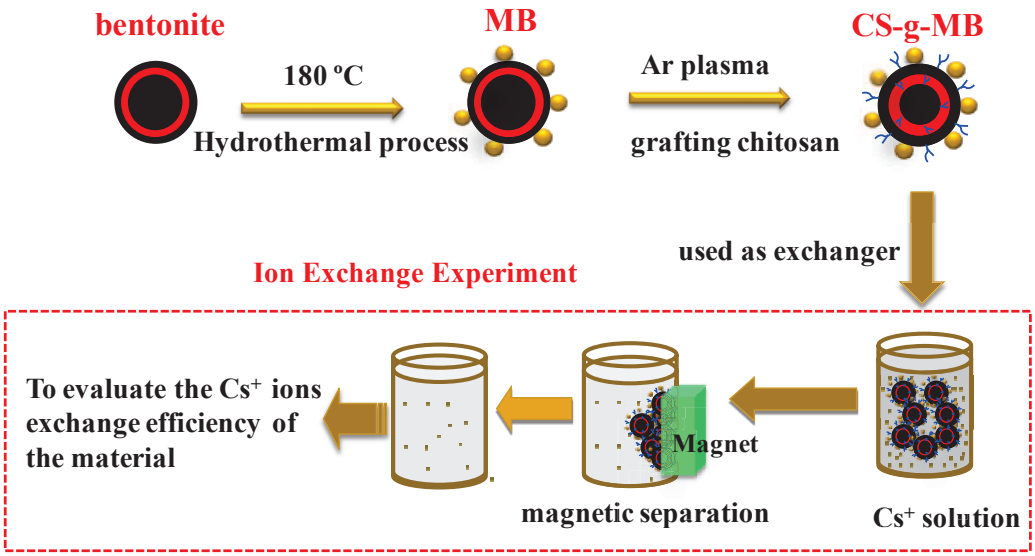

Fig. 5.2.Synthesis route of CS-g-MB and the design for exchange experiment.

Plasma treatment is a useful means of surface modification, since it is solvent-free, time-efficient, versatile, and eco-friendly [29, 30, 31]. During this process, the radicals, electrons, ions, and VUV/UV light generated by the plasma discharge strongly interact with the surfaces of materials and create active sites for the binding of functional groups. In our earlier work, we confirmed that a radio frequency (RF) Ar plasma is able to rupture C=C bonds to increase the reactivity of the multi-walled surfaces of carbon nanotubes as the result of Ar ion bombardment [32, 33, 34, 35]. This plasma-induced method can provide a wide range of different functional groups depending on the grafting material and the plasma discharge parameters, such as power, gas species, reaction time, and operating pressure. However, to the authors' knowledge, only a few studies regarding the modification of bentonite by plasma treatment have been reported.

Previous research studies have shown that -OH groups play a very important role in the Cs^+ ion adsorption process [4, 36, 37]. With this in mind, we attempted to design a novel chitosan-grafted magnetic bentonite (CS-g-MB) with a large Cs^+ ion adsorption capability and low turbidity in water solution, so as to avoid significantly increasing the turbidity of raw untreated water. In the present study, we used an RF-driven Ar plasma technique to obtain the first-ever synthesis of CS-g-MB. A schematic showing the formation of CS-g-MB and the exchange processes is presented in Fig.5.2. The objectives of this study were as follows: 1) to attach chitosan to bentonite; 2) to readily separate the treated bentonite from the adsorption medium by a simple magnetic process; 3) to achieve low turbidity in aqueous solutions; 4) to generate a material that was stable in both groundwater and seawater; and 5) to realize high efficiency in the removal of Cs^+ ions. This combination of goals was made possible by taking advantage of the abundant functional groups of chitosan and the spatial structure of bentonite, as well as through the application of magnetic nanoparticles. In the present study, a series of batch experiments were conducted under different physicochemical conditions, varying the ionic strength, pH, solid/liquid ratio, and competitive cations. A comparison of the performances of the CS-g-MB composite in contaminated actual seawater and in simulated groundwater was also performed.

5.2 Experimental details

5.2.1 Instruments and reagents

Bentonite was obtained from Gaomiaozicounty (Inner Monolia, China).Chitosan 100, ferric chloride ($FeCl_3$•$6H_2O$), anhydrous CH_3COONa, ethylene glycol, sodium dodecyl sulfate, and all other chemicals were purchased from Wako Pure Chemical Industries, Ltd. All reagents used in the experiments were of analytical purity without further purification.

Table 5.1 Summary table of reagents used in this study.

Reagents	degree	Compony

CH_3COONa	Analytical grade	Wako Pure Chemical Industries, Ltd.
Ethylene glycol	Analytical grade	Wako Pure Chemical Industries, Ltd.
Sodium dodecyl sulfate	Analytical grade	Wako Pure Chemical Industries, Ltd.
$FeCl_3•6H_2O$	Analytical grade	Wako Pure Chemical Industries, Ltd.
Bentonite	Gaomiaozi county	Inner Mongolia, China
Chitosan	100%	Wako Pure Chemical Industries, Ltd.
H_3PO_4	Analytical grade	Wako Pure Chemical Industries, Ltd.
CsCl	Analytical grade	Wako Pure Chemical Industries, Ltd.
NaOH	Analytical grade	Wako Pure Chemical Industries, Ltd.
$MgCl_2$	Analytical grade	Wako Pure Chemical Industries, Ltd.
CH_3COOH	Analytical grade	Wako Pure Chemical Industries, Ltd.
KCl	Analytical grade	Wako Pure Chemical Industries, Ltd.
NaCl	Analytical grade	Wako Pure Chemical Industries, Ltd.
HCl	37%	Wako Pure Chemical Industries, Ltd.
CsCl standard solution	1001 mg/L	Wako Pure Chemical Industries, Ltd.
LiCl	Analytical grade	Wako Pure Chemical Industries, Ltd.

Table 5.2 Summary table of instruments used in this study.

Instruments	**Model**	**Compony**
Pipet	200µl, 1000µl	Wako Pure Chemical Industries, Ltd.
FE-SEM	JSM-7001F	JEOL
XRD (Cu Kα radiation)	RINT-Ultima	Rogaku
XPS (Mg Kα X-ray source)	ESCA-3400	Shimadzu

TGA	DTG-60A	Shimadzu
BET	BELSORP MINI II	BELSORP
pH meter	pH 15-7Mo	LABINDIA
Atomic absorption spectroscopy	Solar S4-AA	THERMO ELECTRON

5.2.2 Preparation of magnetic bentonite

In this study, the magnetic bentonite was prepared by the hydrothermal process according to a literature with a few modifications.[38] In general, 0.81g ferric chloride, 40 mL ethylene glycol and 200 mg bentonite were mixed and stirred for 3h. Then 3.6g NaAc and 1.0 g sodium dodecyl sulfate were added with constant stirring for 1h. The mixture was sealed in a Teflon-lined stainless steel autoclave and maintained at 180ºC for 10h. After that, the products were separated with a permanent magnet and then washed with ethanol and Milli-Q water for several times, and finally dried at 50 ºC.

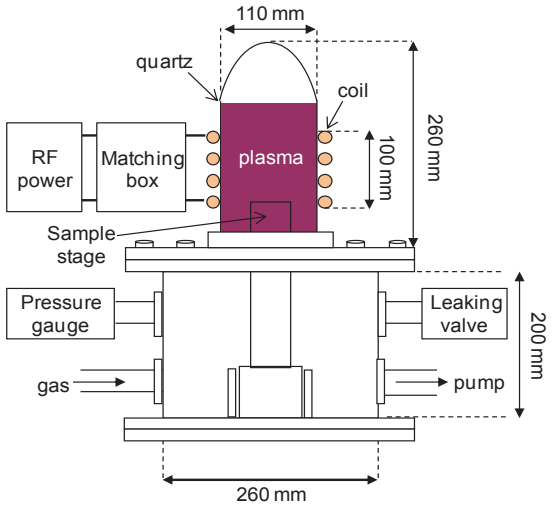

Fig. 5.3 Schematic view of experimental setup for inductively coupled radio frequency plasma.

5.2.3 Preparation of CS-g-MB composites

In our experiments, the inductively-coupled radio frequency plasma device we employed had already been described in our previous papers.[39, 40] A schematic diagram of the compact experimental setup is shown in Fig.5.3. The CS-g-MB composite was synthesized via a two-step method by low-temperature plasma-induced grafting procedure in Ar atmosphere. The plasma induced grafting procedures consist of two successive processes: surface activation and chitosan grafting, as described in Ref.[37]. After the plasma induced grafting procedure, the CS-g-MB composites were gathered by a permanent magnet, washed several time with 0.01 mol/L H_3PO_4 solution and Milli-Q water, and finally dried at 60 ºC. The synthesized particles were characterized by BET (BELSORP MINI II), FE-SEM (JEOL JSM-7001F), XRD equipped with Cu Kα radiation (λ=0.154 nm), XPS (Shimadzu ESCA-3400) with Mg Kα X-ray source, magnetic measurement (MPMS-XL SQUID magnetometer) and TGA (Shimadzu DTG-60A) analysis with a heart rate of 10 ºC/min from 35to 800 ºC.

5.2.4 Cesium adsorption experiment

The CS-g-MB sample was used as cesium cation exchanger to determine its removal efficiency. A sample of 3.6 mgwas immersed in 6 mL CsCl solution in a polypropylene tube, and then $NaClO_4$ solution was added as the background electrolyte solution. The pH was adjusted with NaOH or HCl solution. After ultrasonic treatment for 30 min, the samples were shaking for 24 h. And finally, the solution phases were separated with a permanent magnet. The concentration of Cs^+ ions in the solution phase was determined by atomic absorption spectroscopy (Thermo Scientific Solar S4-AA). The amounts of Cs^+ exchange with the samples were calculated based on the differences between Cs^+ concentrations in the solution before and after the experiment. Similar cation effect experiments were performed using $MgCl_2$, $LiClO_4$, and $KClO_4$. The schematic of the formation of CS-g-MB and the exchange processes are shown in Fig.5.2.

The amount of Cs^+ ions removed by CS-g-MB were calculated according to Eqs.(5-1):

$$Cs^+ \text{ removed } (\%) = \frac{(C_0 - C_t)}{C_0} \times 100\% \qquad (5\text{-}1)$$

where C_0 and C_t represent the initial and at time t concentrations (mg/L) of Cs^+ ions, respectively, W is the mass of sorbent (g), V represents the volume of the suspension (L) and 132.9 is the standard atomic weight of cesium.

5.3 Results and discussion

5.3.1 Material characterization

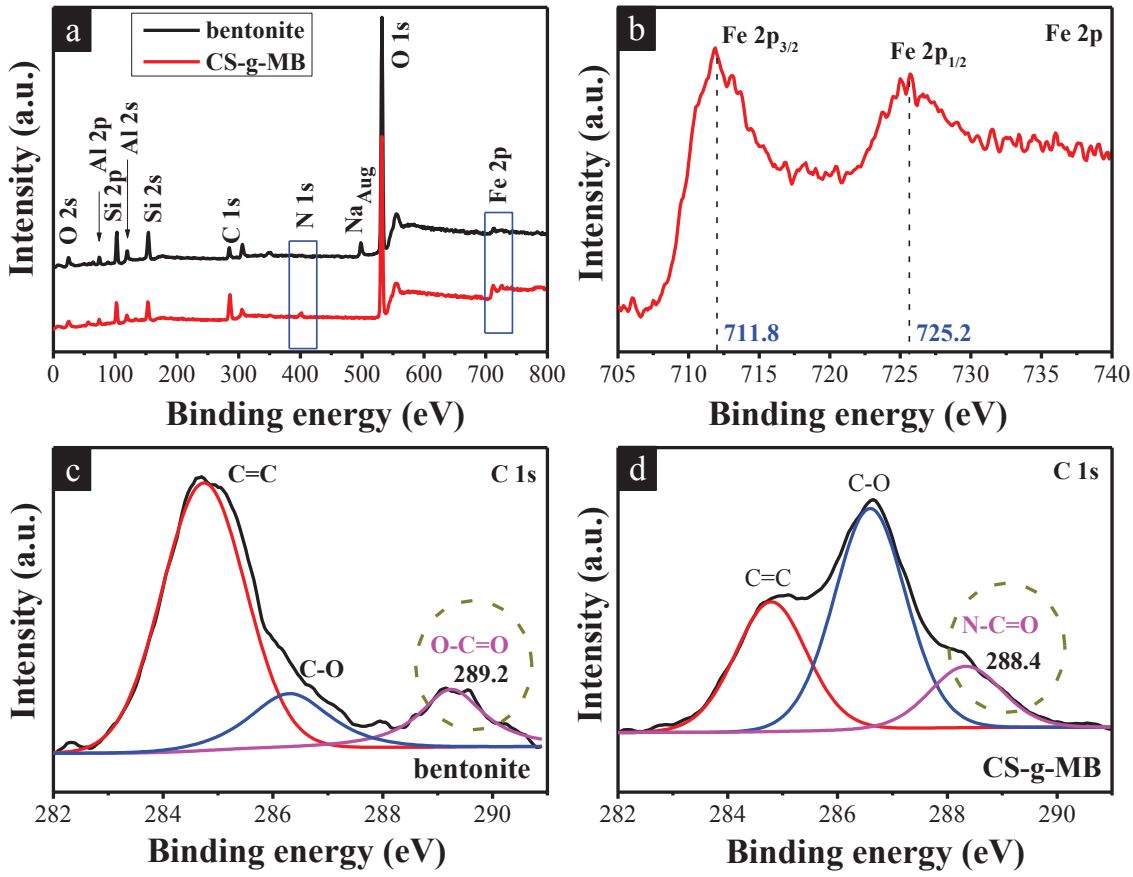

Fig. 5.4 XPS spectra of survey scan (a), Fe 2p spectrum (b), and C 1s spectrum of bentonite (c) and CS-g-MB (d).

The CS-g-MB composite was synthesized via a plasma-induced method. More detailed information on the experimental setup and experimental details are described in supporting information. The surface areas of the original bentonite and the synthesized CS-g-MB

composite were determined by N_2 Brunauer-Emmett-Teller (BET) measurements to be 18.52 and 31.7 m^2/g, respectively. The X-ray photoelectron spectroscopy (XPS) data in Fig. 5.4a indicate the presence of Al, Si, C, O, and Fe on the surfaces of the bentonite and CS-g-MB composite. The spectrum of the CS-g-MB composite shows characteristic peaks for N 1s (402.6 eV), indicating the effective connection of chitosan onto the bentonite structure [37, 41], while the characteristic Si peaks are attributed to the silica sheets of bentonite[25, 42]. The Fe 2p peak of the bentonite is due to the substitution of Fe^{3+} for Si^{4+} in the bentonite structure. In contrast to the bentonite, the Fe 2p peak in the CS-g-MB spectrum is muchmore intense, an effect that is related to the magnetic properties of the bentonite. A twinned Fe 2p peak is seen in Fig.5.4b, and the binding energies of these two peaks indicate the formation of an Fe_3O_4 phase in the composite rather than Fe_2O_3[43, 44].

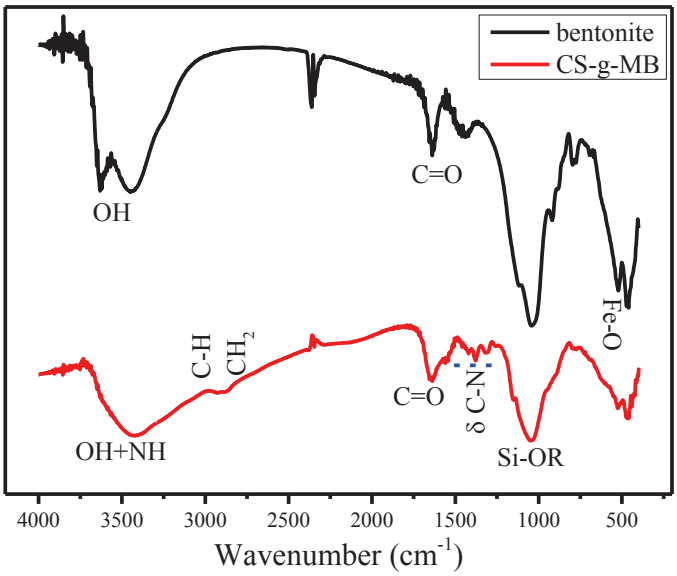

Fig. 5.5 FT-IR spectra of CS-g-MB composite.

It should also be noted that the C 1s spectrum of the CS-g-MB composite is quite different from that of the bentonite (Fig.5.4c and 5.4d). The characteristic C peaks in this spectrum are attributed to the organic carbon in the bentonite. Many studies have shown that organic matter can be stabilized by intimate association between clay mineral particles [45, 46, 47]. The C 1s spectrum of the bentonite in Fig. 5.4c can be deconvoluted into three components: (1) a C=C peak (284.4 eV); (2) a C-O peak (286.2 eV); and (3) a carboxylate carbon peak

(O-C=O, 289.2eV). It is remarkable that the C 1s spectrum of the CS-g-MB composite in Fig.5.4 is different from that of the bentonite. The carboxylate carbon peak has been replaced by an amide peak (N-C=O, 288.4 eV), indicating that chitosan was grafted onto the bentonite through the reaction of amino groups with carboxylate groups. A further proof that the FT-IR spectra also reveal the existence of CO-NH functional group in CS-g-MB composite was offered (Fig.5.5). During the plasma treatment, many reactive species, such as radicals, electrons, and ions, are generated by the plasma discharge and can readily interact with the surface of the material to create active sites for further modification [39, 48]. In our previous work, we have confirmed that an RF Ar plasma can break C-C bonds to increase the reactivity of carbon nanotubes following Ar ion bombardment [32, 33, 34, 35]. The increased intensity of the C 1s and C-O peaks also result from the grafted chitosan. More detailed information and analysis are presented in Table 5.3. These data clearly show that the C, N, and Fe concentrations have greatly increased, indicating that the CS-g-MB composite was synthesized successfully.

Table 5.3 Peak results of XPS Spectra.

	peak	Start BE[a] (eV)	End BE[a] (eV)	FWHM[b] (eV)	%
bentonite	C 1s	281.85	291.35	1.86	9.59
	Si 2p	99.45	106.40	1.69	16.15
	O 1s	527.50	536.35	2.14	73.66
	Fe 2p	704.76	740.50	4.63	0.60
CS-g-MB	C 1s	281.85	291.15	1.54	20.81
	Si 2p	99.45	106.40	1.80	10.92
	O 1s	527.50	533.62	2.50	62.60
	N 1s	396.45	405.45	2.69	2.48
	Fe 2p	704.76	740.5	5.03	3.19

a: binding energy; b: full widths at half maximum.

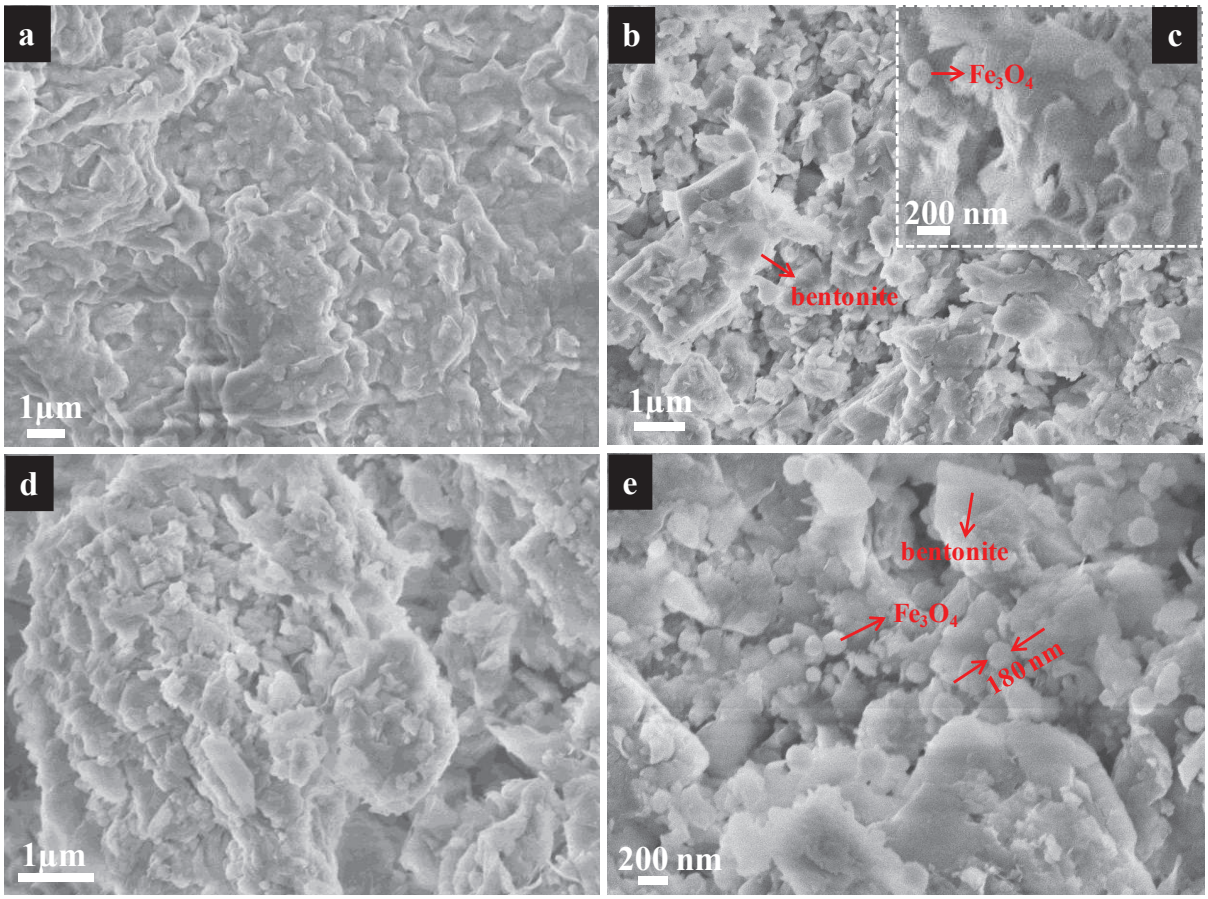

Fig.5.6. SEM images of pristine bentonite (a), MB (b) and CS-g-MB composite (c and d).

In order to verify the above, the morphologies and microstructures of the samples were characterized by SEM. Fig.5.6a shows that the bentonite displays rock-like macroparticles with rough, crumpledsurfaces. Following magnetic modification, some cracks and small structures are observed on the surface of the magnetic bentonite (MB) (Fig.5.6b), indicating the partial exfoliation of the bentonite layer during the hydrothermal process. Several spherical magnetic nanoparticles are also observed on the MB surface, which is consistent with the results of a previous study [38]. After chitosan coating, much thinner structures are observed in the CS-g-MB (Fig.5.6d), and therefore the bentonite structures were exfoliated into smaller pieces. We believe that this change is closely related to the intercalation of the chitosan into the bentonite layers. From the high-resolution SEM images of the CS-g-MB (Fig.5.6e), we can also see that the surface of the CS-g-MB composite consists of spherical,

magnetic Fe_3O_4 nanobeads with diameters of approximately 150 nm. In addition, these sphere-like structures are randomly distributed over the surface.

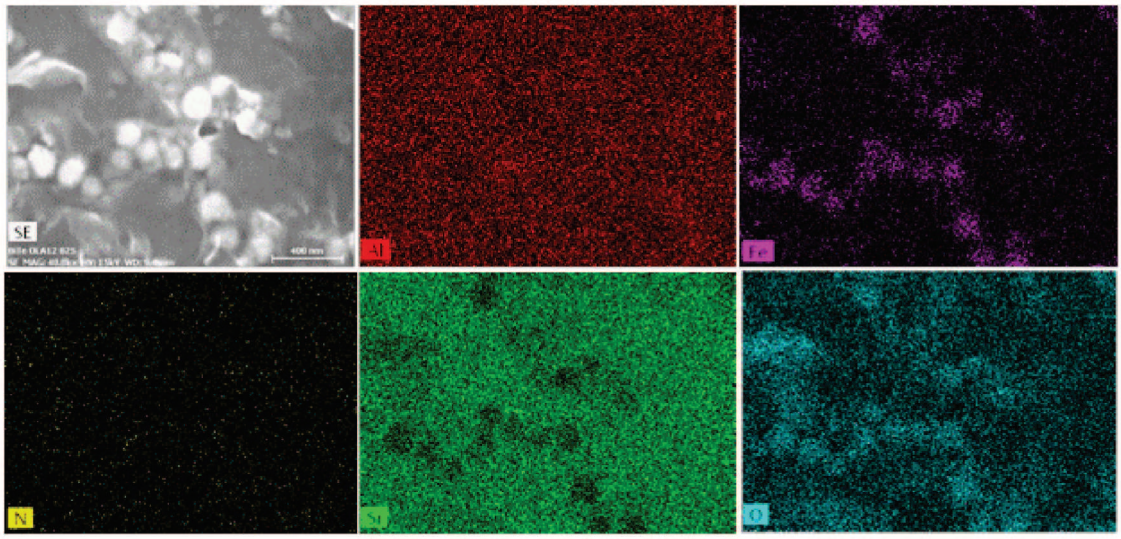

Fig.5.7. The elemental mapping of the homogenous dispersion of Al, Si, Fe, O, and N elements in the CS-g-MB.

In addition, from the high-resolution SEM images of the MB and CS-g-MB composite (Fig. 5.6c and 5.6e), many spherical magnetic Fe_3O_4 nanobeads with diameters of 130-180 nm were observed and randomly distributed over the surface. The further proof about the spherical magnetic particles was provided by the elemental mapping of the CS-g-MB composite (Fig. 5.7). It can be seen that N exists homogeneously in CS-g-MB composite, indicating that chitosan was grafted onto magnetic bentonite.

The XRD patterns of the samples were used to evaluate the basal spacing between layers of the clay, as shown in Fig. 5.8a and Table 5.4. The three curves all show a large peak at 2θ = 26.7º, corresponding to the pattern of quartz, suggesting that the bentonite consists of quartz phase (Fig. 5.8a). [49] Fig. 5.8b shows the comparison XRD patterns of MB with the standard reference materials (Fe_3O_4 and δ-FeOOH). The serious of characteristic peaks of MB at 2θ = 30.3º, 35.6º, 43.3º, and 57.2º, correspond to the diffractions of (220), (311), (400), and (511) crystal faces of Fe_3O_4 with a face-centered cubic structure (JCPDS card No. 19-0629).[50, 51] The weak peaks of the bentonite near 2θ = 35.6º is due to the substitution of Fe^{3+} for Si^{4+} in

the bentonite structure. In contrast to MB and CS-g-MB, the diffraction peaks near diffraction peaks in bentonite patterns are much weaker, which is related to the additional magnetic properties of MB and CS-g-MB. During this series of modification processes, the (001) reflection of the bentonite shifts gradually from 7.06º to 6.05°, implying the formation of an exfoliated structure resulting from the chitosan addition, and confirming that the CS-g-MB composite was successfully synthesized.

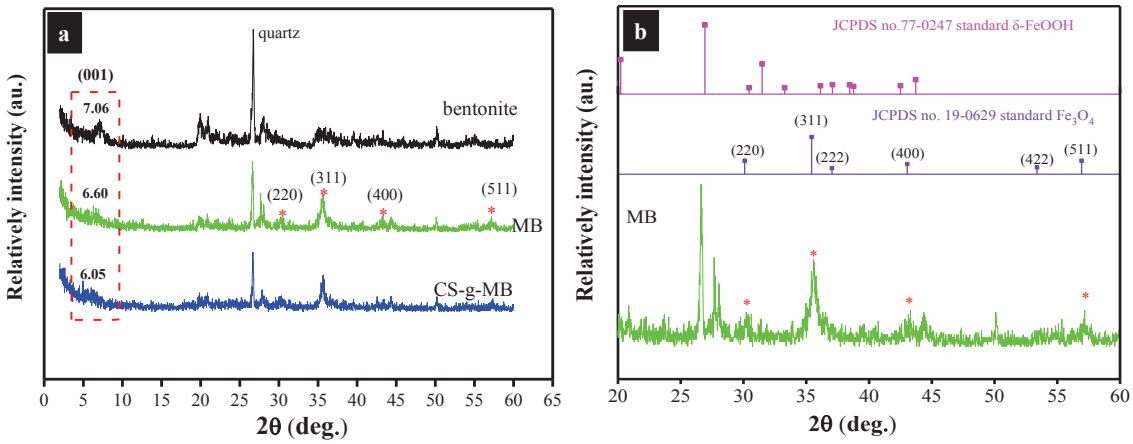

Fig. 5.8. (a and b) XRD curves of bentonite, MB and CS-g-MB.

Table 5.4. The diffraction angle (2θ) and interlayer spacing (d_{001}) of samples.

Samples	2θ	d_{001}(nm)
bentonite	7.06	1.25
MB	6.60	1.34
CS-g-MB	6.05	1.46

From Bragg's Law, we can determine that the chitosan addition had an impact on the spacing of the bentonite layers. Bragg's Law is expressed as in Eq. (5-2):

$$2dsin\theta = n\lambda \qquad (5\text{-}2)$$

where d is the spacing between the planes, θ is the angle between the incident and reflected rays, n is the order of the reflection, and λ is the X-ray wavelength. It was determined that the d_{001} spacing in natural bentonite was 1.25 nm. However, after the additions of the magnetic

Fe_3O_4 nanobeads and the chitosan, the d_{001} values increased to 1.34 and 1.46 nm, respectively, values that are consistent with the SEM results in Fig. 5.6. These results suggest an exfoliated structure resulting from the chitosan addition, and confirm that the CS-g-MB composite was successfully synthesized.

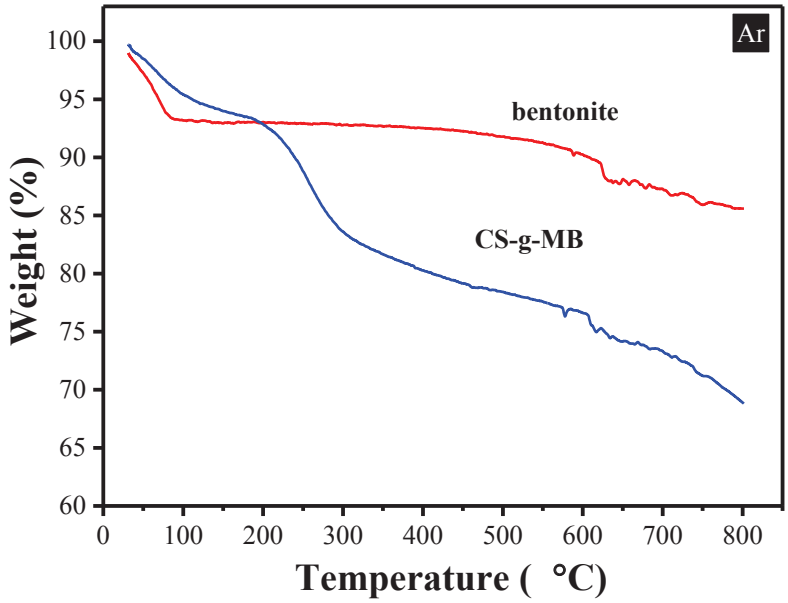

Fig. 5.9. TGA curves of bentonite and CS-g-MB.

The weight percentage of grafted chitosan in the CS-g-MB composite can be estimated by thermogravimetric analysis (TGA). Fig. 5.9 presents the TGA curves of the bentonite and CS-g-MB under a flow of Ar atmosphere. The approximate 6.8% mass loss of the bentonite up to 100 ºC is attributed to the elimination of absorbed water. The weight loss (～ 1.8%) from 100 to 550 ºC can be negligible. The second stage of mass loss (~ 5.8%) from 550 to 800 ºC is due to the self-dehydroxylation of the hydroxyl groups on the surface of the bentonite [52]. The initial mass loss of about 6.3% from 35-160 ºC seen in the TGA curve of the CS-g-MB is primarily attributed to the evaporation of absorbed water and ethanol. A distinct mass loss of approximately 16.2% between 160 and 550 ºC that is not seen in the bentonite is possibly due to the loss of grafted chitosan. In addition, we believe that there are two possible reasons for the mass loss from 550 to 800 ºC. The first is, again, the self-dehydroxylation of hydroxyl groups on the bentonite surface. The second is the phase transition from Fe_3O_4 to

FeO. O'neill [53] had showed that there have following chemical reactions between 560 ºC <T <997 ºC:

$$2Fe_3O_4 \rightleftharpoons 6FeO + O_2$$

$$4Fe_3O_4 + O_2 \rightleftharpoons 6Fe_2O_3$$

$$0.5Fe_3O_4 \rightleftharpoons 1.5Fe + O_2$$

$$Fe_2O_3 \rightleftharpoons FeO + O_2$$

$$2FeO \rightleftharpoons 2Fe + O_2$$

However, FeO is the only thermodynamically stable species during this temperature.[53, 54] Therefore, in the present work, the Fe_3O_4 content was less than 8.7 wt% while the chitosan content was approximately 16.2 wt%.

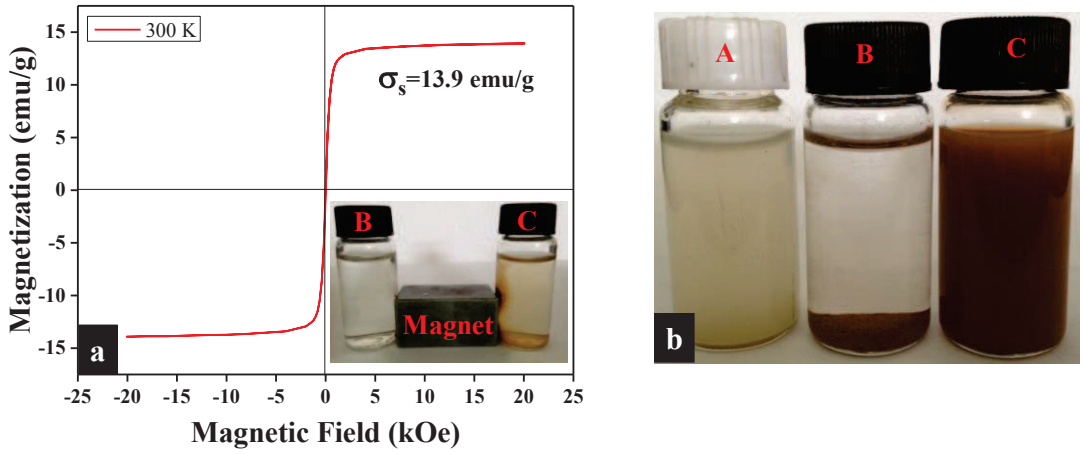

Fig.5.10. Magnetization curve of CS-g-MB composite at 300 K (a) and a comparison of turbidity of (A) bentonite, (B) CS-g-MB composite and (C) MB suspensions imaged after 2.5 hours (b).The inset figure of (a) shows the magnetic property of (B) CS-g-MB composite and (C) MB solution under an external magnetic field.

Further investigations of the CS-g-MB composite were performed using a vibrating sample magnetometer. The magnetic hysteresis curve of the sample measured at 300 K shows features typical of magnetically soft ferrites (Fig. 5.10a). The saturation magnetization value

of the CS-g-MB composite is 13.9 emu/g, indicating the good magnetic property that is critical for separation. The magnetic separation of the sample was also assessed in water by placing a magnet near a glass bottle containing a dispersion of the material. In this manner, complete magnetic separation could be achieved in less than 10 min. The inset to Fig. 5.10a shows that both the CS-g-MB suspension (B) and the MB suspension (C) were attracted toward the magnet within a short time period, demonstrating the high magnetic sensitivity of our product, which could be very convenient with regard to the practical applications of these materials as adsorbents.

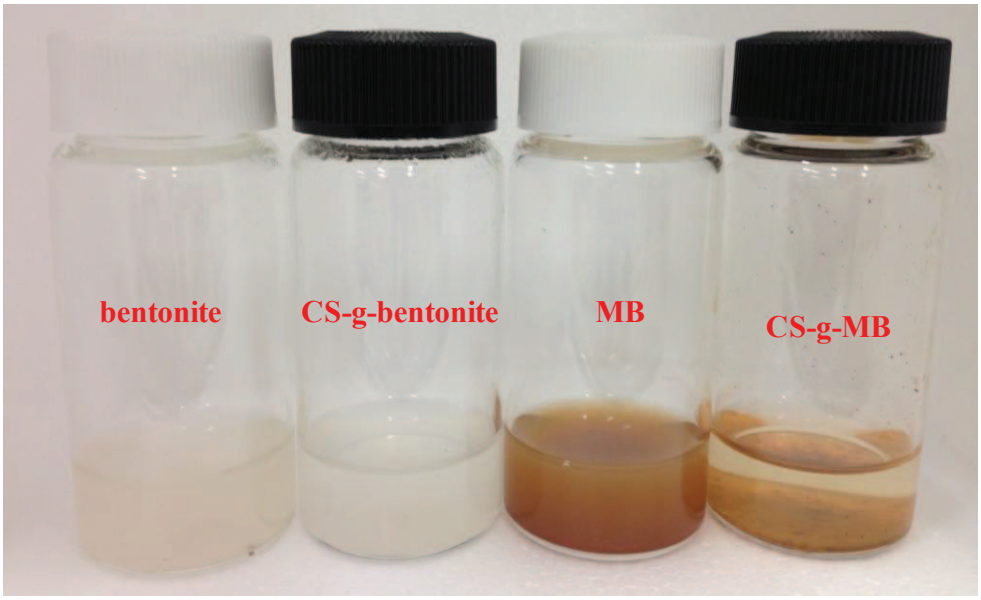

Fig. 5.11 Visual images of bentonite, CS-g-bentonite, MB and CS-g-MB suspensions obtained after 2 days. (Sorbents =1.4 g/L)

Materials with poor dispersion properties will always exist in the form of agglomerates, and this agglomeration can assist in avoiding significant increases in the turbidity of untreated water as well as in the separation of the material from the solution. In Fig. 5.10a, the magnetically separated portion of the CS-g-MB suspension (B) is not clear, an effect that is related to the presence of larger agglomerates than are found in the MB suspension (C). A comparison of the turbidities of bentonite, CS-g-MB composite, and MB suspensions is provided in the inset to Fig. 5.10b, and it is evident that the visual appearance of turbidity is

drastically different among these three samples. The addition of chitosan to the MB greatly changes the turbidity of the MB suspension, and the poor dispersion of the CS-g-MB composite confirms that chitosan was successfully grafted onto the MB. Furthermore, the turbidity of chitosan grafted bentonite (CS-g-bentonite) suspension was also compared, indicating the sorbent without magnetic nanoparticles could not be separated directly from the aqueous solution by gravity (Fig. 5.11). Furthermore, with magnetic nanoparticles, it is a great advantage that we can realize a quick separation the cesium ions and remove the adsorbents to improve the turbidity by the magnet.

These results indicate that the enhanced coagulation by plasma modification represents a viable, advanced technology with applications in wastewater management. These results thus suggest future approaches in which new adsorbents can be readily separated from the solution, thus avoiding any increases in the turbidity or color of the water.

5.3.2 Cation exchange results

The pH-dependence of Cs^+ ion adsorption has been studied by many researchers [4, 55, 56], and the results indicate that the pH of a solution has a significant effect on the uptake of Cs^+ ions. From Fig. 5.12a, it is evident that the removal of Cs^+ ions increases gradually with rising pH. The observed pH-dependence of Cs^+ removal by the CS-g-MB composite may stem from competition for adsorption by hydronium ions, as well as the deprotonation states of functional groups. The pH_{zpc} was detected as 4.3 for CS-g-MB suspension (Fig. 5.13).

The effective hydrated radius of the hydronium ion (0.280 nm as H_3O^+) is smaller than that of Cs^+ (0.329 nm), and therefore the hydronium ions can more readily attach to adsorption sites. At low pH, it is conceivable that the highly concentrated H_3O^+ ions are able to compete with Cs^+ ions, such that there are fewer sites available for Cs^+. As well, the majority of the amino and hydroxyl groups in the CS-g-MB composite, which originate from the grafted chitosan, are protonated at low pH, resulting in electrostatic repulsion between the composite and Cs^+ ions. With increasing pH, the competition from the hydronium ions is reduced, as is the degree of protonation of the functional groups in the composite. Thus, in the combined

bentonite/chitosan structure, the abundant functional groups allow more efficient utilization of adsorption sites at higher pH.

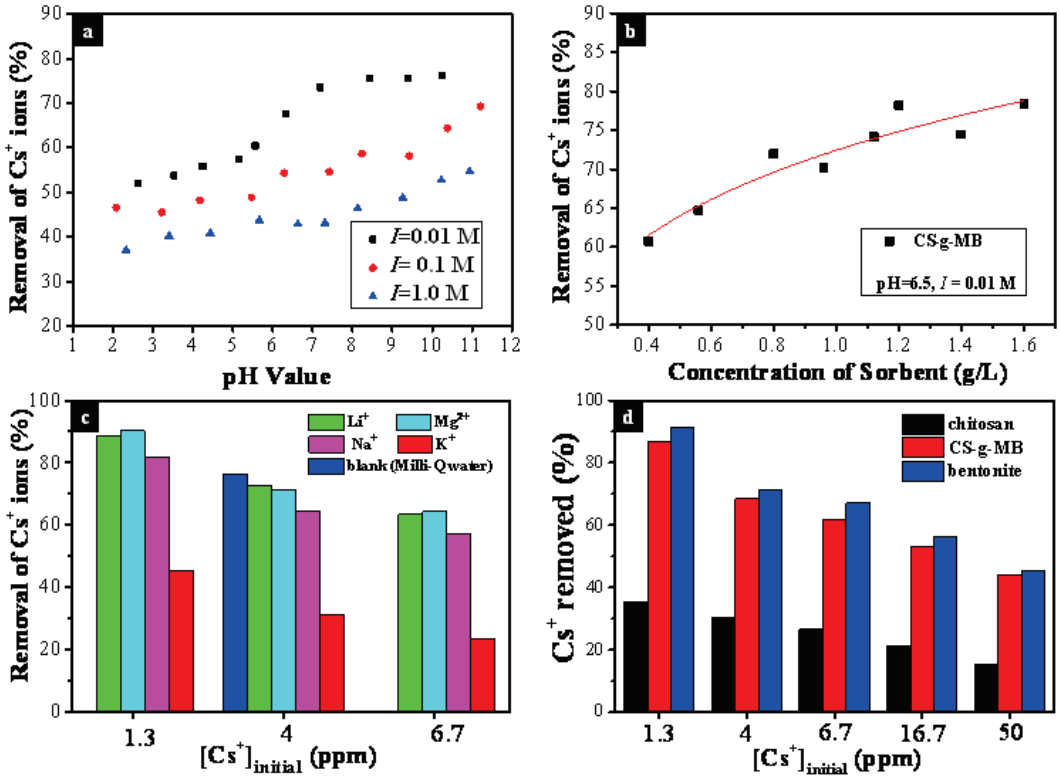

Fig. 5.12. (a) Effect of initial pH and ionic strength ($[Cs^+]_{initial}$=4ppm, m/V=1.0 g/L), (b) effect of adsorbent dose for Cs^+ ion adsorption by CS-g-MB composite ($[Cs^+]_{initial}$=4ppm, pH=6.5), (c) effect of different competitive cations with the different concentration of cesium ion ($[Mn^+]_{initial}$=0.01mol/L, m/V=1.0 g/L and pH=6.5), and (d) the effect of initial Cs^+ concentration for Cs^+ adsorption by materials (m/V=1.0 g/L, pH=6.5 and $[Na^+]_{initial}$=0.01mol/L).

The exchange capacity for Cs^+ ions approaches nearly 80% at pH > 8 and an ionic strength (I) of 0.01 M (using an initial Cs^+ concentration of 4 ppm and a composite concentration of 1.0 g/L). The ionic strength (I) of the solution was calculated by the following equation[57]:

$$I = \frac{1}{2}\sum_{i=1}^{n} c_i z_i^2 \qquad (5\text{-}3)$$

Where c_i is the ionic concentration (M, mol/L), z_i is the charge ofthe ion and the summation is used to account for all ions in the solution.

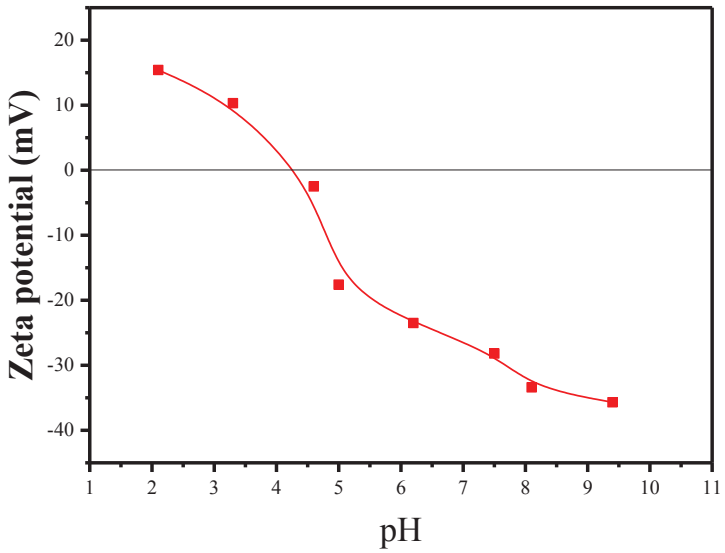

Fig. 5.13. Zeta potential as a function of pH for CS-g-MB composites.

The adsorption of Cs^+ ions thus depends on the type and concentration of cations competing for adsorption. In Fig.5.12a, we primarily consider the concentration of the background electrolyte. Here, the solutions had ionic strengths of 0.01, 0.1, and 1.0 M based on the addition of 0.01, 0.1, and 1.0 M $NaClO_4$, respectively. We can see that, within the ionic strength range of 0.01 to 1.0 M, the removal of Cs^+ ions by the CS-g-MB composite is obviously affected by ionic strength. The percentage removal of Cs^+ions increases with decreasing ionic strength, which is in agreement with the results of previous studies [5, 37]. We propose that there are two main reasons for this phenomenon. The first is the water activity effect and the large difference in ionic hydration energy between the exchanging species[58, 59, 60, 61]. With increasing ionic strength, the water activity decreases and those cations, such as Cs^+, with low hydration energies increase their extent of hydration to a greater extent than ions with high hydration energies, such as Na^+ [62, 63]. The second reason is that, at low ionic strength, fewer Na^+ ions are available to compete with Cs^+ ions as exchangeable cations, either at bentonite layers or at the functional groups of the chitosan. Therefore, the principal mechanism of Cs^+ ion adsorption by CS-g-MB composite is cation exchange. The cation

exchange capacity of a material is thus a very important factor to consider when selecting a highly efficient sorbent to remove Cs^+ ion from radioactive wastewater.

The effects of the CS-g-MB concentration on Cs^+ ion removal were also investigated. As shown in Fig.5.12b, the removal percentage increased rapidly as the solid/liquid ratio was increased. This trend was not unexpected, since higher concentrations of the adsorbent correspond to more active sites for Cs^+ ion adsorption.

An additional important characteristic of Cs^+ adsorption is the significant effect of the competing cation species. In Fig. 5.12c, we assess the effects of competition by monovalent alkali and divalent alkaline-earth II cations (Li^+, Na^+, Mg^{2+}, and K^+) with respect to the removal of Cs^+ ions. These four cations were selected due to their natural abundance in water. Our results indicate that, at a concentration of 0.001 M, the removal of Cs^+ ions is decreased in the order of $Li^+ \approx Mg^{2+} > Na^+ > K^+$. The results therefore demonstrate that the presence of these four cations can inhibit Cs^+ adsorption and that K^+ has the most significant effect. This relative effect is thought to result from the hydrated radius and the hydration energy of the cations in aqueous solution. The bare and hydrated radii of the cations are given in Table 5.5, from which it is evident that, as the atomic number increases, so does the ionic size, resulting in a decrease in the hydrated radius and the absolute value of the enthalpy of hydration. The hydrated radius of 0.331 pm for K^+ is very close to that of 0.329 pm for Cs^+, and both ions also have similar hydration energies [64]. For this reason, K^+ ions can compete more effectively with Cs^+ ions for adsorption on the CS-g-MB composite. It is important to note that the hydrated radii decrease in the order of $Mg^{2+} > Li^+ > Na^+ > K^+ > Cs^+ > H_3O^+$, which is almost the same as the descending order of Cs^+ adsorption capacity. The Cs^+ ions are exchanged in the form of $Cs(H_2O)_n^+$ during the cation exchange process, since ions in solution are always hydrated; that is, tightly bound to water molecules through ion-dipole interactions [63, 65, 66]. In addition, the number of water molecules contained in the primary hydration shell will vary with the radius and charge of the ion and so the structures of hydrated metal ions in aqueous solution display a variety of configurations dependent on the size and electronic properties of

the ion. Persson has demonstrated that $Li(H_2O)_6^+$ and $Mg(H_2O)_6^{2+}$ ions are of the same size and have similar octahedral configurations [67]. Therefore, in the present study, Li^+ and Mg^{2+} ions in the form of $Li(H_2O)_6^+$ and $Mg(H_2O)_6^{2+}$ generated similar reductions in the adsorption of Cs^+.

A comparison of the exchange efficiencies of chitosan, bentonite, and the CS-g-MB composite is provided in Fig. 5.12d. The removal percentagedecreases in the order of chitosan < CS-g-MB < bentonite, and there is thus an obvious difference between chitosan and the CS-g-MB composite.Previous research has shown that the -OH groups play a very important role in the Cs^+ ion adsorption [4, 36, 37]. However, in our case, we consider that the low removal efficiency of chitosan is strongly related to the structure of this material [68, 69]. In addition, decreased removal efficiency was observed for the CS-g-MB composite compared to bentonite, whichresults from a combination of effects, including the exfoliation of the bentonite layers and the exchange reaction between Fe^{3+} and the exchangeable cations of bentonite [28, 37, 70].

Table 5.5 The bare and hydrated radii of cations.

Ion	Ionic radius(nm)	Hydrated radius(nm)
H_3O^+	0.115	0.280
Li^+	0.094	0.382
Na^+	0.117	0.358
K^+	0.149	0.331
Cs^+	0.186	0.329
Mg^{2+}	0.072	0.428

Compiled from Refs.[63, 71, 72, 73]

Equilibrium isotherms can provide useful information on the adsorption mechanism. In this study, we examined the relationships between removed Cs^+ ions and the residual amounts in aqueous solutions at sorption equilibrium, employing different water systems (actual seawater

and simulated groundwater) to estimate the stability of CS-g-MB (Fig. 5.14a). The seawater used in the present research was taken from the Pacific Ocean near Hamamatsu, Japan. Simulated groundwaterwas also prepared and further information about the two water systems is provided in Table 5.6.

Table 5.6. Concentration of some selected major cation ions and pH value of the two water systems.

Water system	Na^+ (ppm)	Mg^{2+} (ppm)	Ca^{2+} (ppm)	K^+ (ppm)	pH
Seawater	4381	1002	544.8	403.2	7.61
Simulated groundwater	115	120	35	195	5.02

We chose the Langmuir and Freundlich isotherm models[74, 75], both of which are widely used to simulate experimental data (Fig. 5.14a). The Langmuir (Eq. 5-4) and Freundlich (Eq. 5-5) models are expressed as follows:

$$Q_e = \frac{Q_m K_L C_e}{1 + K_L C_e} \tag{5-4}$$

$$Q_e = K_F C_e^{1/n} \tag{5-5}$$

where Q_e is the equilibrated Cs^+ concentration, Q_m (mg/g) is the maximum sorption capacity, K_L (L/mg) is the Langmuir adsorption constant, K_F (mol^{1-n} L^n/g) is the adsorption capacity when the Cs^+ equilibrium concentration is equal to 1, and *1/n* is the Freundlich adsorption.

Table 5.7. Sorption constants for Langmuir and Freundlich isotherm models.

CS-g-MB	Langmuir			Freundlich		
	Q_m (mmol/g)	K_L (L/mmol)	R^2	n	K_F (mmol/g)	R^2
Simulated groundwater	1.21	7.72	0.936	2.28	1.35	0.918

Seawater	1.12	4.38	0.913	1.96	1.13	0.826

Very similar Cs^+ adsorption isotherms were determined for adsorption from contaminated seawater and simulated groundwater, as shown in Fig. 5.14a. The maximum adsorption capacity (Q_m) of Cs^+ on the CS-g-MB composite in the contaminated simulated groundwater (1.21 mmol/g) was greater than that in contaminated seawater (1.12 mmol/g), as can be seen from the data in Table 5.7. The synthesized material was able to remove 76% of Cs^+ ions from the contaminated pure water at CsCl(aq) concentration as 4 ppm (Fig. 5.14b), while a rapid decrease in simulated groundwater and seawater. We believe that these results are closely related to the ionic strengths of the three water systems. The concentrations of the four competitive cations (Li^+, Mg^{2+}, Na^+, and K^+) in the actual seawater were higher than in the simulated groundwater and pure water, indicating a higher ionic exchange in seawater. During these trials, it was also found that the adsorption material was stable in both the contaminated seawater and groundwater over long periods of time.

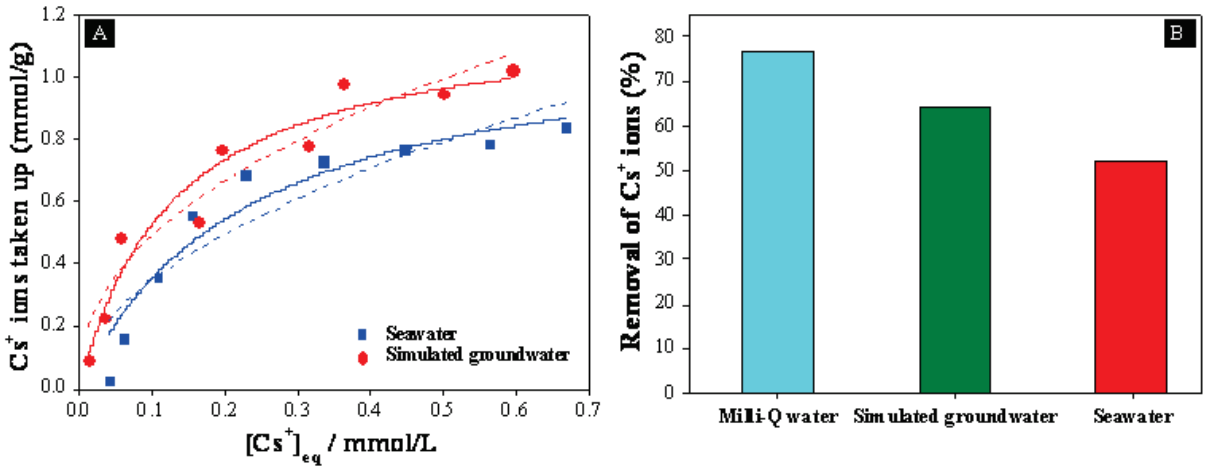

Fig. 5.14. Adsorption isotherms (a) and removal efficiency (b) for Cs+ions by CS-g-MB composite in Milli-Q water, real seawater and simulated groundwater ($[Cs+]_{initial}$=4ppm, m/V=1.0 g/L). Symbols denote experimental data, solid lines represent model fitting of the Langmuir equation, and dash lines represents the model fitting of the Freundlich equationconstant.

From Table 5.7, it is also apparent that the Langmuir isotherm generated a better fit to our experimental data compared to the Freundlich model, which indicating that monolayer coverage of the adsorbate is the main adsorption mechanism. In addition, the maximum adsorption of Cs^+ ions on the CS-g-MB composite was 10.0% lower than the amount adsorbed on pure bentonite (1.33 mmol/g), which is consistent with the results in Fig. 5.12d. As noted, the decreased adsorption of Cs^+ions on the composite is attributed to the exfoliated bentonite structure and the isomorphic substitution of Fe^{3+} for Si^{4+}. The adsorption capacities of Cs^+ ions on various materials as reported in the literature are summarized in Table 5.8, and the CS-g-MB composite shows a higher adsorption capacity than a number of other sorbents. Taking into consideration the good magnetic properties, low turbidity, and stability in aqueous solution of the CS-g-MB composite, it appears to be a good candidate for the removal of Cs^+ions from contaminated groundwater and seawater. These results should thus assist in the application of bentonite-based materials to the remediation of nuclear waste and drinking water and thus allow the development of new adsorbents that can be easily removed from solution and that do not increase either the turbidity or color of the water being treated.

Table 5.8. Comparison of maximum sorption capacity for Cs^+ ions by various sorbents.

Sorbents	C_{smax} (mmol/g)	References
CNTs	0.24	[37]
bentonite	1.33	[37]
Prussian blue	0.99	[4]
Prussian blue+CNT	1.08	[4]
SAMMS	1.14	[76]
CoFC@Glass-Py	1.30	[77]
CS-g-MB	1.21	This work

5.3.3 Mechanisms of Cs^+ ion adsorption by the CS-g-MB composite

Based on the characterization and Cs^+ ion exchange experimental investigations, a cation exchange mechanism involving hydrated Cs^+ ions is considered to be the main mechanism for Cs^+ ion adsorption on the CS-g-MB composite. In the present study, the cation exchange mechanism appears to consist of two parts: the $Cs(H_2O)_n^+$ ions exchange with the exchangeable hydrated cations ($[M(H_2O)_n]^{a+}$) consisting of monovalent Group I (a=1) and divalent Group II (a=2) metals (such as Na, Ca, and K) between the layers, while $Cs(H_2O)_n^+$ ions exchange with chitosan functional groups such as -OH groups.Possible cation exchange mechanisms are described schematically in Fig.5.15.

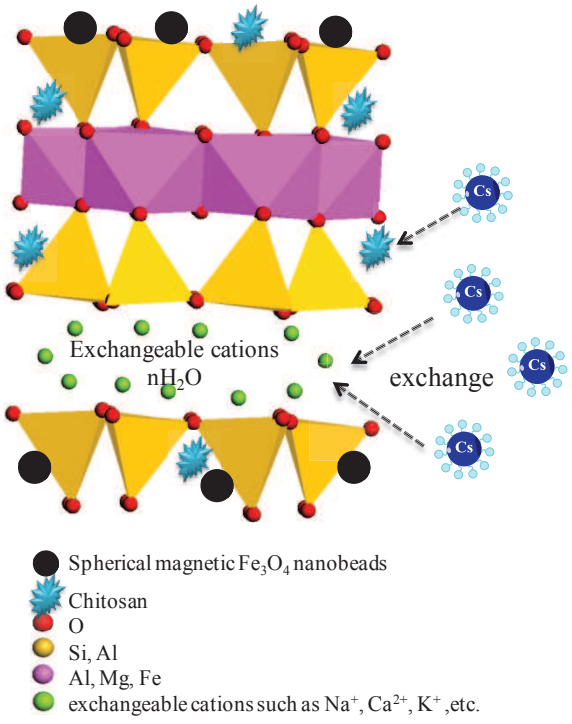

Fig.5.15 The possible cation exchange mechanism of Cs^+ ion sorption on the CS-g-MB composite.

5.4 Conclusions

We successfully synthesized chitosan-modified magnetic bentonite via an RF Ar plasma method. The CS-g-MB composite shows very good magnetic properties as well as low turbidity and high stability in seawater and aqueous solutions and has a significant adsorption capacity for Cs^+ ions. The Cs^+ ion exchange reaction of the CS-g-MB was found to vary with

both pH and ionic strength, and is primarily controlled by a cation exchange mechanism.In the presence of Mg^{2+}, K^+, Li^+, and Na^+ ions, the Cs^+ ion exchange reaction is reduced in the order of $Li^+ \approx Mg^{2+} < Na^+ < K^+$, largely as the result of variations in the hydrated radius and hydration energy between these cations in aqueous solution. The results indicated that enhanced coagulation generated by plasma modification is an advanced yet feasible process with applications in wastewater management. The results presented herein should therefore be helpful with regard to the application of bentonite-based materials for the remediation of nuclear waste and drinking water.We hope that this work will allow for the future development of new adsorbents that are readily separated from solution and that do not negatively affect either the turbidity or color of the water being treated.

Reference:

[1]. Yamaguchi, S.; Kondo, K.; Kodera, S.,Fukushima Daiichi Nuclear Power Plant accident and its effect. *National Diet Library* **2011.6.23,** (Issue Brief 718).
[2]. Sato, K.; Fujimoto, K.; Dai, W.; Hunger, M.,Molecular Mechanism of Heavily Adhesive Cs: Why Radioactive Cs is not Decontaminated from Soil. *J. Phys. Chem. C* **2013,** *117* (27), 14075-14080.
[3]. Mizuno, T.; Kubo, H.,Overview of active cesium contamination of freshwater fish in fukushima and eastern Japan. *Sci. Rep.* **2013,** *3*, 1-4.
[4]. Vipin, A. K.; Hu, B.; Fugetsu, B.,Prussian blue caged in alginate/calcium beads as adsorbents for removal of cesium ions from contaminated water. *J. Hazard. Mater.* **2013,** *258–259* (0), 93-101.
[5]. Yang, D.; Sarina, S.; Zhu, H.; Liu, H.; Zheng, Z.; Xie, M.; Smith, S. V.; Komarneni, S.,Capture of radioactive cesium and iodide ions from water by using titanate nanofibers and nanotubes. *Angew. Chem. Int. Ed.* **2011,** *50* (45), 10594-10598.
[6]. Ding, N.; Kanatzidis, M. G.,Selective incarceration of caesium ions by Venus flytrap action of a flexible framework sulfide. *Nat. Chem.* **2010,** *2* (3), 187-191.
[7]. Clearfield, A.,Ion-exchange materials seizing the caesium. *Nat. Chem.* **2010,** *2* (3), 161-162.
[8]. Celestian, A. J.; Kubicki, J. D.; Hanson, J.; Clearfield, A.; Parise, J. B.,The mechanism responsible for extraordinary Cs ion selectivity in crystalline silicotitanate. *J. Am. Chem. Soc.* **2008,** *130* (35), 11689-11694.
[9]. Kaufhold, S.; Dohrmann, R.; Klinkenberg, M.; Siegesmund, S.; Ufer, K.,N_2-BET specific surface area of bentonites. *J. Colloid Interface Sci.* **2010,** *349* (1), 275-282.

[10]. Huang, R.; Zheng, D.; Yang, B.; Wang, B.; Zhang, Z.,Preparation and characterization of CTAB-HACC bentonite and its ability to adsorb phenol from aqueous solution. *Water Sci. Technol.* **2011,** *64* (1), 286-292.

[11]. Seckin, T.; Gultek, A.; Onal, Y.; Yakinci, M. E.; Aksoy, I.,Synthesis, characterization and thermal properties of bentonite-polyacrylate sol-gel materials. *J. Mater. Chem.* **1997,** *7* (2), 265-269.

[12]. Matthes, W.; Madsen, F. T.; Kahr, G.,Sorption of heavy-metal cations by Al and Zr-hydroxy-intercalated and pillared bentonite. *Clay Clay Min.* **1999,** *47* (5), 617-629.

[13]. Kozaki, T.; Sato, H.; Sato, S.; Ohashi, H.,Diffusion mechanism of cesium ions in compacted montmorillonite. *Eng. Geol.* **1999,** *54* (1-2), 223-230.

[14]. Calagui, M. J. C.; Senoro, D. B.; Kan, C. C.; Salvacion, J. W. L.; Futalan, C. M.; Wan, M.-W.,Adsorption of indium(III) ions from aqueous solution using chitosan-coated bentonite beads. *J. Hazard. Mater.* **2014,** *277* (0), 120-126.

[15]. Ma, J.; Zou, J.; Li, L.; Yao, C.; Zhang, T.; Li, D.,Synthesis and characterization of Ag_3PO_4 immobilized in bentonite for the sunlight-driven degradation of orange II. *Appl. Catal. B* **2013,** *134–135* (0), 1-6.

[16]. McLachlan, D. R. C.,Aluminium and the risk for alzheimer's disease. *Environmetrics* **1995,** *6* (3), 233-275.

[17]. Walton, J. R.,Chronic Aluminum Intake Causes Alzheimer's Disease: Applying Sir Austin Bradford Hill's Causality Criteria. *J. Alzheimers Dis.* **2014,** *40* (4), 765-838.

[18]. Chatterjee, T.; Chatterjee, S.; Woo, S. H.,Enhanced coagulation of bentonite particles in water by a modified chitosan biopolymer. *Chem. Eng. J.* **2009,** *148* (2–3), 414-419.

[19]. Renault, F.; Sancey, B.; Badot, P. M.; Crini, G.,Chitosan for coagulation/flocculation processes–An eco-friendly approach. *Eur. Polym. J.* **2009,** *45* (5), 1337-1348.

[20]. Ahmad, A. L.; Mat Yasin, N. H.; Derek, C. J. C.; Lim, J. K.,Optimization of microalgae coagulation process using chitosan. *Chem. Eng. J.* **2011,** *173* (3), 879-882.

[21]. Anirudhan, T. S.; Rijith, S.; Tharun, A. R.,Adsorptive removal of thorium(IV) from aqueous solutions using poly(methacrylic acid)-grafted chitosan/bentonite composite matrix: process design and equilibrium studies. *Colloids Surf., A* **2010,** *368* (1-3), 13-22.

[22]. Kyzas, G. Z.; Deliyanni, E. A.,Mercury(II) removal with modified magnetic chitosan adsorbents. *Molecules* **2013,** *18* (6), 6193-6214.

[23]. Ravi Kumar, M. N. V.,A review of chitin and chitosan applications. *React. Funct. Polym.* **2000,** *46* (1), 1-27.

[24]. Anirudhan, T. S.; Rijith, S.,Synthesis and characterization of carboxyl terminated poly(methacrylic acid) grafted chitosan/bentonite composite and its application for the recovery of uranium(VI) from aqueous media. *Journal of environmental radioactivity* **2012,** *106*, 8-19.

[25]. Wan Ngah, W. S.; Teong, L. C.; Hanafiah, M. A. K. M.,Adsorption of dyes and heavy metal ions by chitosan composites: A review. *Carbohydr. Polym.* **2011,** *83* (4), 1446-1456.

[26]. Dutta, P. K.; Ravikumar, M. N.; Dutta, J.,Chitin and chitosan for versatile applications. *J. Macromol. Sci., Polym. Rev.* **2002,** *C42* (3), 307-354.

[27]. Guo, J.; Chen, S.; Liu, L.; Li, B.; Yang, P.; Zhang, L.; Feng, Y.,Adsorption of dye from wastewater using chitosan-CTAB modified bentonites. *J. Colloid Interface Sci.* **2012,** *382* (1), 61-66.

[28]. Kurtbay, H. M.; Bekci, Z.; Merdivan, M.; Yurdakoc, K.,Reduction of ochratoxin A levels in red wine by bentonite, modified bentonites, and chitosan. *J. Agric. Food Chem.* **2008,** *56* (7), 2541-2545.

[29]. Wei, Y.; Liu, Z. G.; Yu, X. Y.; Wang, L.; Liu, J. H.; Huang, X. J.,O_2-plasma oxidized multi-walled carbon nanotubes for Cd(II) and Pb(II) detection: Evidence of adsorption capacity for electrochemical sensing. *Electrochem. Commun.* **2011,** *13* (12), 1506-1509.

[30]. Chen, C. L.; Ogino, A.; Wang, X. K.; Nagatsu, M.,Plasma treatment of multiwall carbon nanotubes for dispersion improvement in water. *Appl. Phys. Lett.* **2010,** *96* (13), 131504-131503.

[31]. Shao, D. D.; Hu, J.; Wang, X. K.; Nagatsu, M.,Plasma induced grafting multiwall carbon nanotubes with chitosan for 4,4'-dichlorobiphenyl removal from aqueous solution. *Chem. Eng. J.* **2011,** *170* (2-3), 498-504.

[32]. Chen, C. L.; Liang, B.; Lu, D.; Ogino, A.; Wang, X. K.; Nagatsu, M.,Amino group introduction onto multiwall carbon nanotubes by NH3/Ar plasma treatment. *Carbon* **2010,** *48* (4), 939-948.

[33]. Chen, C. L.; Wang, X. K.; Nagatsu, M.,Europium adsorption on multiwall carbon nanotube/iron oxide magnetic composite in the presence of polyacrylic acid. *Environ. Sci. Technol.* **2009,** *43*, 2362-2367.

[34]. Yang, S. B.; Hu, J.; Chen, C. L.; Shao, D. D.; Wang, X. K.,Mutual effects of Pb(II) and humic acid adsorption on multiwalled carbon nanotubes/polyacrylamide composites from aqueous solutions. *Environ. Sci. Technol.* **2011,** *45* (8), 3621-3627.

[35]. Yang, S. B.; Shao, D. D.; Wang, X. K.; Nagatsu, M.,Localized in situ polymerization on carbon nanotube surfaces for stabilized carbon nanotube dispersions and application for cobalt(II) removal. *RSC Adv.* **2014,** *4* (10), 4856-4863.

[36]. Dwivedi, C.; Kumar, A.; Ajish, J. K.; Singh, K. K.; Kumar, M.; Wattal, P. K.; Bajaj, P. N.,Resorcinol-formaldehyde coated XAD resin beads for removal of cesium ions from radioactive waste: synthesis, sorption and kinetic studies. *RSC Adv.* **2012,** *2* (13), 5557-5564.

[37]. Yang, S.; Han, C.; Wang, X.; Nagatsu, M.,Characteristics of cesium ion sorption from aqueous solution on bentonite- and carbon nanotube-based composites. *J. Hazard. Mater.* **2014,** *274* (0), 46-52.

[38]. Jia, B.; Gao, L.; Sun, J.,Self-assembly of magnetite beads along multiwalled carbon nanotubes via a simple hydrothermal process. *Carbon* **2007,** *45* (7), 1476-1481.

[39]. Saraswati, T. E.; Ogino, A.; Nagatsu, M.,Plasma-activated immobilization of biomolecules onto graphite-encapsulated magnetic nanoparticles. *Carbon* **2012,** *50* (3), 1253-1261.

[40]. Saraswati, T. E.; Matsuda, T.; Ogino, A.; Nagatsu, M.,Surface modification of graphite encapsulated iron nanoparticles by plasma processing. *Diamond Relat. Mater.* **2011,** *20* (3), 359-363.

[41]. Yang, M. H.; Jong, S. B.; Lu, C. Y.; Lin, Y. F.; Chiang, P. W.; Tyan, Y. C.; Chung, T. W.,Assessing the responses of cellular proteins induced by hyaluronic acid-modified surfaces utilizing a mass spectrometry-based profiling system: over-expression of CD36, CD44, CDK9, and PP2A. *Analyst* **2012,** *137* (21), 4921-4933.

[42]. Dietsche, F.; Thomann, Y.; Thomann, R.; Mülhaupt, R.,Translucent acrylic nanocomposites containing anisotropic laminated nanoparticles derived from intercalated layered silicates. *J. Appl. Polym. Sci.* **2000,** *75* (3), 396-405.

[43]. Lu, J.; Jiao, X.; Chen, D.; Li, W.,Solvothermal Synthesis and Characterization of Fe_3O_4 and γ-Fe_2O_3 Nanoplates. *J. Phys. Chem. C* **2009,** *113* (10), 4012-4017.

[44]. Liu, M. C.; Chen, C. L.; Hu, J.; Wu, X. L.; Wang, X. K.,Synthesis of magnetite/graphene oxide composite and application for cobalt(II) removal. *J. Phys. Chem. C* **2011,** *115* (51), 25234-25240.

[45]. Six, J.; Conant, R. T.; Paul, E. A.; Paustian, K.,Stabilization mechanisms of soil organic matter: Implications for C-saturation of soils. *Plant and Soil* **2002,** *241* (2), 155-176.

[46]. Tosca, N. J.; Johnston, D. T.; Mushegian, A.; Rothman, D. H.; Summons, R. E.; Knoll, A. H.,Clay mineralogy, organic carbon burial, and redox evolution in Proterozoic oceans. *Geochim. Cosmochim. Acta* **2010,** *74* (5), 1579-1592.

[47]. Du, J.; Wu, D.; Xiao, H.; Li, P.,Adsorption of fluoride on clay minerals and their mechanisms using X-ray photoelectron spectroscopy. *Front. Environ.l Sci. Engin. China* **2010,** *5* (2), 212-226.

[48]. Zhao, Y.; Singh, M. K.; Ogino, A.; Nagatsu, M.,Effects of VUV/UV radiation and oxygen radicals on low-temperature sterilization in surface-wave excited O-2 plasma. *Thin Solid Films* **2010,** *518* (13), 3590-3594.

[49]. Teixeira, S. R.; De Souza, A. E.; De Almeida Santos, G. T.; Vilche Peña, A. F.; Miguel, Á. G.,Sugarcane Bagasse Ash as a Potential Quartz Replacement in Red Ceramic. *J. Am. Ceram. Soc.* **2008,** *91* (6), 1883-1887.

[50]. Zhou, Q.; Zhao, Z.; Wang, Z.; Dong, Y.; Wang, X.; Gogotsi, Y.; Qiu, J.,Low temperature plasma synthesis of mesoporous Fe3O4 nanorods grafted on reduced graphene oxide for high performance lithium storage. *Nanoscale* **2014,** *6* (4), 2286-2291.

[51]. Chen, P.; Xu, K.; Li, X.; Guo, Y.; Zhou, D.; Zhao, J.; Wu, X.; Wu, C.; Xie, Y.,Ultrathin nanosheets of feroxyhyte: a new two-dimensional material with robust ferromagnetic behavior. *Chem. Sci.* **2014,** *5* (6), 2251-2255.

[52]. Abdou, M. I.; Al-sabagh, A. M.; Dardir, M. M.,Evaluation of Egyptian bentonite and nano-bentonite as drilling mud. *Egy. J. Petro.* **2013,** *22* (1), 53-59.

[53]. O'Neill, H. S. C.,Systems Fe-O and Cu-O: Thermodynamic data for the equilibria Fe-"FeO," Fe-Fe_3O_4, "FeO"-Fe_3O_4, Fe_3O_4-Fe_2O_3, Cu-Cu_2O, and Cu_2O-CuO from emf measurements. *Mineralogical Society of America* **1988,** *73*, 470-486.

[54]. Spencer, P. J.; Kubaschewski, O.,A thermodynamic assessment of the iron-oxygen system. *Calphad* **1978,** *2* (2), 147-167.

[55]. Parajuli, D.; Tanaka, H.; Hakuta, Y.; Minami, K.; Fukuda, S.; Umeoka, K.; Kamimura, R.; Hayashi, Y.; Ouchi, M.; Kawamoto, T.,Dealing with the Aftermath of

Fukushima Daiichi Nuclear Accident: Decontamination of Radioactive Cesium Enriched Ash. *Environ. Sci. Technol.* **2013,** *47* (8), 3800-3806.

[56]. Torad, N. L.; Hu, M.; Imura, M.; Naito, M.; Yamauchi, Y.,Large Cs adsorption capability of nanostructured Prussian Blue particles with high accessible surface areas. *J. Mater. Chem.* **2012,** *22* (35), 18261-18267.

[57]. Solomon, T.,The Definition and Unit of Ionic Strength. *J. Chem. Educ.* **2001,** *78* (12), 1691.

[58]. Barrer, R. M.; Klinowski, J.,Ion-exchange selectivity and electrolyte concentration. *J. Chem. Soc., Faraday Trans.* **1974,** *70* (0), 2080-2091.

[59]. Brouwer, E.; Baeyens, B.; Maes, A.; Cremers, A.,Cesium and rubidium ion equilibriums in illite clay. *J. Phys. Chem.* **1983,** *87* (7), 1213-1219.

[60]. Liu, C. X.; Zachara, J. M.; Smith, S. C.; McKinley, J. P.; Ainsworth, C. C.,Desorption kinetics of radiocesium from subsurface sediments at Hanford Site, USA. *Geochim. Cosmochim. Acta* **2003,** *67* (16), 2893-2912.

[61]. Liu, C. X.; Zachara, J. M.; Smith, S. C.,A cation exchange model to describe Cs^+ sorption at high ionic strength in subsurface sediments at Hanford site, USA. *J. Contam. Hydrol.* **2004,** *68* (3-4), 217-238.

[62]. Tansel, B.; Sager, J.; Rector, T.; Garland, J.; Strayer, R. F.; Levine, L.; Roberts, M.; Hummerick, M.; Bauer, J.,Significance of hydrated radius and hydration shells on ionic permeability during nanofiltration in dead end and cross flow modes. *Sep. Purif. Technol.* **2006,** *51* (1), 40-47.

[63]. O'M. B, J.,Review: Ionic hydration in chemistry and biophysics, by B. E. Conway, Elsevier Publishing Company, 1981. *J Solution Chem* **1982,** *11* (3), 221-222.

[64]. Bouzidi, A.; Souahi, F.; Hanini, S.,Sorption behavior of cesium on ain oussera soil under different physicochemical conditions. *J. Hazard. Mater.* **2010,** *184* (1-3), 640-646.

[65]. Nightingale, E. R.,Phenomenological Theory of Ion Solvation. Effective Radii of Hydrated Ions. *J. Phys. Chem.* **1959,** *63* (9), 1381-1387.

[66]. Zhou, J.; Lu, X.; Wang, Y.; Shi, J.,Molecular dynamics study on ionic hydration. *Fluid Phase Equilib.* **2002,** *194–197* (0), 257-270.

[67]. Persson, I.,Hydrated metal ions in aqueous solution: How regular are their structures? *Pure Appl. Chem.* **2010,** *82* (10), 1901-1917.

[68]. Crini, G.,Non-conventional low-cost adsorbents for dye removal: a review. *Bioresour. Technol.* **2006,** *97* (9), 1061-1085.

[69]. Koev, S. T.; Dykstra, P. H.; Luo, X.; Rubloff, G. W.; Bentley, W. E.; Payne, G. F.; Ghodssi, R.,Chitosan: an integrative biomaterial for lab-on-a-chip devices. *Lab on a Chip* **2010,** *10* (22), 3026-3042.

[70]. Xu, Y.; Fang, Z.; Tong, L.,On promoting intercalation and exfoliation of bentonite in high-density polyethylene by grafting acrylic acid. *J. Appl. Polym. Sci.* **2005,** *96* (6), 2429-2434.

[71]. Volkov, A. G., Liquid-liquid interfaces : theory and methods. Deamer, D. W., Ed. CRC Press: Boca Raton, New York :, 1996.

[72]. Gourary, B. S.; Adrian, F. J., Wave Functions for Electron-Excess Color Centers in Alkali Halide Crystals. In *Solid State Physics*, Frederick, S.; David, T., Eds. Academic Press: 1960; Vol. Volume 10, pp 127-247.

[73]. Volkov, A. G.; Paula, S.; Deamer, D. W.,Two mechanisms of permeation of small neutral molecules and hydrated ions across phospholipid bilayers. *Bioelectrochem. Bioenerg.* **1997,** *42* (2), 153-160.

[74]. Markham, E. C.; Benton, A. F.,The adsorption of gas mixtures by silica. *J. Am. Chem. Soc.* **1931,** *53*, 497-507.

[75]. Digiano, F. A.; Baldauf, G.; Frick, B.; Sontheimer, H.,A simplified competitive equilibrium adsorption model. *Chem. Eng. Sci.* **1978,** *33* (12), 1667-1673.

[76]. Park, Y.; Shin, W. S.; Choi, S.-J.,Removal of Co, Sr and Cs from aqueous solution using self-assembled monolayers on mesoporous supports. *Korean J. Chem. Eng.* **2012,** *29* (11), 1556-1566.

[77]. Delchet, C.; Tokarev, A.; Dumail, X.; Toquer, G.; Barre, Y.; Guari, Y.; Guerin, C.; Larionova, J.; Grandjean, A.,Extraction of radioactive cesium using innovative functionalized porous materials. *RSC Adv.* **2012,** *2* (13), 5707-5716.

CHAPTER 6 Conclusions

This thesis focuses on the management of Cs^+constaiminated wastewater within the adsorption method. The carbon nanotube- and bentonite-based composites were successfully synthesized by the plasma-induced grafting method and application them for the remediate Cs^+ ions from the contaminated wastewater.

This thesis contributes to not only the development of application of plasma modification in wastewater management and the high-efficiency adsorbent for Cs^+ ions, but also clarifying Cs^+ adsorption mechanisms in aqueous solution.

The key points provided by this thesis are following:

1) We have demonstrates that cation-exchange mechanism is much more effective than the hydroxyl group to Cs^+ adsorption. In addition, the effect of hydroxyl groups to Cs^+ adsorption is dependent on the property of the matrix. We cannot improve the Cs^+ adsorption capacity of material only by increasing the amount of hydroxyl groups in any case.
2) The spatial structure and cation-exchange capacity of the material are very important factors for high-efficiency sorbent for Cs^+ ions. Our findings are important for estimating and optimizing the sorbent of Cs^+ ions and give the future directions of new and selective adsorbents for the removal of Cs^+ ions in groundwater or wastewater.
3) We designed the chitosan-grafted magnetic bentonite (CS-g-MB) by plasma-induced grafting method to enhance coagulation of magnetic bentonite in water.
4) The CS-g-MB composite shows good magnetic properties, low turbidity, and high stability in aqueous solution and exhibits significant adsorption capacity for Cs^+ ions.
5) The adsorption of Cs^+ by CS-g-MB is dependent on both pH and ionic strength. In the presence of Mg^{2+}, K^+, Li^+, and Na^+ ions, the Cs^+ exchange is constrained in

the order of $Li^+ \approx Mg^{2+} < Na^+ < K^+$, primarily as a result of the hydrated radii and hydration energies of these cations in aqueous solution.

6) The enhanced coagulation achieved by plasma modification represents a viable yet advanced technology for wastewater management, and is capable of synthesizing new adsorbents that can be readily separated from solution and that avoid increasing the turbidity and color of the water being treated.

Activity

■ Publications

1) S.B. Yang, N. Okada, X.K. Wang and M.Nagatsu. A Highly Effective Cs^+ Removal Property of Chitosan-Grafted Magnetic Bentonite with Low Turbidity, *J. Hazard. Mater.*(accept)
2) S.B. Yang, D.D. Shao, X.K. Wang, G.S. Hou, M. Nagatsu, X.L. Tan, X.M. Ren and J.T. Yu, Design of Chitosan-Grafted Carbon Nanotubes: Evaluation of How the -OH Functional Group Affects Cs^+ Adsorption, *Mar. Drugs*., 13(5), 3116-313, 2015.
3) S.B. Yang, C.C. Ding, W.C. Cheng, Z.X. Jin, Y.B. Sun, Effect of microbes on Ni(II) diffusion onto sepiolite, *J.Mol. Liq.*, 204, 170-175, 2015.
4) S.B. Yang, Y. Chen, C.L. Chen, J.X. Li, D.Q. Wang, X.K. Wang, and W.P. Hu, Competitive Adsorption of Pb(II), Ni(II) and Sr(II) Ions on Graphene Oxides: A Combined Experimental and Theoretical Study, *ChemPusChem*, 80, 480-484, 2015.
5) Y.B. Sun, S.B. Yang, Y. Chen, C.C. Ding, W.C. Cheng, and X.K. Wang, Adsorption and desorption of U(VI) on functionalized graphene oxide: A Combined Experimental and Theoretical study, *Environ. Sci. Technol.* 49, 4255-4262, 2015 (co-first author)
6) S.B. Yang, C. Han, X.K. Wang and M. Nagatsu. Characteristics of Cesium Ion Sorption from Aqueous Solution on Bentonite- and Carbon Nanotube-based Composites, *J. Hazard. Mater*., 274, 46-52, 2014.
7) S.B. Yang, D.D. Shao, X.K. Wang and M. Nagatsu. Localized In-situ Polymerization on Carbon Nanotube Surfaces for Stabilized Carbon Nanotube Dispersions and Application for Cobalt(II) Removal, *RSC Advances*, 4, 4856-4863, 2014.
8) Y.B. Sun, D.D. Shao, C.L. Chen, S.B. Yang, and X.K. Wang, Highly Efficient Enrichment of Radionuclides on Graphene Oxide-Supported Polyaniline, *Environ. Sci. Technol*., 47, 9904-9910, 2013.
9) X.L. Wu, Tao Wen, H.L. Guo, S.B. Yang, X.K. Wang, and A.W. Xu, Biomass-Derived Sponge-like Carbonaceous Hydrogels and Aerogels for Supercapacitors, *ACS Nano*, 7,

3589-3597, 2013.

10) Y.B. Sun, S.B. Yang, G.X. Zhao, Qi Wang, and X.K. Wang, Adsorption of Polycyclic Aromatic Hydrocarbons on Graphene Oxides and Reduced Graphene Oxides, CHEMISTRY- ASIAN J., 8, 2755-2761, 2013.
11) S.B. Yang, X.L. Wu, C.L. Chen, H.L. Dong, W.P. Hu, and X.K. Wang, Spherical α-$Ni(OH)_2$ nanoarchitecture grown on graphene as advanced electrochemical pseudocapacitor materials, *Chem. Commun*., 48, 2773-2775, 2012.
12) G.X. Zhao, T. Wen, X. Yang, S.B. Yang, J.L. Liao, J. Hu, D.D. Shao, X.K. Wang, Preconcentration of U(VI) ions on few-layered graphene oxide nanosheets from aqueous solutions, *Dalton Tran*.,41, 6182-6188,2012.
13) Y.B. Sun, C.L. Chen, X.L. Tan, D.D. Shao, J.X. Li, G.X. Zhao, S.B. Yang, Q. Wang,X.K. Wang, Enhanced adsorption of Eu(III) on mesoporous Al_2O_3/expanded graphite composites investigated by macroscopic and microscopic techniques, *Dalton Tran.*,41, 13388-13394,2012.
14) Y.B. Sun, C.L. Chen, D.D. Shao, J.X. Li, X.L. Tan, G.X. Zhao, S.B. Yang; X.K. Wang, Enhanced adsorption of ionizable aromatic compounds on humic acid-coated carbonaceous adsorbents, *RSC Advances*2, 10359-10364, 2012.
15) S.B. Yang, J. Hu, C.L. Chen, D.D. Shao, and X.K. Wang, Mutual Effects of Pb(II) and Humic Acid Adsorption on Multiwalled Carbon Nanotubes/PolyacrylamideComposites from Aquesous Solutions, *Environ. Sci. Technol.* 45, 3621-3627, 2011.
16) X. Yang, S.B. Yang, S.T. Yang, J. Hu, X.L. Tan, X.K. Wang, Effect of pH, ionic strength and temperature on sorption of Pb(II) on NKF-6 zeolite studied by batch technique. *Chem. Eng. J.*, 168, 86-93, 2011.
17) D.L. Zhao, S.B. Yang, S.H. Chen, Z.Q. Guo, and X. Yang, Effect of pH, ionic strength and humic substances on the adsorption of Uranium (VI) onto Na-rectorite, *J RadioanalNucl Chem.*, 287, 557-565, 2011.
18) D.L. Zhao, S.H. Chen, S.B. Yang, X. Yang, and S.T. Yang, Investigation of the sorption behavior of Cd(II) on GMZ bentonite as affected by solution chemistry, *Chem. Eng. J.*,

166,1010-1016, 2011.

■ Conferences International conferences

1) Shubin Yang, Naoya Okada, Xiangke Wang, and Masaaki Nagatsu, Synthesis of Chitosan-coated Magnetic Bentonite by Plasma-Induced Graft Chitosan and Its Application in Cs+ Capture, 2015 International Symposium toward the Future of Advanced Researches in Shizuoka University, Hamamatsu, Japan: 2015.1.27-28 (poster, No. PS-42)
2) Shubin Yang, Okada Naoya, Xiangke Wang, Masaaki Nagatsu, Understanding the Sorption of Cesium ion on bentonite by Plasma Jet, ISPlasma2014 / IC-PLANTS 2014,Nagoya: 2014, 3. 2-6 (poster, 06aP17)
3) Shubin Yang, Chou Han, Xiangke Wang, Masaaki Nagatsu, Removal Mechanism of Cesium Ion from Aqueous Solution with Bentonite- and Carbon Nanotube-based Composites, ICRP-8/SPP-31,Fukuoka: 2014, 2. 3-7 (poster,6P-AM-S10-P41)
4) Shubin Yang, Chou Han, Xiangke Wang, Masaaki Nagatsu, Sorption Mechanism of Cesium Ions from Aqueous Solution by Chitosan-grafted Carbon Nanotubes and Bentonite by Plasma-induced Grafting Method, MRS-J, Yokohama: 2013, 12. 9-11 (poster, 10564-P-P10-011)
5) Shubin Yang, Chou Han, Xiangke Wang, Masaaki Nagatsu, Removal of Cs ion from aqueous solution using plasma functionalized chitosan-grafted graphite-encapsulated magnetic nanoparticles, APPC-12, Chiba:2013. 7.14-19 (poster, A3-PWe-6)

■ Domestic conferences

1) Shubin Yang, Naoya Okada, Masaaki Nagatsu, Study of Adsorption and Desorption of Cs^{+} Ions on Chitosan-Grafted Magnetic Bentonite, The 62^{nd} JSAP Spring Meeting, 2015, 3.11 -14 Shibuya, (Oral, 11a-A20-7).
2) Shubin Yang, Naoya Okada, Xiangke Wang, and Masaaki Nagatsu, Synthesis and

characterization of bentonite-based composites by plasma-induced graft chitosan for separation of cesium ions from waste solutions, 306th Monday Morning Forum, 2014. 12.15, Hamamatsu, Japan (Oral).

3) Shubin Yang, Naoya Okada, Xiangke Wang, Masaaki Nagatsu, Characteristics of cesium ion sorption from aqueous solution on plasma-induced chitosan grafted magnetic bentonite composites, Plasma Conference, 2014.11.18-21, Niigata (Poster and short oral, No. 19PB-117).
4) Shubin Yang, Xiangke Wang, Masaaki Nagatsu, Study of the Sorption of Cobalt(II) Ion on Magnetic Carbon Nanotubes by Atmospheric Pressure Plasma Jet, The 61nd JSAP Spring Meeting, 2014, 3.17 -20 Sagamihara, (Poster, 18p-PA8-2).
5) Shubin Yang, Chou Han, Xiangke Wang, Masaaki Nagatsu"Study on the Sorption Mechanism of Cesium ion by Chitosan-grafted Nanomaterials", JSPF Annual Meeting, 2013.12.3-6, Tokyo (Poster, 04aE20P).
6) Shubin Yang, Chou Han, Xiangke Wang, Masaaki Nagatsu, Capture of Cesium from Water by Using Plasma Induced Chitosan-grafted Magnetic Bentonite，第 26 回プラズマ材料科学シンポジウム(SPSM-26), 九州大学: 2013.9.23
7) Shubin Yang, Chou Han, Xiangke Wang, Masaaki Nagatsu,Capture of Cesium from Water by Using Plasma Induced Chitosan-grafted Magnetic Carbon Nanotubes, 応用物理学会秋季学術講演会, 2013. 9.17
8) 楊樹斌，王祥科,永津雅章, プラズマ酸化多層カーボンナノチューブ/酸化鉄を用いた水溶液中セシウムイオンの吸着, 第 60 回応用物理学会春季学術講演会, 神奈川工科大学, 厚木: 2013.03, 講演番号 29p-PA1-9.
9) 楊樹斌，邵大冬，王祥科, 永津雅章,分散性改善のためのプラズマ修飾多層カーボンナノチューブ表面のポリマリゼーションとコバルト除去への応用, 第30回プラズマプロセシング研究会(SPP-30), アクトシティ浜松・研修交流センター, 浜松: 2013.01, 講演番号 P4-41.